

Conceptual Basis for Distribution of Highly Sorbed Contaminants in 100 Areas Vadose Zone

Prepared for the U.S. Department of Energy
Assistant Secretary for Environmental Management

Contractor for the U.S. Department of Energy
under Contract DE-AC06-08RL14788

 **CH2MHILL**
Plateau Remediation Company
P.O. Box 1600
Richland, Washington 99352

Conceptual Basis for Distribution of Highly Sorbed Contaminants in 100 Areas Vadose Zone

Document Type: RPT

Program/Project: EP&SP

R. Khaleel
INTERA

Date Published
February 2012

Prepared for the U.S. Department of Energy
Assistant Secretary for Environmental Management

Contractor for the U.S. Department of Energy
under Contract DE-AC06-08RL14788

 **CH2MHILL**
Plateau Remediation Company
P.O. Box 1600
Richland, Washington 99352

APPROVED

By Shauna E. Adams at 9:35 am, Mar 09, 2012

Release Approval

Date

Approved for Public Release;
Further Dissemination Unlimited

TRADEMARK DISCLAIMER

Reference herein to any specific commercial product, process, or service by tradename, trademark, manufacturer, or otherwise, does not necessarily constitute or imply its endorsement, recommendation, or favoring by the United States Government or any agency thereof or its contractors or subcontractors.

This report has been reproduced from the best available copy.

Printed in the United States of America

Contents

| | |
|--|-----------|
| 1. Introduction..... | 7 |
| 2. Overview of 100 Areas Vadose Zone | 8 |
| 3. Composite Vertical Distribution of High K_d Contaminants..... | 13 |
| 4. Remedial Investigation/Feasibility Study Borehole Data | 22 |
| 4.1 Borehole C7864 (100-H Area) | 22 |
| 4.2 Borehole C7691 (100-K Area) | 27 |
| 4.3 Borehole C7683 (100-K Area) | 31 |
| 4.4 Borehole C7689 (100-K Area) | 36 |
| 4.5 Borehole C7506 (100-B/C Area) | 41 |
| 4.6 Borehole C7843 (100-B/C Area) | 45 |
| 4.7 Borehole C7844 (100-B/C Area) | 50 |
| 5. Plausible Conceptual Models | 55 |
| 5.1 Lead-Cadmium Burial Grounds. | 55 |
| 5.2 Media and Chemical Heterogeneities..... | 56 |
| 5.3 Conceptual Model #1 | 57 |
| 5.4 Conceptual Model #2 | 60 |
| 5.5 Conceptual Model #3 | 62 |
| 6. Concluding Remarks | 65 |
| 7. References | 66 |

Figures

| | |
|--|----|
| Figure 2-1. Variability of Various Stratigraphic Units for the 100 Areas..... | 9 |
| Figure 2-2. Representative Gravel-dominated Hanford formation for 100 Areas | 9 |
| Figure 2-3. Schematic Illustrating Columbia River, Aquifer and Vadose Zone Exchange Flow for 100 Areas 11 | |
| Figure 2-4. Schematic Illustrating Unsaturated Flow Conditions for Low Fluxes in Coarse-textured Gravelly Media..... | 12 |
| Figure 3-1. 100-F Area Lead Measurements | 14 |
| Figure 3-2. 100-H Area Lead Measurements..... | 14 |
| Figure 3-3. 100-D Area Lead Measurements..... | 15 |
| Figure 3-4. 100-K Area Lead Measurements..... | 15 |
| Figure 3-5. 100-B/C Area Lead Measurements | 16 |
| Figure 3-6. 100-F Area Arsenic Measurements..... | 16 |
| Figure 3-7. 100-H Area Arsenic Measurements | 17 |

| | |
|--|----|
| Figure 3-8. 100-D Area Arsenic Measurements | 17 |
| Figure 3-9. 100-K Area Arsenic Measurements | 18 |
| Figure 3-10. 100-B/C Area Arsenic Measurements..... | 18 |
| Figure 3-11. 100-F Area Mercury Measurements | 19 |
| Figure 3-12. 100-H Area Mercury Measurements..... | 19 |
| Figure 3-13. 100-D Area Mercury Measurements..... | 20 |
| Figure 3-14. 100-K Area Mercury Measurements..... | 20 |
| Figure 3-15. 100-B/C Area Mercury Measurements | 21 |
| Figure 3-16. Diagrams Illustrating Distribution of Detects/Non-Detects and Below/Above Background Data for Arsenic, Mercury and Lead..... | 21 |
| Figure 4-1. Borehole C7864 Location | 23 |
| Figure 4-2. C7864 Borehole Logging Data | 24 |
| Figure 4-3. Borehole C7864 Lead Measurements | 25 |
| Figure 4-4. Borehole C7864 Arsenic Measurements..... | 25 |
| Figure 4-5. Borehole C7864 Mercury Measurements..... | 26 |
| Figure 4-6. Borehole C7691 (199-K-191) Location | 28 |
| Figure 4-7. Borehole Logging Data for C7691 | 29 |
| Figure 4-8. Borehole C7691 Lead Measurements | 30 |
| Figure 4-9. Correlation of Borehole C7691 Lead Measurements with Other Measurements | 30 |
| Figure 4-10. Borehole C7683 (199-K-183) Location | 32 |
| Figure 4-11. Borehole C7683 Logging Data | 33 |
| Figure 4-12. Borehole C7683 Lead Measurements | 34 |
| Figure 4-13. Borehole C7683 Arsenic Measurements..... | 34 |
| Figure 4-14. Borehole C7683 Mercury Measurements..... | 35 |
| Figure 4-15. Borehole C7689 (199-K-189) Location | 37 |
| Figure 4-16. Borehole C7689 Logging data | 38 |
| Figure 4-17. Borehole C7689 Lead Measurements | 39 |
| Figure 4-18. Borehole C7689 Arsenic Measurements..... | 39 |
| Figure 4-19. Borehole C7689 Mercury Measurements..... | 40 |
| Figure 4-20. Borehole C7506 (199-B3-50) Location | 42 |
| Figure 4-21. Borehole C7506 Logging Data | 43 |
| Figure 4-22. Borehole C7506 Lead Measurements | 44 |
| Figure 4-23. Borehole C7506 Arsenic Measurements..... | 44 |
| Figure 4-24. Borehole C7843 (199-B3-52) Location | 46 |
| Figure 4-25. Borehole C7843 Logging Data | 47 |
| Figure 4-26. Borehole C7843 Lead Measurements | 48 |
| Figure 4-27. Borehole C7843 Arsenic Measurements..... | 48 |
| Figure 4-28. Borehole C7843 Mercury Measurements..... | 49 |
| Figure 4-29. Borehole C7844 Location | 51 |

| | |
|--|----|
| Figure 4-30. Borehole C7844 Logging Data | 52 |
| Figure 4-31. Borehole C7844 Lead Measurements | 53 |
| Figure 4-32. Borehole C7844 Arsenic Measurements | 53 |
| Figure 4-33. Borehole C7844 Mercury Measurements..... | 54 |
| Figure 5-1. Location of 100 Areas Burial Grounds (in red) which received Lead-Cadmium Poison Pieces; Other nearby burial grounds are shown in green..... | 55 |
| Figure 5-2. Borehole C7864 Location | 58 |
| Figure 5-3. Lead Contamination Measurements for Waste Site 100-H-21..... | 59 |
| Figure 5-4. Borehole C7864 Lead, Antimony and Copper Concentration Profiles | 59 |
| Figure 5-5. Perspective on Thermal Plume Profiles during Reactor Operations in 100-H Area | 61 |
| Figure 5-6. Head Data in Well 199-H4-1 | 61 |
| Figure 5-7. An Interacting Dual Media Representation of 100 Area Gravelly Vadose Zone; Macropore (fast flow) and Porous Matrix (slow flow) (after Mohanty et al. 2011) | 63 |
| Figure 5-8. An Interacting Physiochemical Hypothesis – Transients in Ionic Strengths May Mobilize Colloids across the Macropore-Matrix Interface (after Mohanty et al. 2011)..... | 64 |
| Figure 5-9. Macropore-matrix Exchange Caused by Hysteresis of Colloids and Metal Mobilization (after Mohanty et al. 2011) | 64 |

Tables

| | |
|--|----|
| Table 4-1. Batch Leach Testing Results for Lead for Borehole C7864 Samples | 26 |
| Table 5-1. Composition of Lead-Cadmium Poison Pieces | 56 |

Terms

| | |
|-------|---|
| bgs | below ground surface |
| CHPRC | CH2M Hill Plateau Remediation Company |
| EPA | U.S. Environmental Protection Agency |
| ERDF | Environmental Restoration Disposal Facility |
| K_d | contaminant distribution coefficient |
| LFI | Limited Field Investigation |
| PNNL | Pacific Northwest National Laboratory |
| PRG | preliminary remediation goal |
| PRZ | periodically rewetted zone |
| RI/FS | Remedial Investigation/Feasibility Study |
| RUM | Ringold upper mud |
| SSL | soil screening level |

Unit Abbreviations

| | |
|---------------------|----------------------------------|
| ft | feet |
| gal/min | gallons per minute |
| g/cm^3 | grams per cubic centimeter |
| ℓ/min | liters per minute |
| m | meter(s) |
| μm | micrometers |
| $\mu\text{Ci/cm}^3$ | microcuries per cubic centimeter |
| $\mu\text{g}/\ell$ | micrograms per liter |
| mg/kg | milligrams per kilogram |
| mm/yr | millimeters per year |

1. Introduction

For the 100 Areas Remedial Investigation/Feasibility Study (RI/FS) process, the calculated soil screening levels (SSLs) and preliminary remediation goals (PRGs) represent the maximum quantity, whether soil concentration or radionuclide activity, of a contaminant that can remain in the vadose zone without causing an exceedance of standards. SSL and PRG values for a particular contaminant depend on a number of key factors. These include, among others, individual waste site characteristics including contaminant mass loading, distance to the water table, the land use scenario and the associated net infiltration (recharge) rate, vadose zone hydrostratigraphy and its physical and hydraulic characteristics, and contaminant chemistry.

In calculating SSLs and PRGs, in the absence of sufficient data to determine the subsurface extent of contaminants at individual waste sites, the contaminated interval is assumed to be the entire vadose zone thickness below the waste site. This can, however, be an overly conservative assumption for many of the 100 Area waste sites. In this report, site characterization data from the deep boreholes specified in the RI Work Plans for those 100 Areas waste sites where large volumes of liquid wastes were discharged to the vadose zone are used to assess this conservatism. It should be noted that the deep borehole measurements targeted in the RI Work Plan were identified with a bias towards locating contaminants throughout the vadose zone and targeted areas at or near the waste sites.

Contaminant distribution coefficients (K_d 's) describe the partitioning of the adsorbed phase concentration to its dissolved phase concentration. The focus of this report is on the extent of vertical distribution of analytes that are known to be relatively less mobile (such as lead, arsenic and mercury) within the vadose zone under the near neutral pH and oxygenated conditions present in the vadose zone within the River Corridor portion of the Hanford Site. The characterization data presented in this report suggest that, for these analytes that are less mobile within the vadose zone, the soil column is not uniformly contaminated from the waste site to the water table. For incidents where a deep measurement indicates an elevated level for the high K_d contaminant, this report provides the plausible conceptual site models for these occurrences.

Section 2 provides a background of the 100 Areas, its characteristics and the important role they play in developing plausible conceptual models for the high K_d contaminant transport. Section 3 provides, for the recently drilled RI/FS boreholes, the composite vertical distribution of concentration profiles for high K_d analytes. Section 4 presents the detailed data for individual RI/FS borehole locations. Section 5 presents three plausible conceptual models to help explain the deeper than expected location within the vadose zone for the high K_d analytes. Section 6 provides the concluding remarks.

2. Overview of 100 Areas Vadose Zone

This section provides a brief discussion of the 100 Areas vadose zone including its hydrogeologic framework, nature and extent of contamination during reactor operations, and migration potential for nonreactive (mobile) and reactive (relatively immobile) contaminants. The stream-aquifer interaction and its relevance to vadose zone contamination and the importance of preferential flow are discussed. The 100 Areas vadose zone characteristics and the behavior of similar reactive high K_d analytes provide guidance on the development of postulated conceptual models for high K_d contaminant transport considered later in Section 5.

The average thickness of the vadose zone in the 100 Areas ranges from 6 m (100-F Area) to over 30 m (100-B/C Area) with each reactor area being slightly different. The large volume of liquid discharges during operations created water table mounds 6 to 9 m above the nominal water table under the retention basins and other liquid disposal facilities (PNNL-14702, *Vadose Zone Hydrology Data Package for Hanford Assessments*). The groundwater mounding reduced the thickness of the vadose zone during operations.

The hydrogeologic framework of the vadose zone is complex; however, locally within the 100 Areas, it can be divided into two primary hydrostratigraphic units: (1) the gravel-dominated facies association of the Hanford formation and (2) the conglomeratic member of Wooded Island, Unit E, of the Ringold Formation (PNNL-14702). The Ringold Formation makes up the lower portion of the vadose zone at the 100-K, 100-N, and the 100-D Areas (Figure 2-1). It is only partially present in the 100-B/C Area and absent in the 100-H and 100-F Areas. The Hanford formation extends from the surface to just above the water table where the Ringold Formation is present. The Hanford formation extends beneath the water table and makes up the unconfined aquifer in the 100-H and 100-F Areas. The relatively thick Ringold upper mud (RUM)/basalt constitute the lower boundary (Figure 2-1).

The Ringold Formation Unit E is fluvial deposited pebble-to-cobble gravel with a sandy matrix. It is characterized by complex interstratified beds and lenses of sand and gravel with low to moderate degrees of cementation. As illustrated in Figure 2-2, the gravel-dominated facies of the Hanford formation is generally composed of uncemented, clast-supported pebble, cobble, and boulder gravel with a poorly sorted silty sandy matrix and minor sand and silt interbeds or stringers. It occasionally exhibits an open framework texture with little or no matrix. The physical and hydraulic properties for the 100 Areas vadose zone sediment samples vary widely, reflecting the heterogeneity of the vadose zone. These data are described in the vadose zone flow parameters catalog for the 100 Areas (SGW-46279, *Conceptual Framework and Numerical Implementation of 100 Areas Groundwater Flow and Transport Model*).

The contact (Figure 2-1) between Ringold Unit E and the Hanford formation is important because the saturated hydraulic conductivity for the gravel-dominated sequence of the Hanford formation is one to two orders of magnitude higher than the more compacted and locally cemented Ringold Unit E. Because hydraulic conductivity varies with the formation, different groundwater level responses may occur where channels now filled with the Hanford formation have been scoured into the Ringold Unit E. These buried channels can potentially function as preferential pathways for contaminated groundwater during high river stages.

Results from the geochemical characterization studies in the 100 Areas show a contaminant zoning (chromatographic) effect in the vadose zone (PNNL-14702). For radionuclides and inorganic contaminants that are not adsorbed (i.e., tritium, nitrate), large releases of water, during reactor operations, at retention basin and liquid waste disposal facilities quickly pushed these contaminants through the vadose zone, into the unconfined aquifer, and subsequently out to the Columbia River. BNWL-CC-2326 (*Analysis of Travel Time of I-131 from the 1301-N Crib to the Columbia River During*

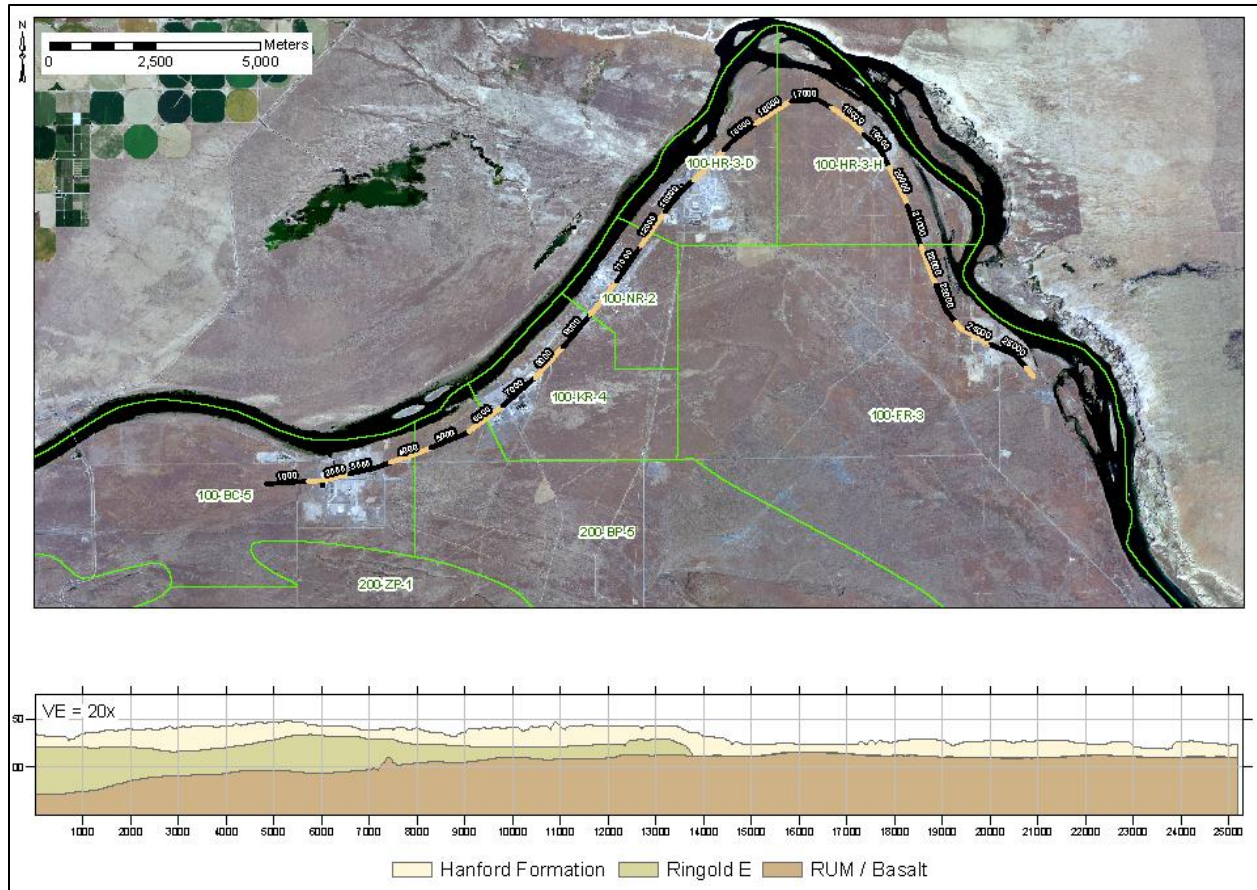


Figure 2-1. Variability of Various Stratigraphic Units for the 100 Areas

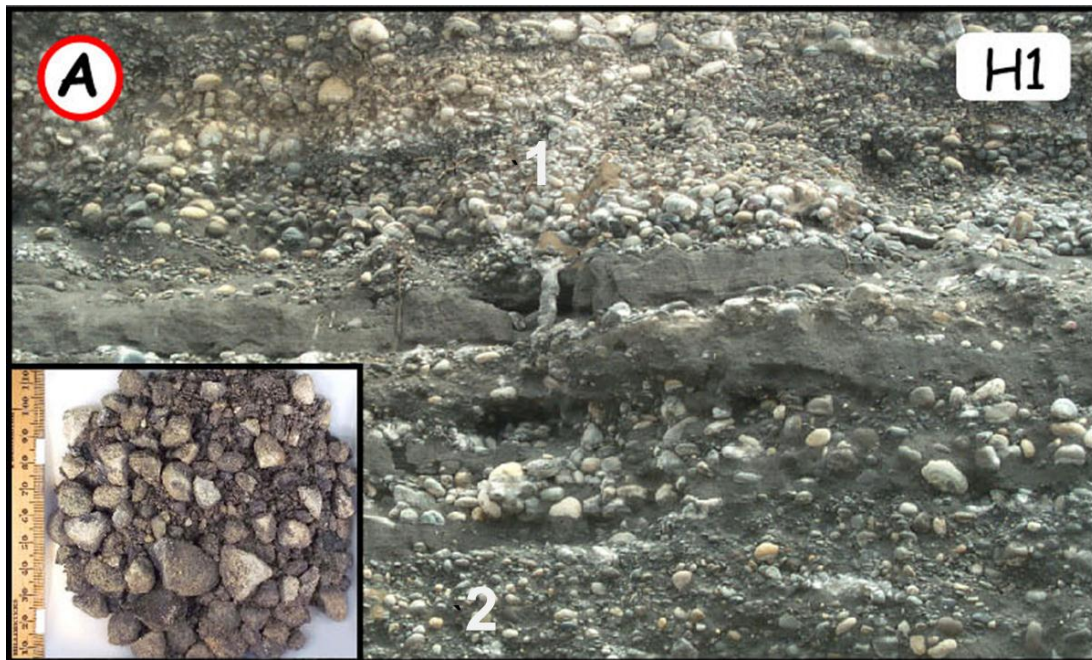


Figure 2-2. Representative Gravel-dominated Hanford formation for 100 Areas

July 1969) for example, using iodine-131 isotopic analysis, estimated the travel time to the Columbia River from the 1301-N (116-N-1) liquid waste disposal facility to be approximately 10 days during active disposal (a distance of some 225 m).

Because highly sorbed contaminants are the focus of this report, it is worth noting the observed vadose zone migration behavior of other high K_d analytes in 100 Areas. Contaminants that show moderate adsorption such as strontium-90 show a differential distribution (i.e., chromatographic zoning) within the vadose zone (PNNL-14702). PNL-10899 (*Strontium-90 Adsorption-Desorption Properties and Sediment Characterization at the 100-N Area*) examined characterization data from 12 boreholes within the 100-N Area and found that strontium-90 in the vadose zone is bound to sediment directly underneath the liquid waste disposal facilities in a relatively thin layer at depths that correspond to the elevated water table formed during operations. Contaminants with strong adsorption (i.e., high K_d) such as cobalt-60, cesium-137, and plutonium-239/240 remained within 1 m of the bottom of the disposal facility.

A complicating aspect of release of contaminants from the vadose zone in the 100 Areas is the seasonal and diurnal fluctuations of the Columbia River (Figure 2-3). A high river stage can cause the water table to rise into vadose zone sediments containing higher concentrations of contaminants. Additionally, the chemistry changes within the periodically rewetted zone (PRZ) caused by the constant re-wetting of the soil due to diurnal and seasonal fluctuations could affect the release of contaminants from the vadose zone. This aspect of interaction among the river, aquifer, and the vadose zone is considered in postulating a conceptual basis for the deeper than expected location for high K_d analytes.

Also, as discussed in Section 5, colloid formation and colloid-facilitated transport are noted as potential mechanisms for the deep penetration of high K_d analytes. In general, under saturated flow conditions, the potential exists for formation of colloids and their migration. Under unsaturated conditions, however, due to the low water content and significant filtration at the air-water/solid interfaces, conditions are generally not conducive to colloid formation or colloid-facilitated transport. Nonetheless, Hanford waste sites that received large-volume discharges or highly concentrated wastes, conditions may have existed for both colloid formation and colloid-facilitated transport. The formation of colloids and occurrence of colloid-facilitated transport of contaminants were identified in the tank farm vadose zone by a DOE-RL Expert Panel as potentially an important process affecting vadose zone transport (DOE/RL-97-49, *TWRS Vadose Zone Contamination Issue, Expert Panel Status Report*). Field data, however, are insufficient to adequately characterize the potential for colloidal transport. Various interacting mechanisms might be involved simultaneously during colloid transport, but their importance depends on the chemical and physical properties of the colloids and transport media as well as the environmental conditions. These are discussed in Section 5, in the context of developing conceptual models.

A variety of preferential flow pathways such as macropores and discontinuities are capable of concentrating or contributing to preferential flow phenomena as well as fingering and funnel flow (DOE/RL-97-49). Preferential flow has been recognized and widely studied under saturated or near-saturated flow conditions (Nkedi-Kizza et al. 1983; De Smedt and Wierenga 1984). Preferential flow is less of an occurrence for arid and semiarid climates or under low water fluxes, particularly where soils are coarse-textured and gravel-dominated, such as those in 100 Areas vadose zone (Figure 2-2). Under natural recharge conditions, precipitation at arid sites is usually too low (in relation to saturated hydraulic conductivity) to invoke preferential flow; much of the water in the dry soils is simply adsorbed onto the grain surfaces as film flow and cannot move along preferred pathways (Figure 2-4). In the context of conceptual models for highly sorbed contaminants, flow through macropores and the potential development for preferential flow is discussed in Section 5.

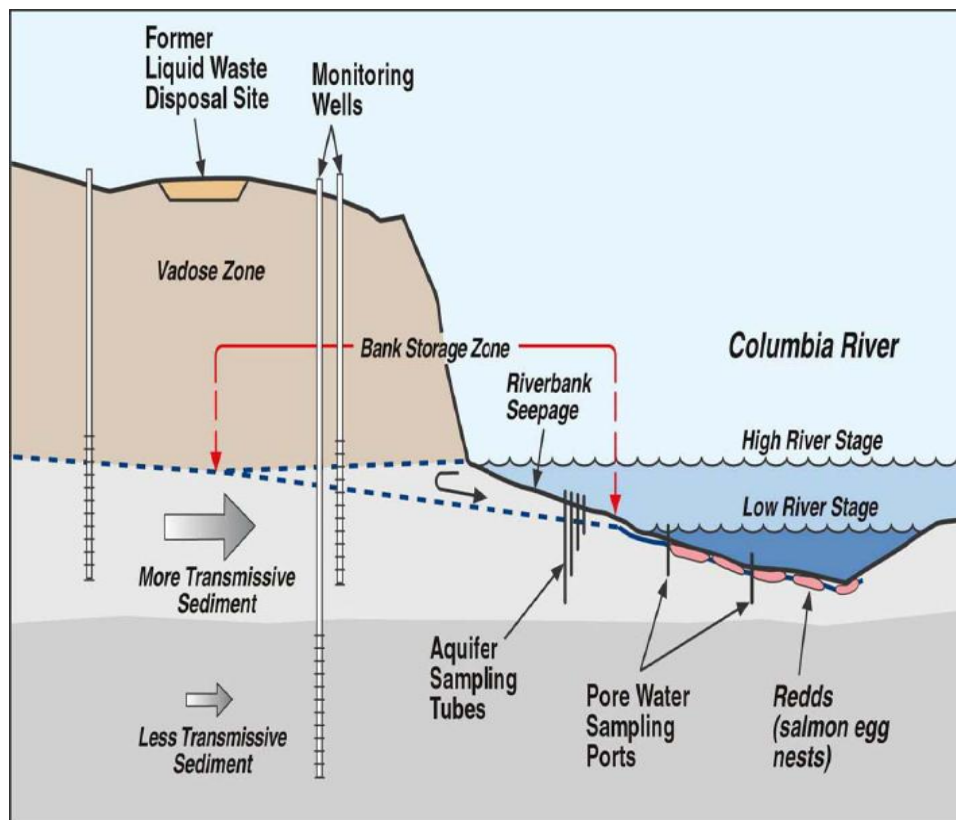
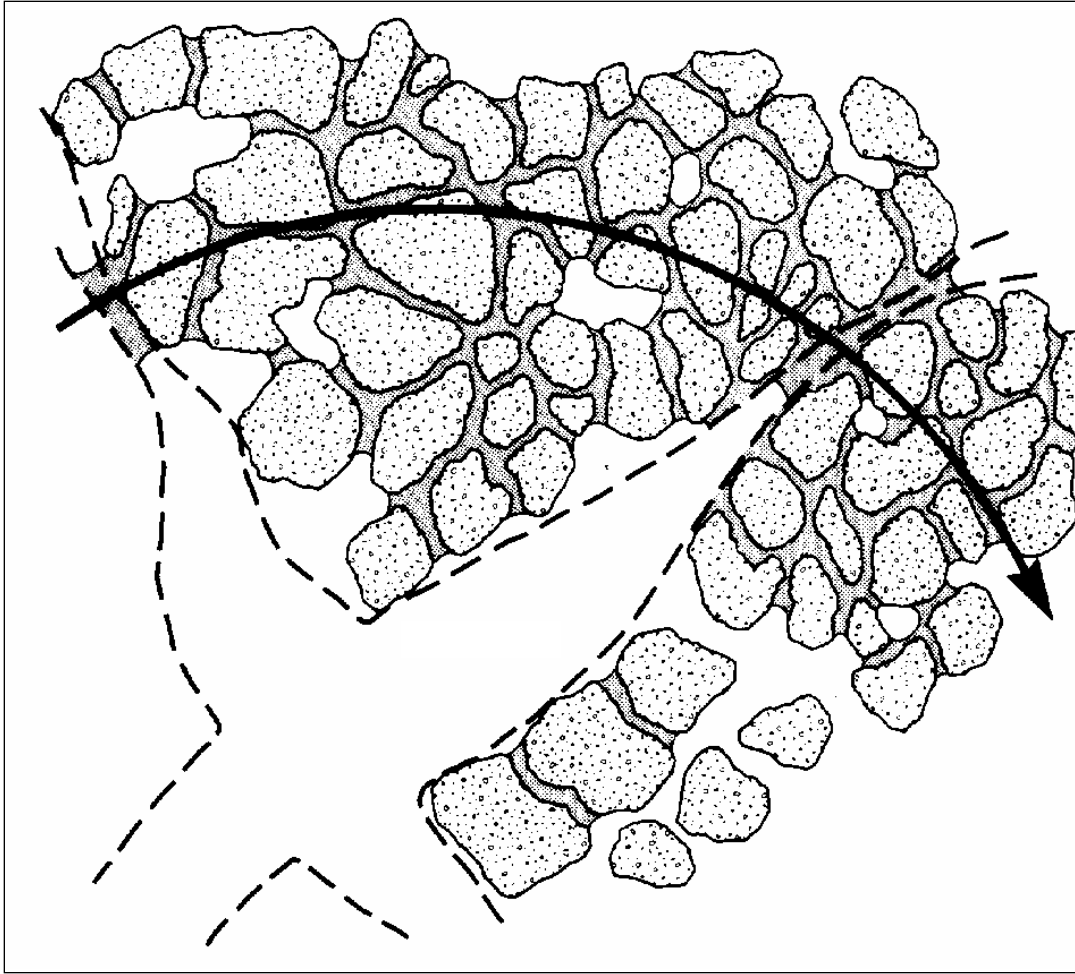


Figure 2-3. Schematic Illustrating Columbia River, Aquifer and Vadose Zone Exchange Flow for 100 Areas



Source: Wang and Narasimhan (1985)

Note: The expanded vertical slice illustrates the fact that under unsaturated conditions and low recharge, the bulk flow bypasses the pathway formed by larger pore sizes (i.e., macropores) and essentially follows the pathway formed by the smaller pore size network. The large, open spaces in the figure mimic macropores such as those existing for 100 Areas gravelly media.

Figure 2-4. Schematic Illustrating Unsaturated Flow Conditions for Low Fluxes in Coarse-textured Gravelly Media

3. Composite Vertical Distribution of High K_d Contaminants

As was discussed earlier, the borehole measurements targeted in the RI Work Plan were identified with a bias towards locating contaminants throughout the vadose zone and targeted areas at or near the waste sites. A detailed description of data for individual boreholes is presented in Section 4. Here we present a summary of the composite set of measurements for lead, arsenic and mercury for 100-F, 100-H, 100-D, 100-K, and 100-B/C Areas.

Figure 3-1 through Figure 3-5 illustrate the vertical distributions of vadose zone lead measurements for 100-F, 100-H, 100-D, 100-K, and 100-B/C Areas, respectively. As indicated, the figures show the composite representation based on one-time measurements for the boreholes. Also indicated in these figures are the background concentration levels for lead. The vertical axis represents the fraction of depth calculated as the depth of measurement divided by depth to water table. Note that a line connecting two markers in these figures do not necessarily represent a continuous contamination between the two sampling locations; in many cases, there are non-detects that occur between these locations.

As expected, because of the high K_d and low mobility, the bulk of the measurements are in the shallow vadose zone (Figure 3-1 through Figure 3-5). However, some of the measurements which are above background lie in the deeper portion of the vadose zone (i.e., close to the water table). Three plausible models are conceptualized to explain the deep penetration for the apparently immobile high K_d contaminants; these are discussed in Section 5.

Figure 3-6 through Figure 3-10 illustrate the vertical distributions of vadose zone arsenic measurements for 100-F, 100-H, 100-D, 100-K, and 100-B/C Areas, respectively. The bulk of the arsenic measurements (> 90%) are below background levels. Unlike lead measurements, high arsenic values above background are sporadic within the vadose zone. Again, three plausible models are conceptualized to explain the deep penetration for the apparently immobile high K_d contaminants; these are discussed in Section 5.

Figure 3-11 through Figure 3-15 illustrate the vertical distributions of vadose zone mercury measurements for 100-F, 100-H, 100-D, 100-K, and 100-B/C Areas, respectively. The majority of mercury data show a general trend of decreasing concentration with increasing depth below ground. Unlike lead and arsenic measurements, the bulk of the mercury measurements are in the shallow vadose zone.

Figure 3-16 illustrates the partitioning of arsenic, mercury and lead measurements based on whether the vadose zone sampling resulted in detectable or non-detectable values. Also shown are the fraction of data which are above or below background levels for the three analytes. As indicated, bulk of the measurements is below background for all three analytes.

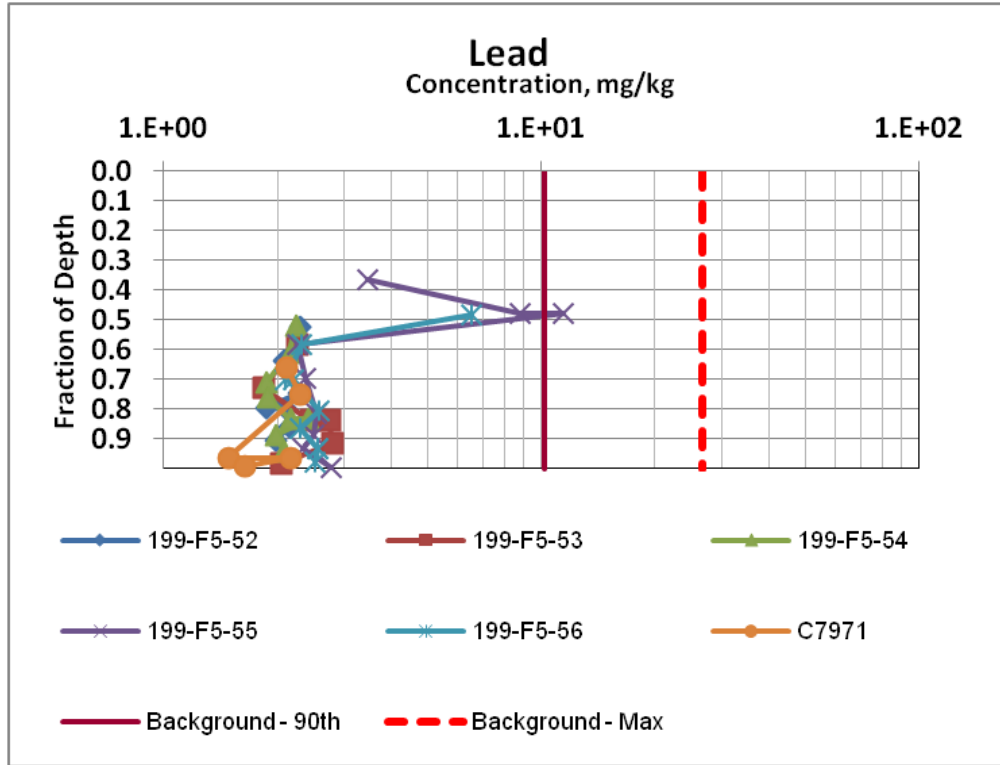


Figure 3-1. 100-F Area Lead Measurements

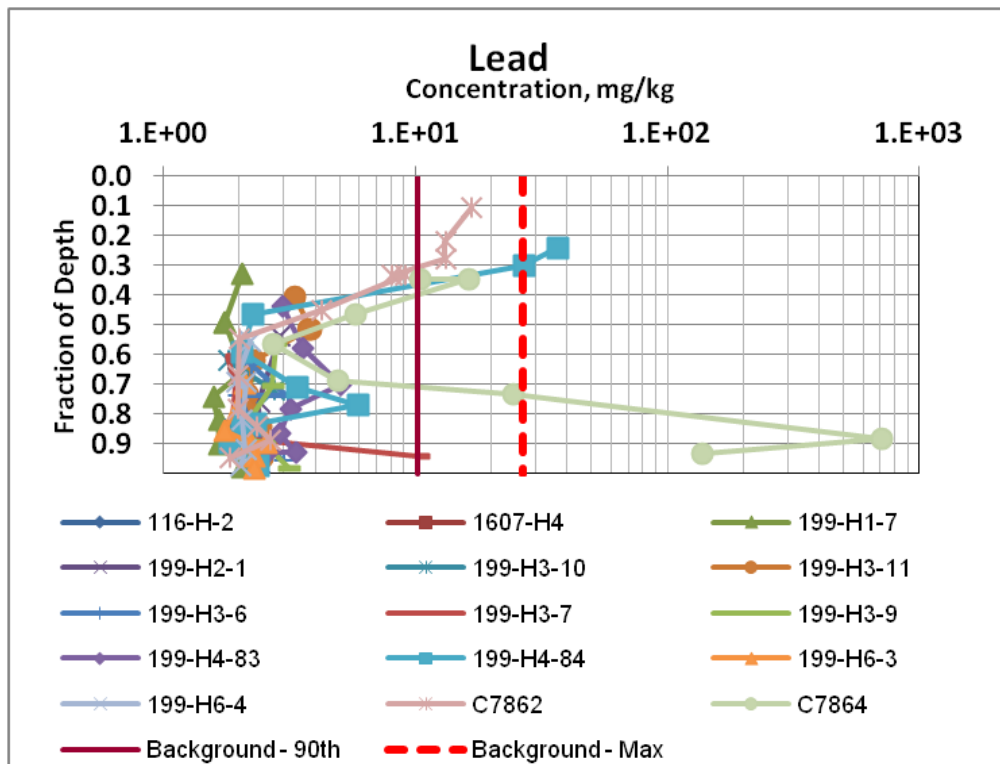


Figure 3-2. 100-H Area Lead Measurements

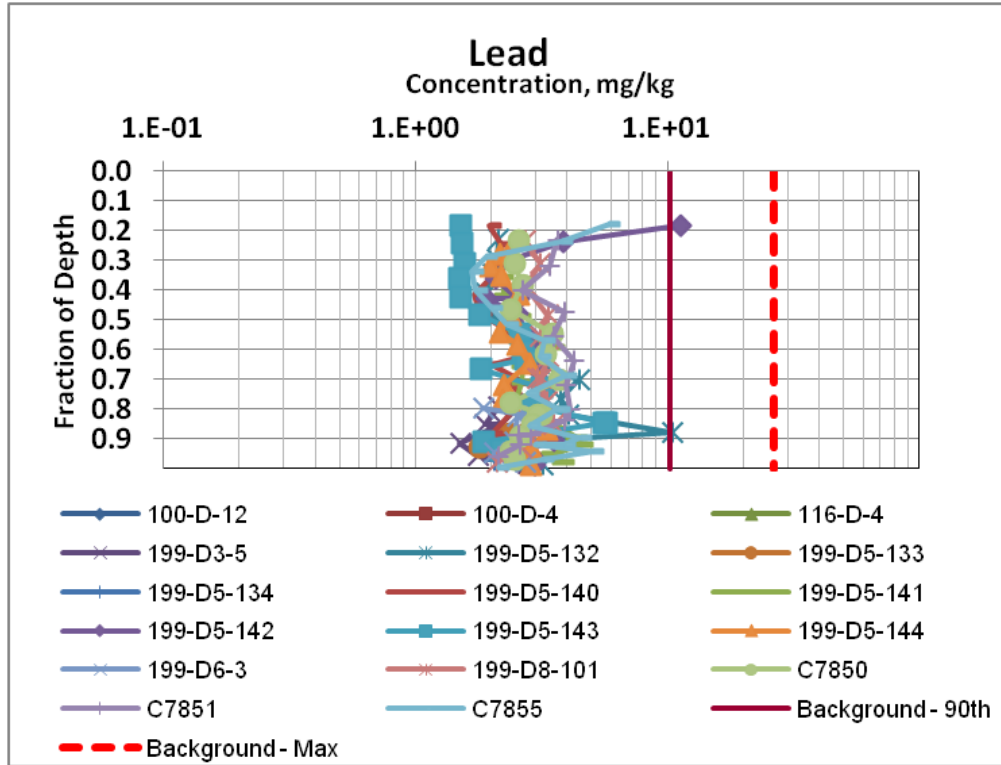


Figure 3-3. 100-D Area Lead Measurements

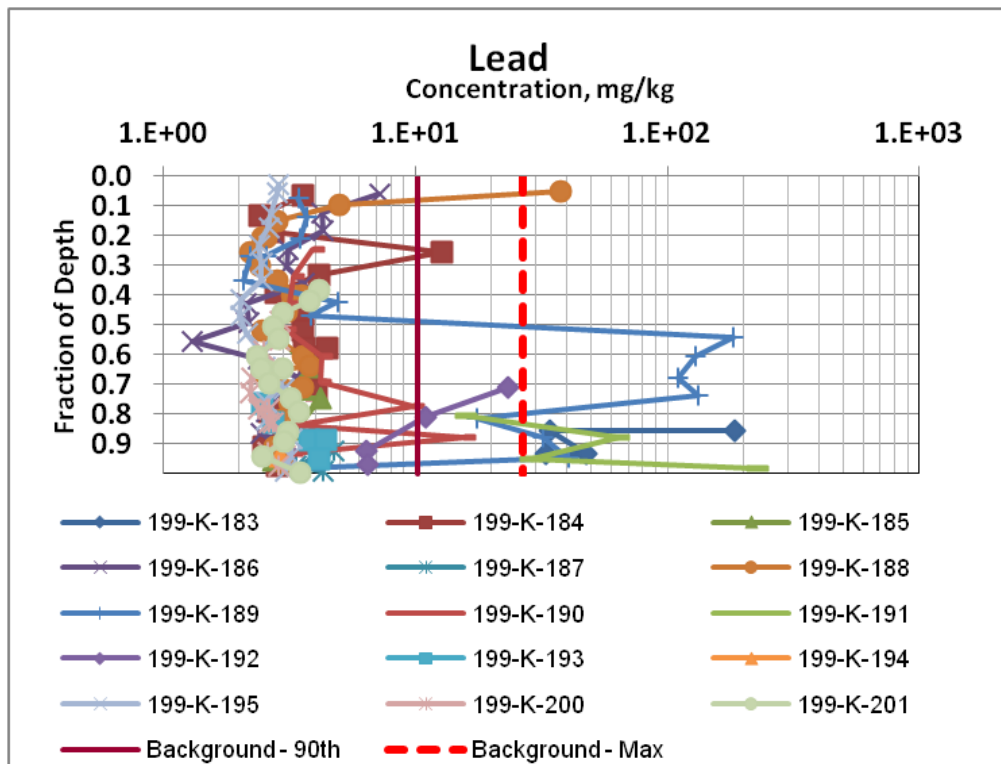


Figure 3-4. 100-K Area Lead Measurements

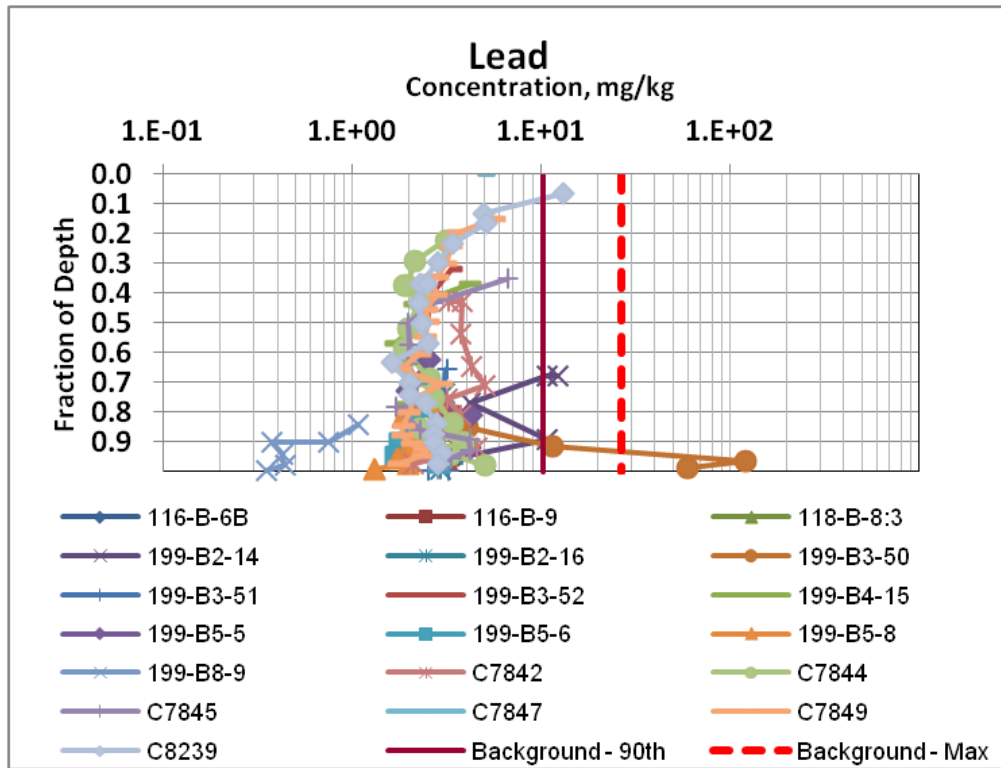


Figure 3-5. 100-B/C Area Lead Measurements

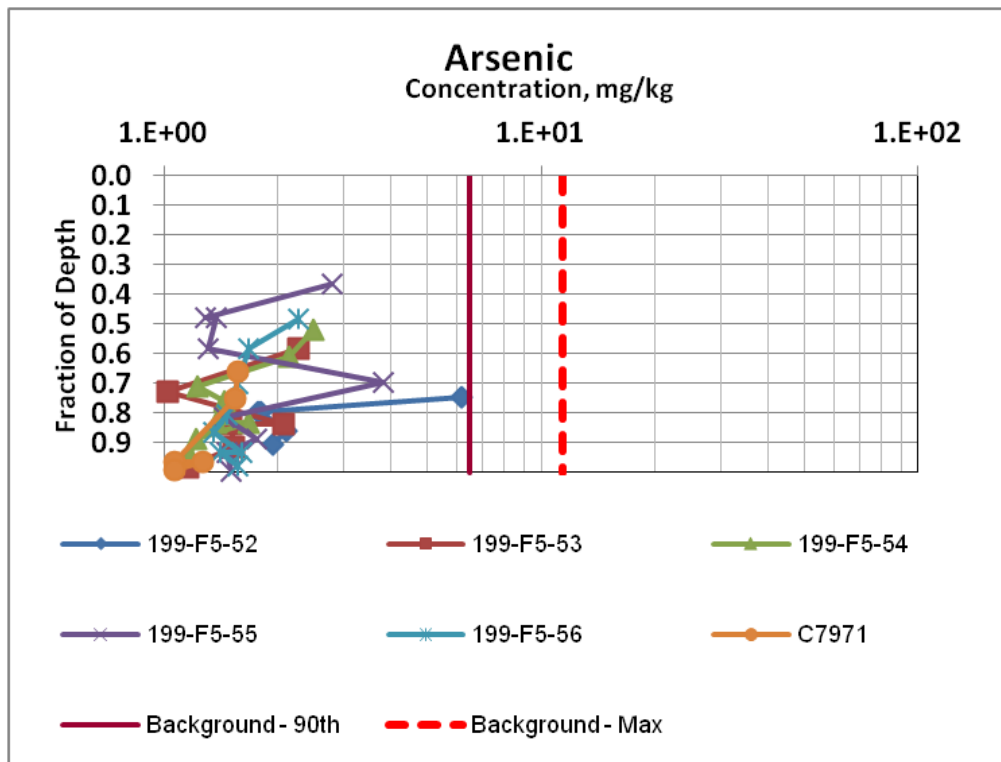


Figure 3-6. 100-F Area Arsenic Measurements

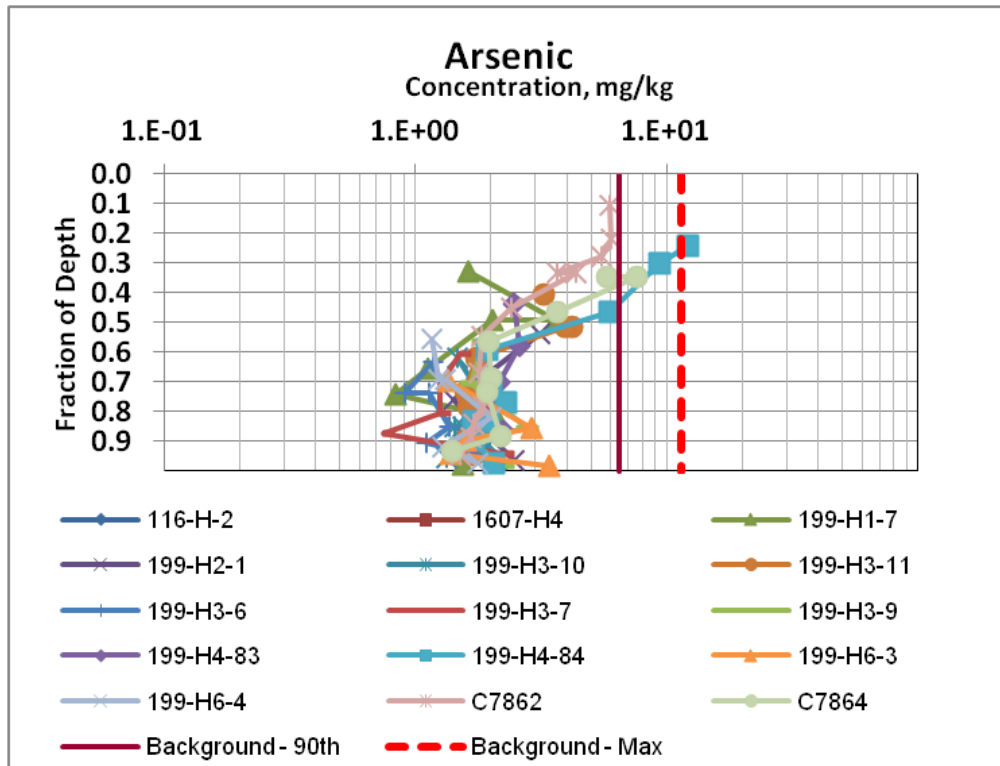


Figure 3-7. 100-H Area Arsenic Measurements

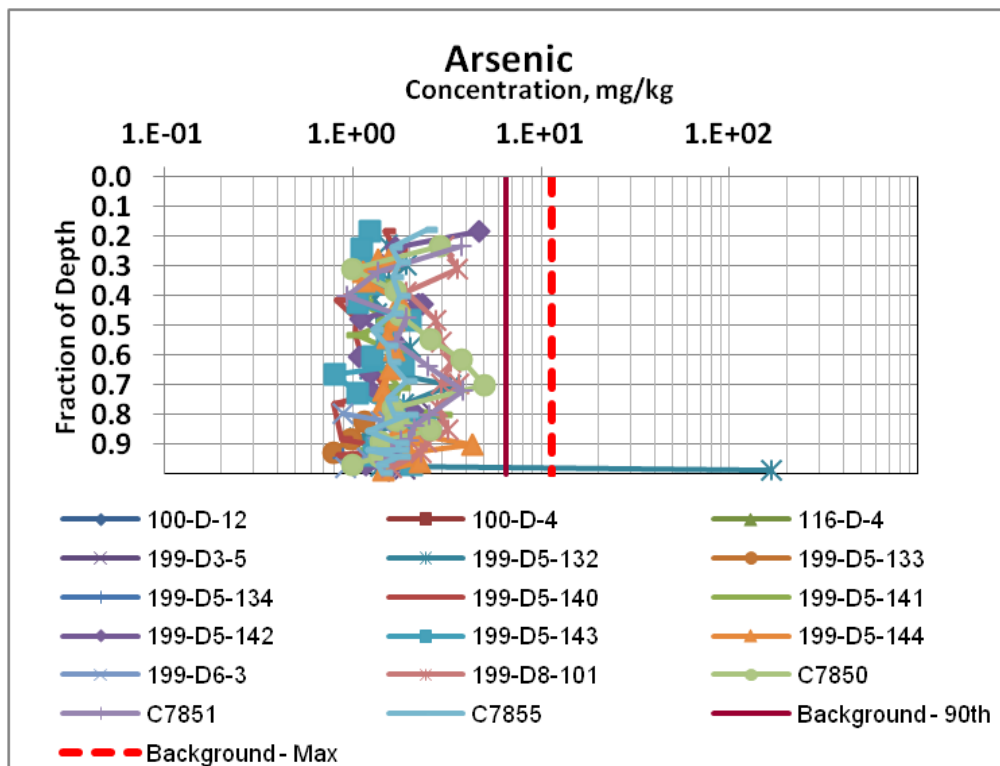


Figure 3-8. 100-D Area Arsenic Measurements

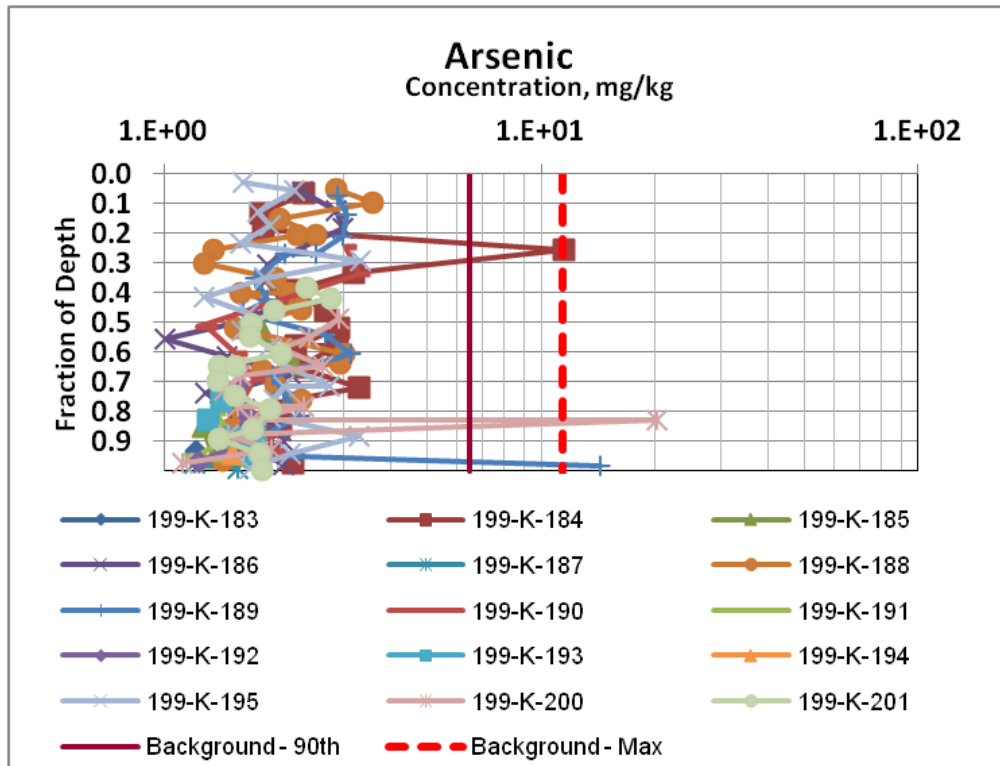


Figure 3-9. 100-K Area Arsenic Measurements

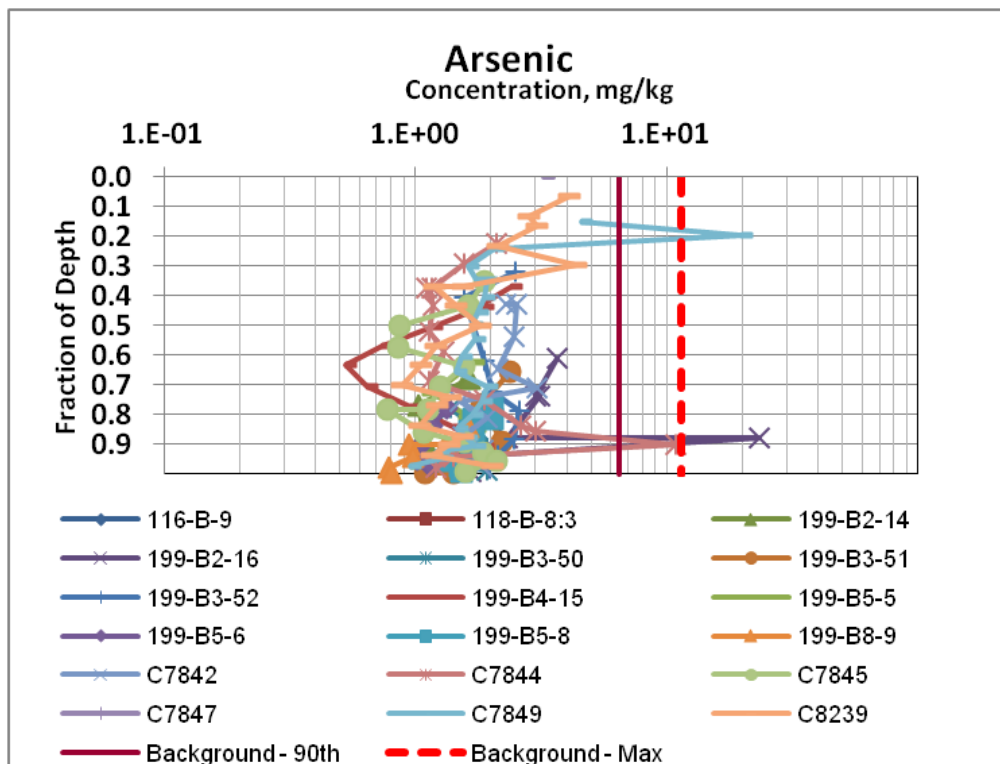


Figure 3-10. 100-B/C Area Arsenic Measurements

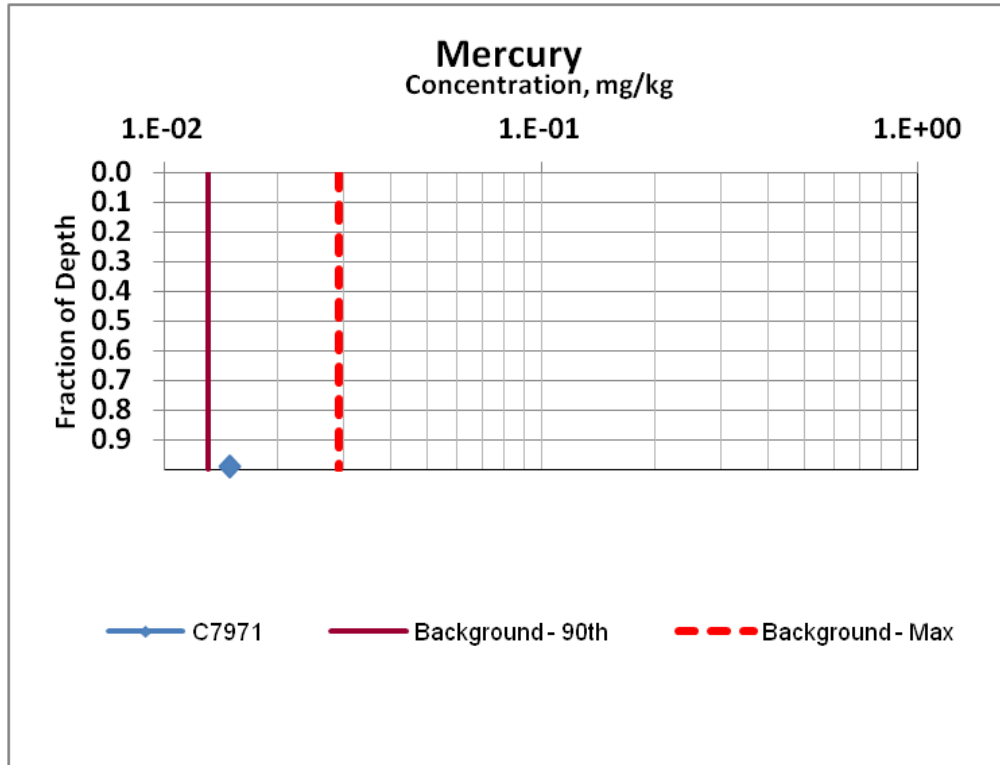


Figure 3-11. 100-F Area Mercury Measurements

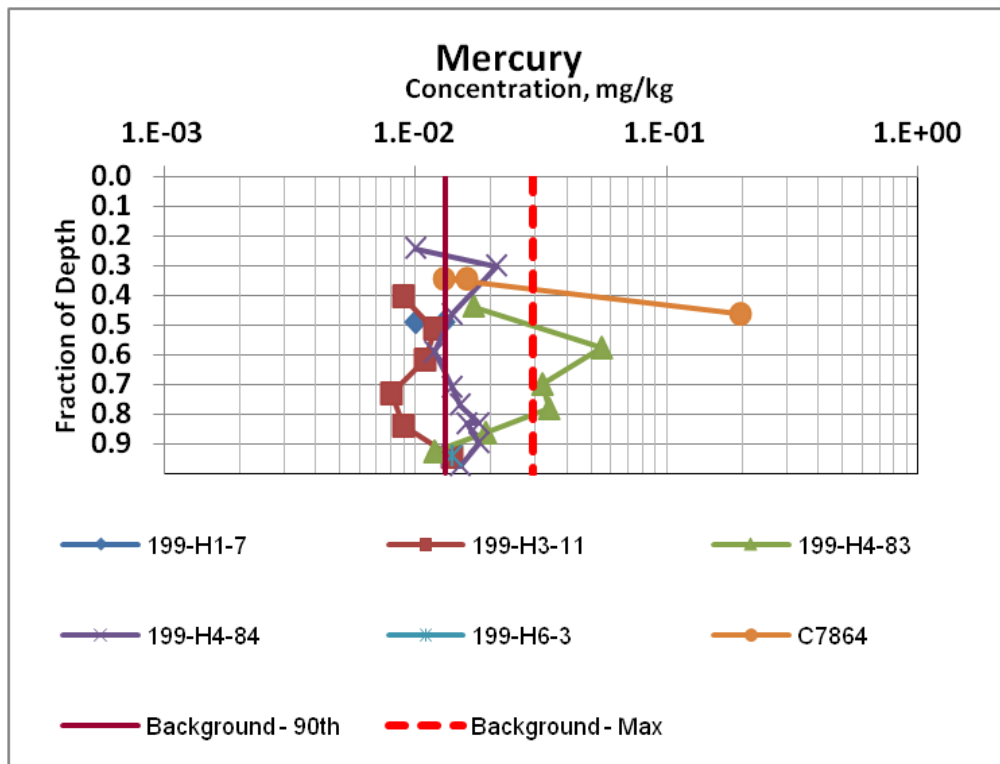


Figure 3-12. 100-H Area Mercury Measurements

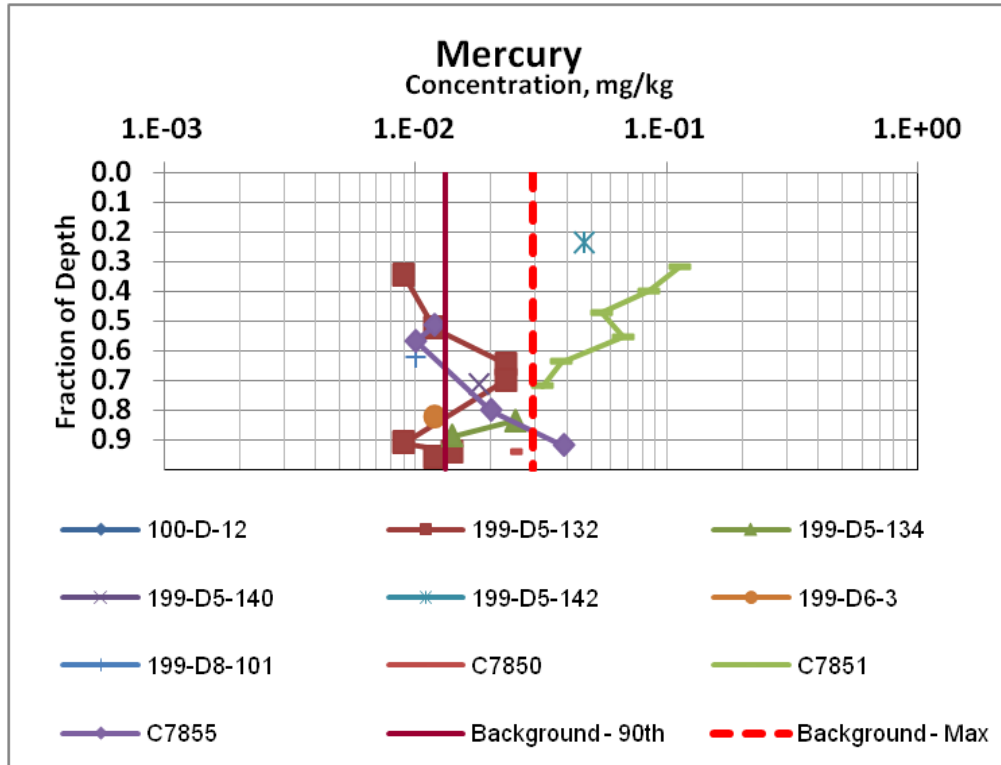


Figure 3-13. 100-D Area Mercury Measurements

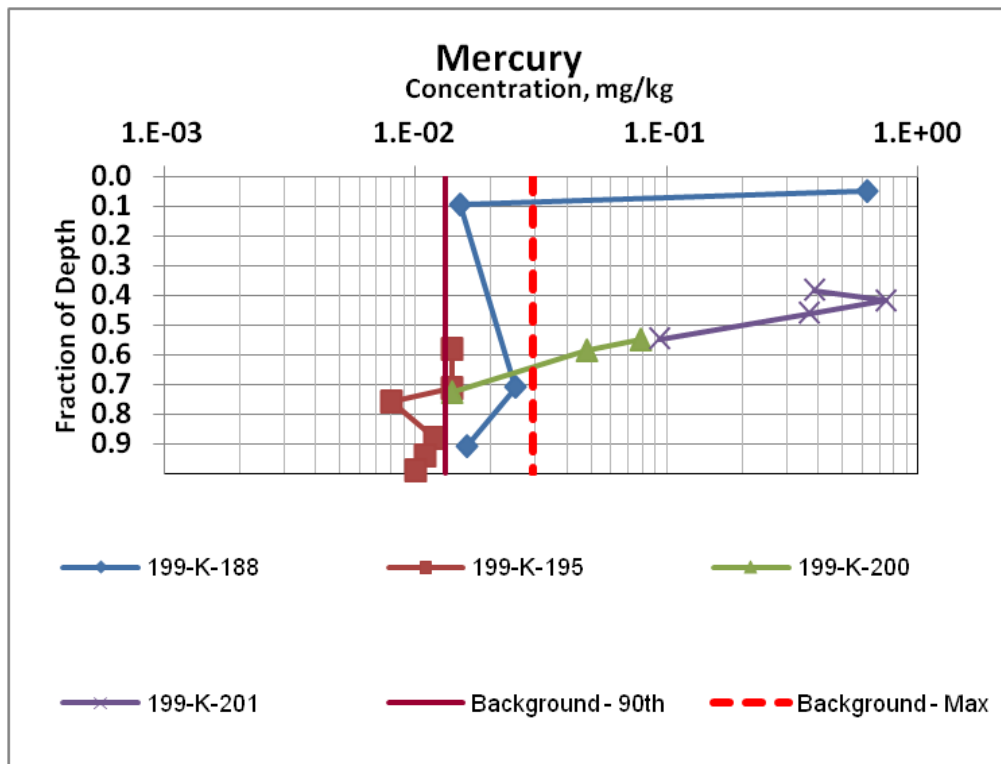


Figure 3-14. 100-K Area Mercury Measurements

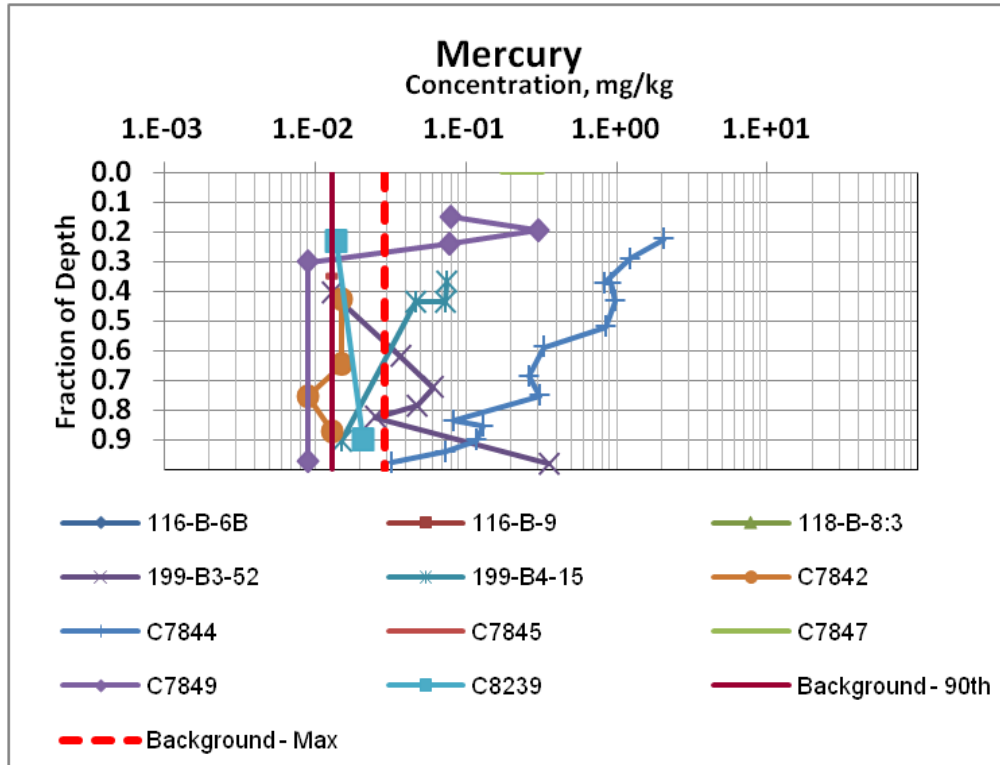


Figure 3-15. 100-B/C Area Mercury Measurements

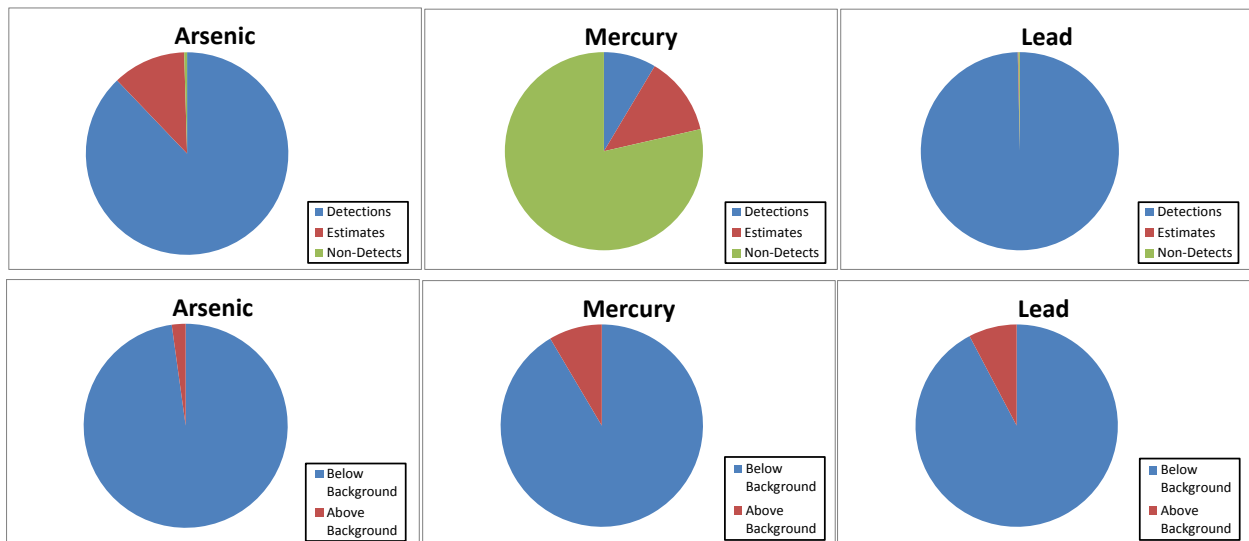


Figure 3-16. Diagrams Illustrating Distribution of Detects/Non-Detects and Below/Above Background Data for Arsenic, Mercury and Lead

4. Remedial Investigation/Feasibility Study Borehole Data

This section provides data for seven RI/FS boreholes including available information on operational history for the nearest waste sites, borehole logs, and measurements. The concentration measurements in these seven boreholes exceed lead, arsenic or mercury background levels:

- C7864
- C7691
- C7683
- C7689
- C7506
- C7843
- C7844

4.1 Borehole C7864 (100-H Area)

Figure 4-1 shows the borehole location. The nearest waste site is 116-H-1 (Figure 4-1) and that site has been remediated and closed out. The waste site disposal trench was oriented in a north-south direction and was divided into three separate lobes. The trench operated from 1952 until 1958, receiving mixed waste effluent from the 116-H-7 Retention Basin during reactor shutdowns caused by fuel element ruptures. The process effluent coolant received by this trench reportedly contained debris from fuel element ruptures. Additionally, the trench received water and sludge removed from the 116-H-7 Retention Basin in April and May 1965, during basin deactivation.

Figure 4-2 illustrates the borehole logging data. The lead, arsenic and mercury measurements for C7864 are shown in Figure 4-3, Figure 4-4, and Figure 4-5, respectively. A review of the pertinent data for C7864 suggests the following:

- Waste site contamination is observed throughout the vadose zone based on chromium and strontium-90 concentration data. [Note that the top 15 ft (4.6 m) has been remediated]
- A change in lithology occurs at about 32 ft (9.8 m) bgs from muddy sandy gravel to sandy gravel (Figure 4-2).
- The water table is located at about 43 ft (13.1 m) bgs (Figure 4-2). The vadose zone is impacted by PRZ smearing.
- The zone of high lead contamination is located just above the current water table (Figure 4-3); this is the largest observed lead contamination among all 100 Areas.
- Batch leaching tests (Table 4-1) for three sampling depths close to the water table [39.5 -41.1 ft (12.0 -12.5 m), 40.6-43.1 ft (12.4 -13.1 m), and 48.3-50.8 ft (14.7-15.5 m)] indicate that lead is practically immobile and non-exchangeable. No significant leachate concentration was detected.
- Nearby boreholes as well as this borehole measurements do not indicate lead contamination in groundwater.

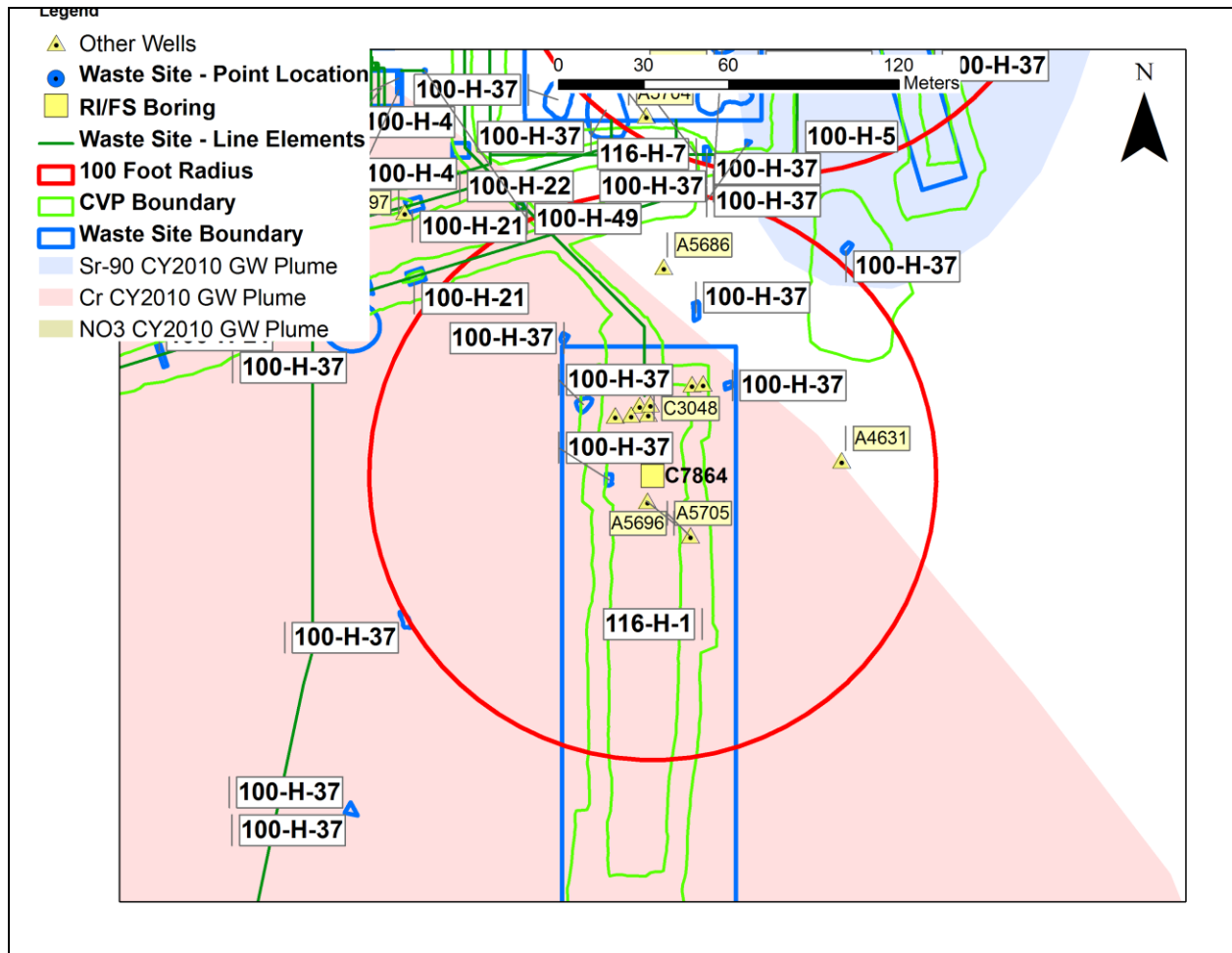
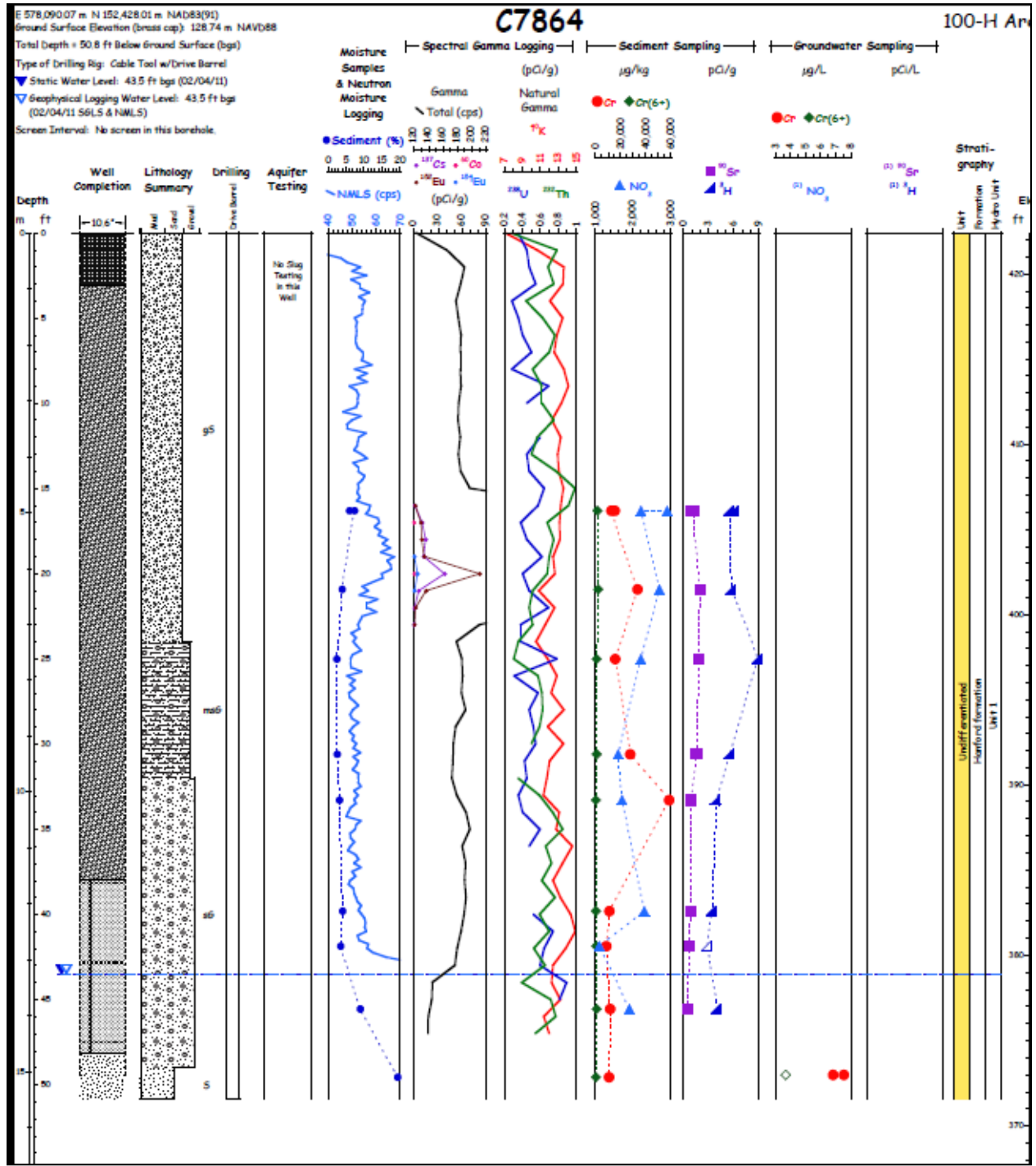


Figure 4-1. Borehole C7864 Location



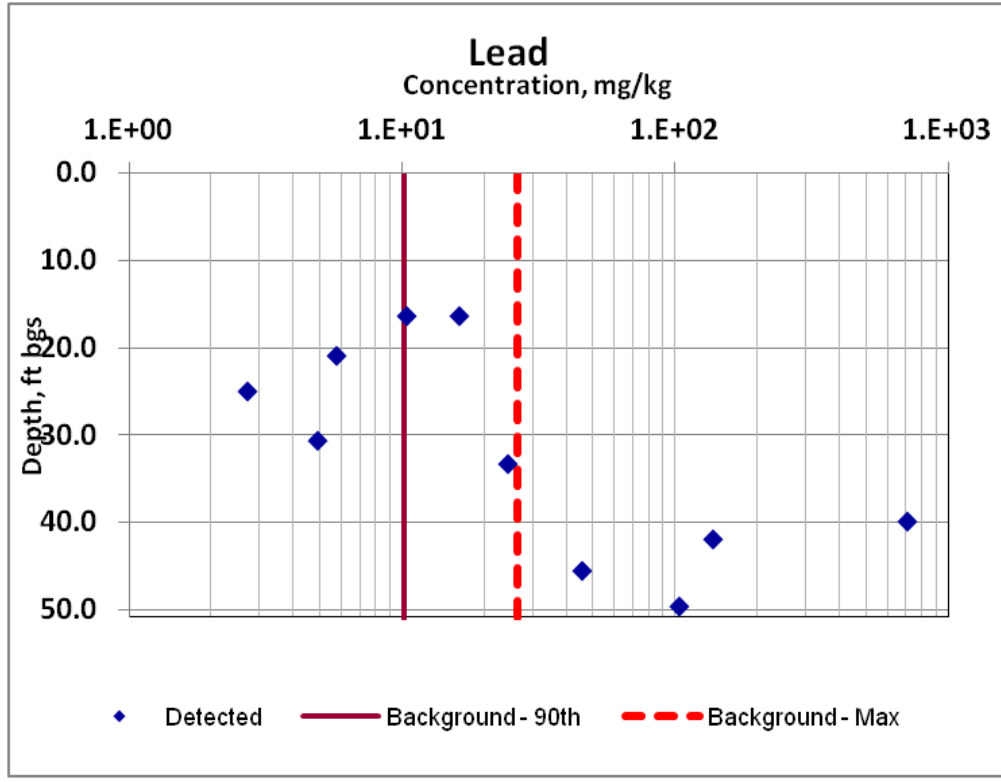


Figure 4-3. Borehole C7864 Lead Measurements

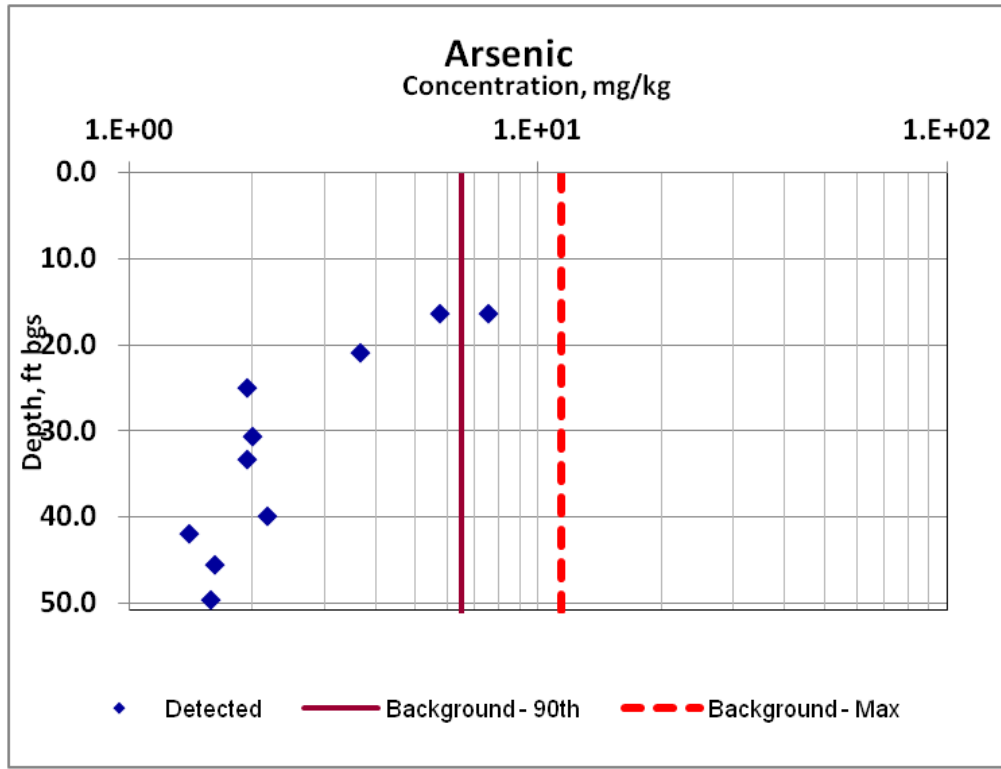


Figure 4-4. Borehole C7864 Arsenic Measurements

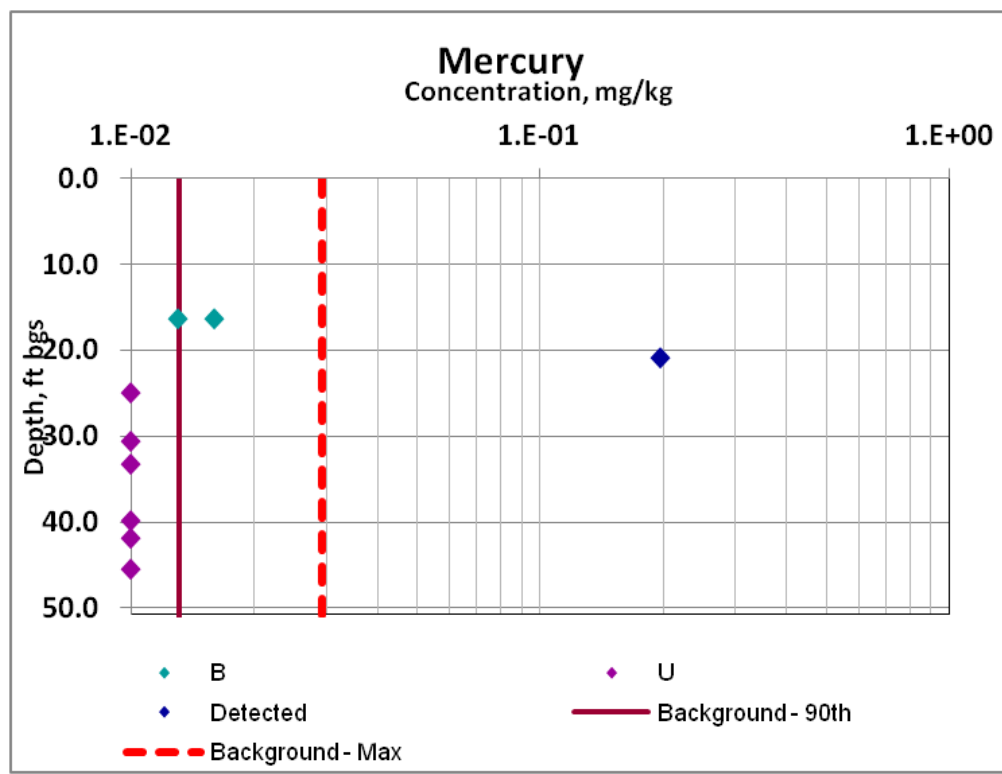


Figure 4-5. Borehole C7864 Mercury Measurements

Table 4-1. Batch Leach Testing Results for Lead for Borehole C7864 Samples

| | | | | | | | | | | | | | | | | | | | | | |
|--|----------------------------|--------------|--------------|--------------|------|-------------------------------|-----------|-----------|-----------|---|--------------------------------------|------|---|-------|---|-------|-------|------|-------|-------|-------|
| Borehole #C7864, Interval I-006 | | | | | | | | | | 39.5 - 41.1 | | | | | | | | | | | |
| Analyte | Soil Concentration (mg/kg) | | | | | Leachate Concentration (mg/L) | | | | | Percent Leached per Soil:Water Ratio | | | | Estimated K _d per Soil:Water Ratio | | | | | | |
| | Replicate #1 | Replicate #2 | Replicate #3 | Replicate #4 | | B28VH4-A1 | B28VH4-A2 | B28VH4-B1 | B28VH4-C1 | | | | | | | | | | | | |
| | B28VH4-1 | B28VH4-2 | B28VH4-3 | B28VH4-4 | Avg | 1:1 | Q | 1:1 | Q | 1:2.5 | Q | 1:5 | Q | 1:1 | 1:1 | 1:2.5 | 1:5 | 1:1 | 1:1 | 1:2.5 | 1:5 |
| Lead | 31.4 | 10.4 | 19.1 | 30.9 | 23.0 | 0.15 | U | 0.15 | U | 0.03 | U | 0.03 | U | <0.65 | <0.65 | <0.33 | <0.65 | >152 | >152 | >763 | >760 |
| Avg = average | | | | | | | | | | K _d = distribution coefficient | | | | | Q = laboratory qualifier | | | | | | |
| B = analyte was detected at less than the contract required detection limit but greater than or equal to the minimum detection limit | | | | | | | | | | N/A = not applicable | | | | | U = undetected | | | | | | |
| Borehole #C7864, Interval I-007 | | | | | | | | | | 40.6 - 43.1 | | | | | | | | | | | |
| Analyte | Soil Concentration (mg/kg) | | | | | Leachate Concentration (mg/L) | | | | | Percent Leached per Soil:Water Ratio | | | | Estimated K _d per Soil:Water Ratio | | | | | | |
| | Replicate #1 | Replicate #2 | Replicate #3 | Replicate #4 | | B28VH7-A1 | B28VH7-B1 | B28VH7-B2 | B28VH7-C1 | | | | | | | | | | | | |
| | B28VH7-1 | B28VH7-2 | B28VH7-3 | B28VH7-4 | Avg | 1:1 | Q | 1:2.5 | Q | 1:2.5 | Q | 1:5 | Q | 1:1 | 1:2.5 | 1:2.5 | 1:5 | 1:1 | 1:2.5 | 1:2.5 | 1:5 |
| Lead | 54.6 | 27.6 | 62.4 | 52.0 | 49.2 | 0.15 | U | 0.03 | U | 0.03 | U | 0.03 | U | <0.31 | <0.15 | <0.15 | <0.31 | >327 | >1640 | >1640 | >1630 |
| Borehole #C7864, Interval I-015 | | | | | | | | | | 48.3 - 50.8 | | | | | | | | | | | |
| Analyte | Soil Concentration (mg/kg) | | | | | Leachate Concentration (mg/L) | | | | | Percent Leached per Soil:Water Ratio | | | | Estimated K _d per Soil:Water Ratio | | | | | | |
| | Replicate #1 | Replicate #2 | Replicate #3 | Replicate #4 | | B28VK7-A1 | B28VK7-A2 | B28VK7-B1 | B28VK7-C1 | | | | | | | | | | | | |
| | B28VK7-1 | B28VK7-2 | B28VK7-3 | B28VK7-4 | Avg | 1:1 | Q | 1:1 | Q | 1:2.5 | Q | 1:5 | Q | 1:1 | 1:1 | 1:2.5 | 1:5 | 1:1 | 1:1 | 1:2.5 | 1:5 |
| Lead | 96.2 | 14.9 | 92.2 | 52.0 | 63.8 | 0.15 | U | 0.15 | U | 0.03 | U | 0.03 | U | <0.24 | <0.24 | <0.12 | <0.24 | >425 | >425 | >2120 | >2120 |

4.2 Borehole C7691 (100-K Area)

Figure 4-6 shows the borehole C7691 (199-K-191) location. The two nearest waste sites are 126-K-1 and 100-K-84 (Figure 4-6).

The 126-K-1 waste site has been reclassified as being rejected. The 100-K Gravel Pit was dug in the 1950s as a borrow pit that was used to obtain fill material needed during construction activities in the 100-K Area. The site was later used in the 1970s through 1989 as an inert waste and demolition waste landfill. The wastes consisted of predominantly concrete, wood, steel pipe, structural steel, conduit, wire, and asphalt generated at 100-K and from closure of the Basalt Waste Isolation Project Near Surface Test Facility at Gable Mountain and the Exploratory Shaft site. The inert/demolition waste was located in a 5 ft (1.5 m) thick layer in the southwest corner of the gravel pit and was covered with approximately 1 ft (0.3 m) of pit-run backfill. Approximately 80% of the gravel pit was unused as a landfill.

The waste site 100-K-84 consists of red stained soil. Five small areas were identified. Some of the material appeared crushed while other pieces looked like "slag." Similar piles of material have been found south of the 200 West Area, 100-B/C Area, and Riverland (McGee Ranch) Area. Crushed iron ore was a component of the concrete used in reactor and other facility construction, as it provided additional shielding. The material is highly magnetic.

Figure 4-7 illustrates the borehole logging data. The lead measurements for C7691 are shown in Figure 4-8 and correlation of lead measurements to other measurements is shown in Figure 4-9. A review of the pertinent data for C7691 suggests the following:

- A change in lithology occurs at about 75 ft (22.9 m) bgs from muddy gravel to muddy sandy gravel (Figure 4-7).
- The water table is located at about 72 ft (22.0 m) bgs (Figure 4-7).
- A zone of higher lead concentration is observed between 60-80 ft (18.3-24.4 m) bgs (Figure 4-8). The higher concentration at about 71 ft (21.6 m) bgs also corresponds with increase in copper and antimony concentration (Figure 4-9).
- There is no evidence of waste site contamination; chromium and strontium-90 are near background concentrations.

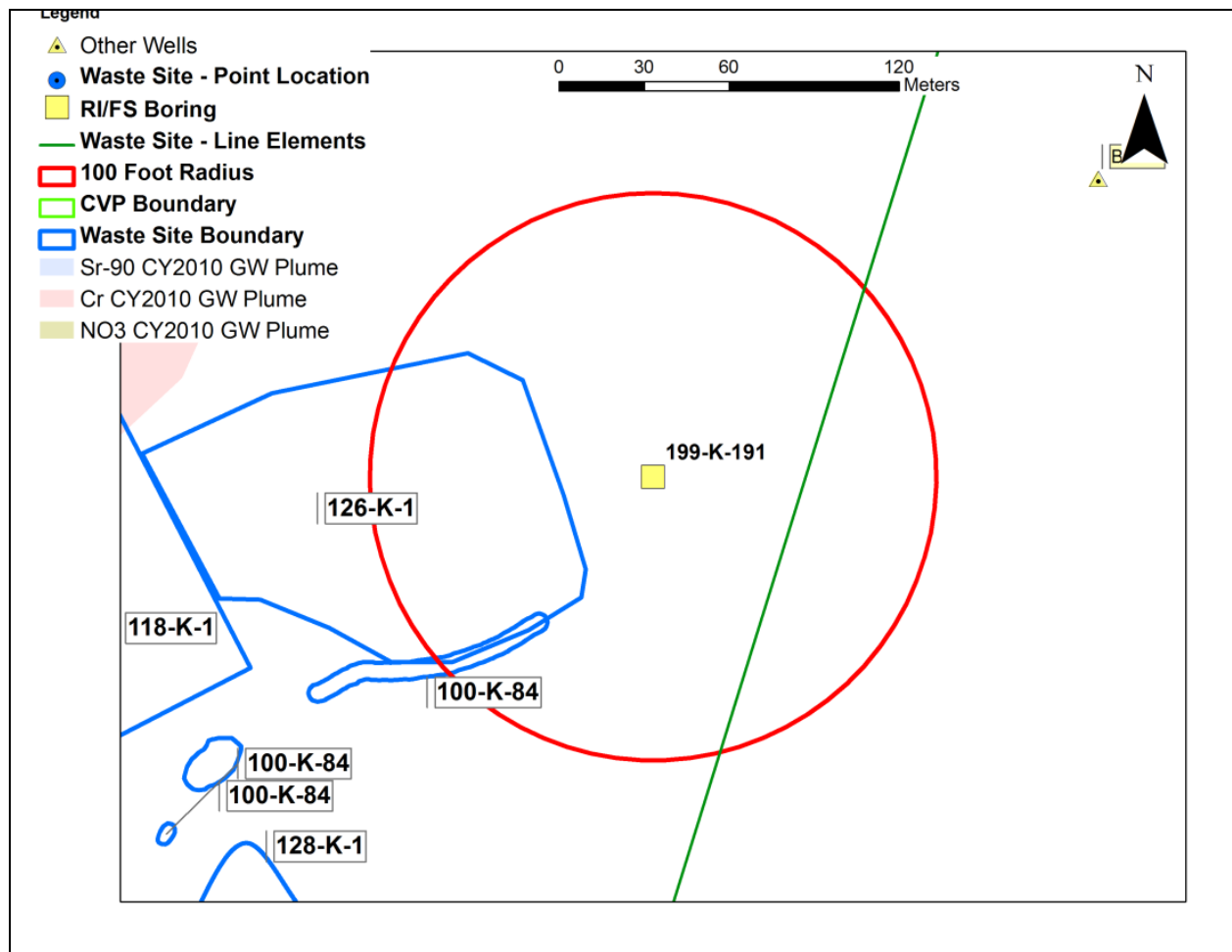


Figure 4-6. Borehole C7691 (199-K-191) Location

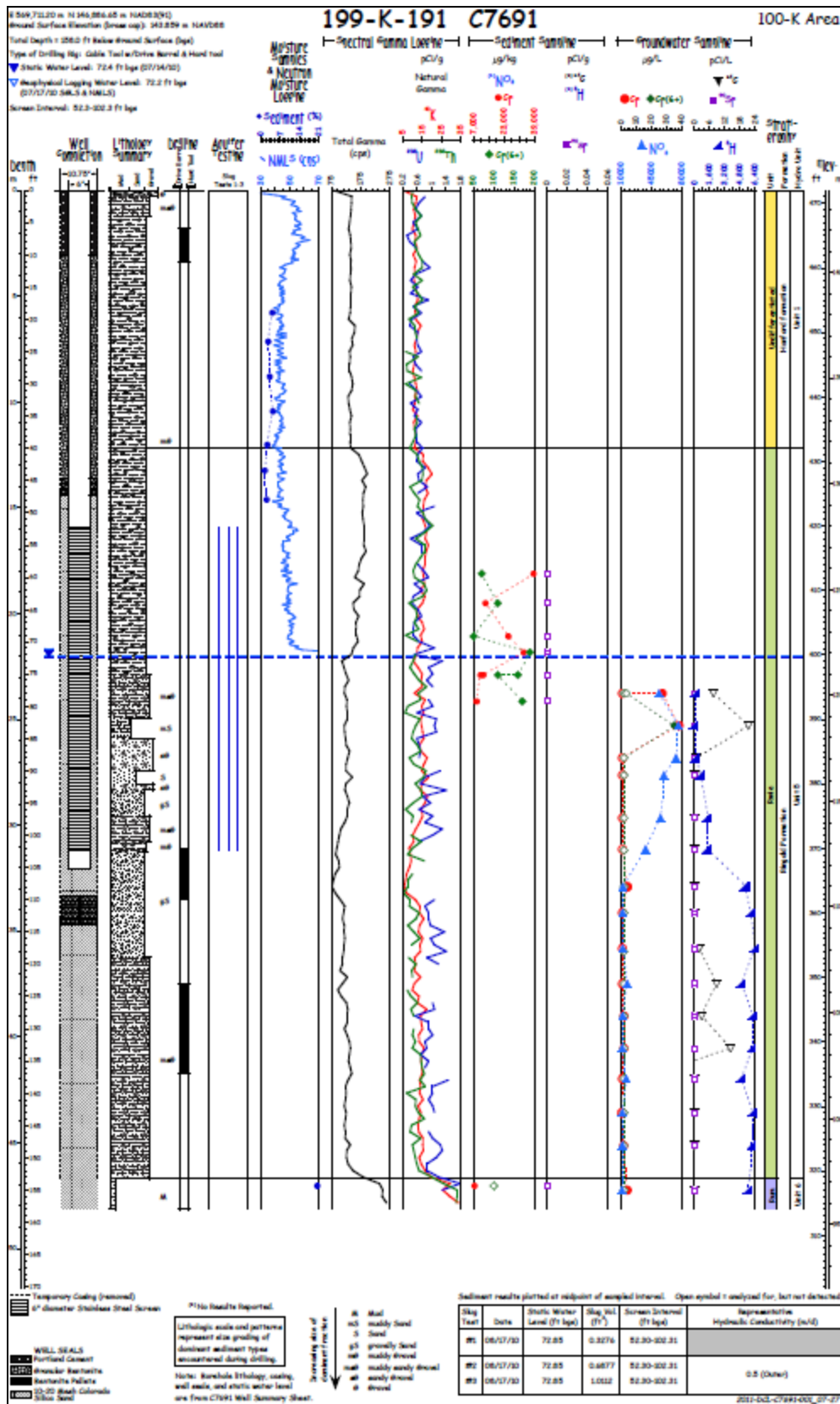


Figure 4-7. Borehole Logging Data for C7691

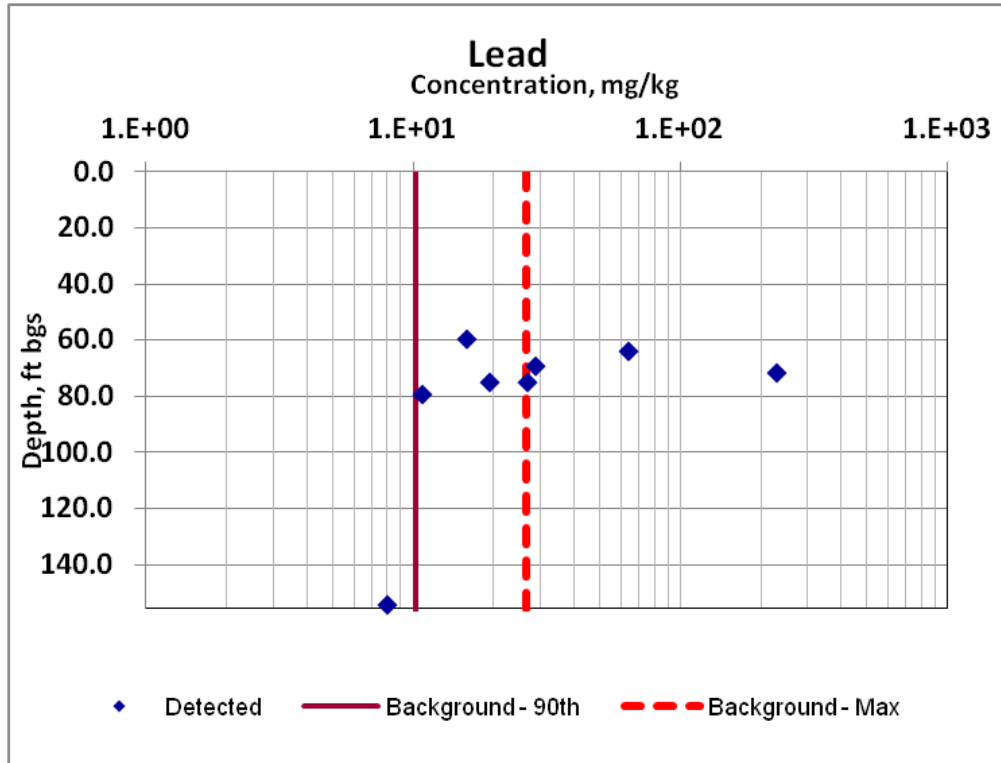


Figure 4-8. Borehole C7691 Lead Measurements

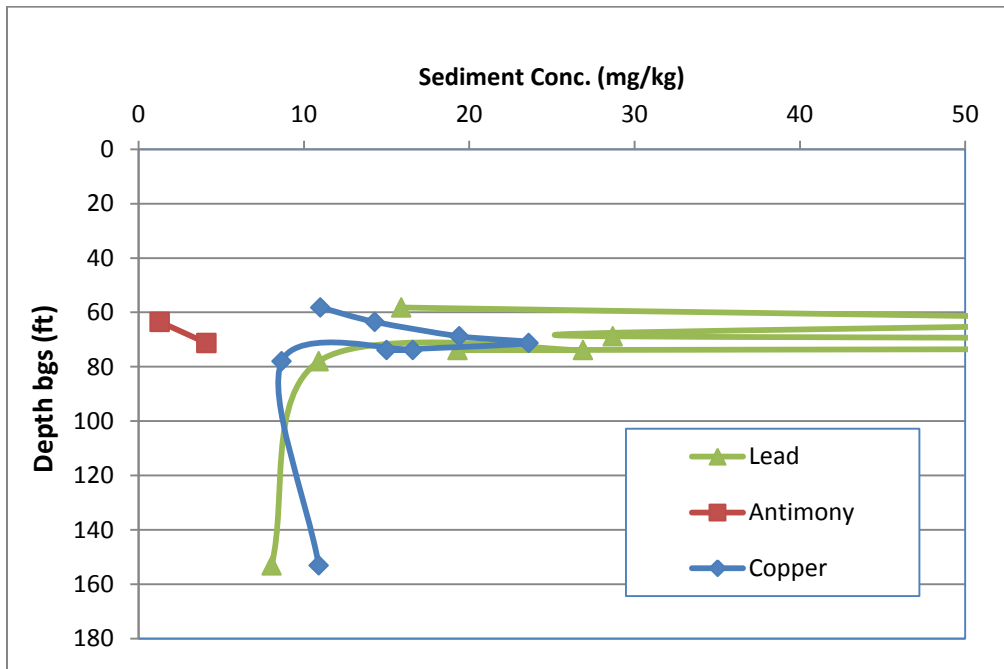


Figure 4-9. Correlation of Borehole C7691 Lead Measurements with Other Measurements

4.3 Borehole C7683 (100-K Area)

Figure 4-10 shows borehole C7683 (199-K-183) location. The closest waste sites are 116-KW-3, and the 107-KW and 107-KW Retention Basins.

The 116-KW-3 waste site (Figure 4-10) has been remediated and closed out. The unit consisted of three open-top, carbon steel tanks with steel bottoms. The tanks were 20 ft (6.1 m) apart. Decommissioning activities included removal of large steel access plates. This site received cooling water effluent from the 105-KW Reactor for radioactive decay and thermal cooling prior to release to the Columbia River. Eighty percent of the total radionuclide inventory is contained within the soil adjacent to the basin.

The 107-KW and 107-KW Retention Basins and their effluent lines developed leaks during their operating life. The leak rate from the butterfly valves (that went to an adjacent trench) could have been as high as 5,000 to 10,000 gal/min (18,930 to 37,850 ℓ/min). Most of the basin leakage was diverted to an open canal and discharged to the Columbia River.

Figure 4-11 illustrates the borehole logging data. The lead, arsenic and mercury measurements for C7683 are shown in Figure 4-12, Figure 4-13, and Figure 4-14, respectively. A review of the pertinent data for C7683 suggests the following:

- The zone of high lead contamination corresponds with gravelly sandy mud lithology at ~53 to 65 ft (~16.2 to 19.8 m) bgs (Figure 4-8).
- A zone of higher lead concentration is observed between 55 and 62 ft (16.8 and 18.9 m) bgs and corresponds with the zone of chromium contamination. Higher antimony concentration is also observed (Figure 4-12).
- The water table is located at about 65 ft (19.8 m) bgs, and is affected by PRZ smearing.
- C7683 arsenic and mercury concentrations are below background (Figure 4-13 and Figure 4-14).
- The possible source of lead could be both natural and anthropogenic.

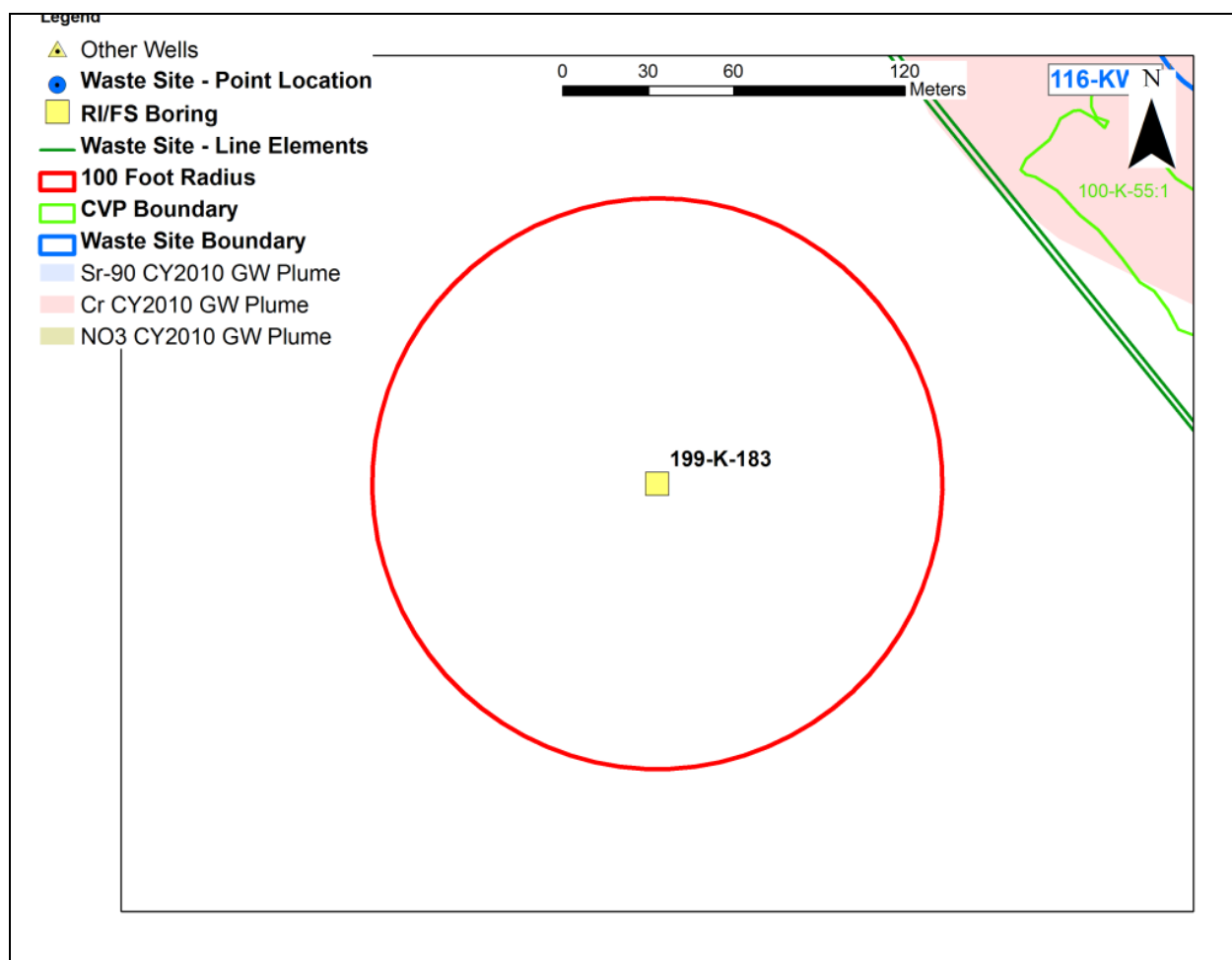


Figure 4-10. Borehole C7683 (199-K-183) Location

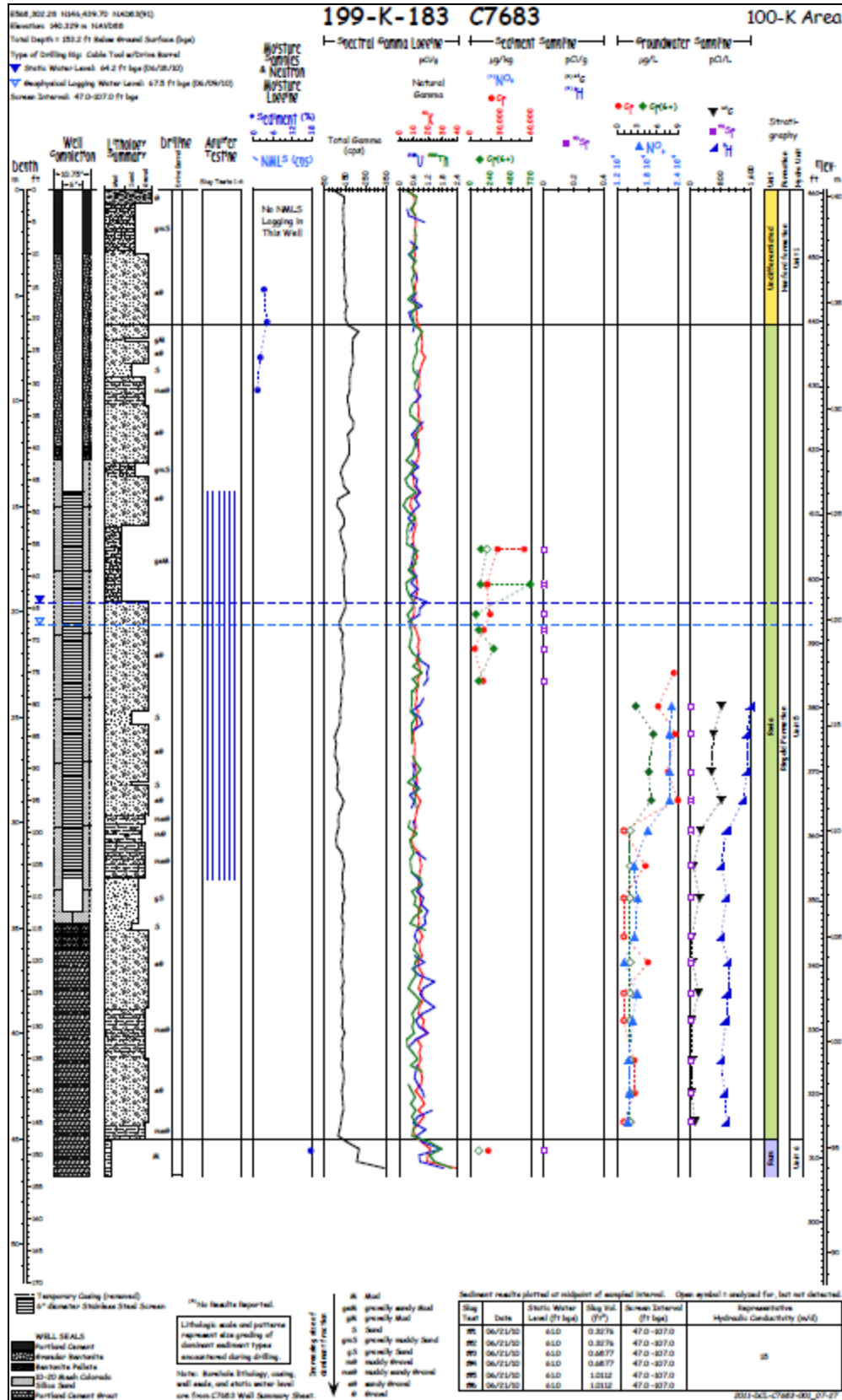


Figure 4-11. Borehole C7683 Logging Data

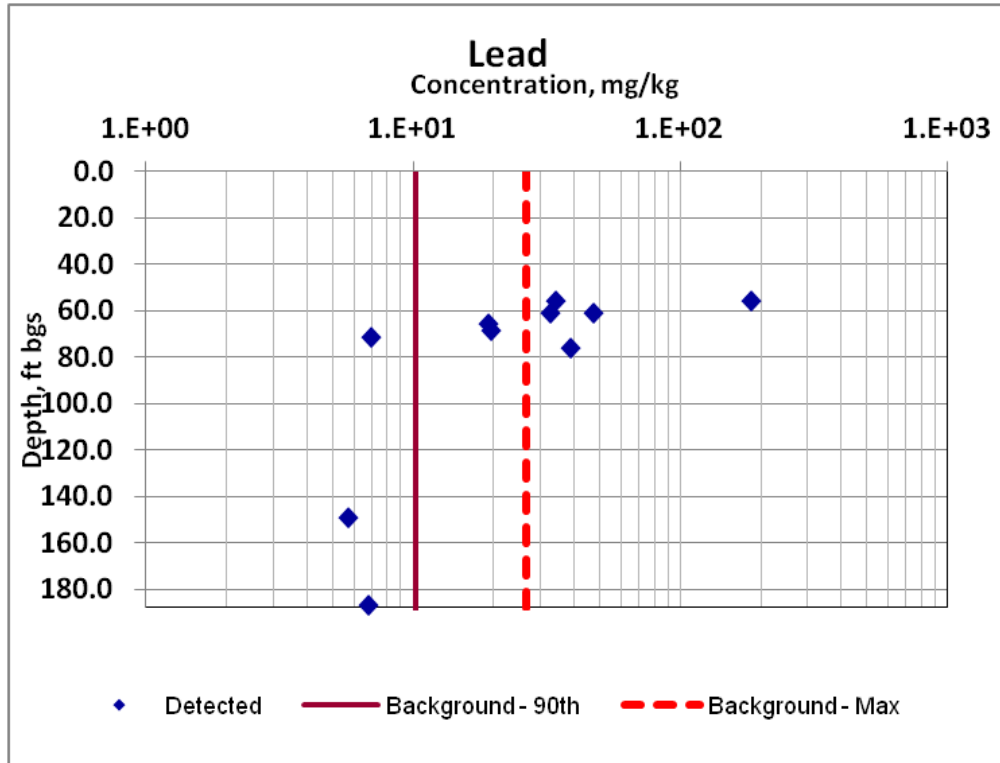


Figure 4-12. Borehole C7683 Lead Measurements

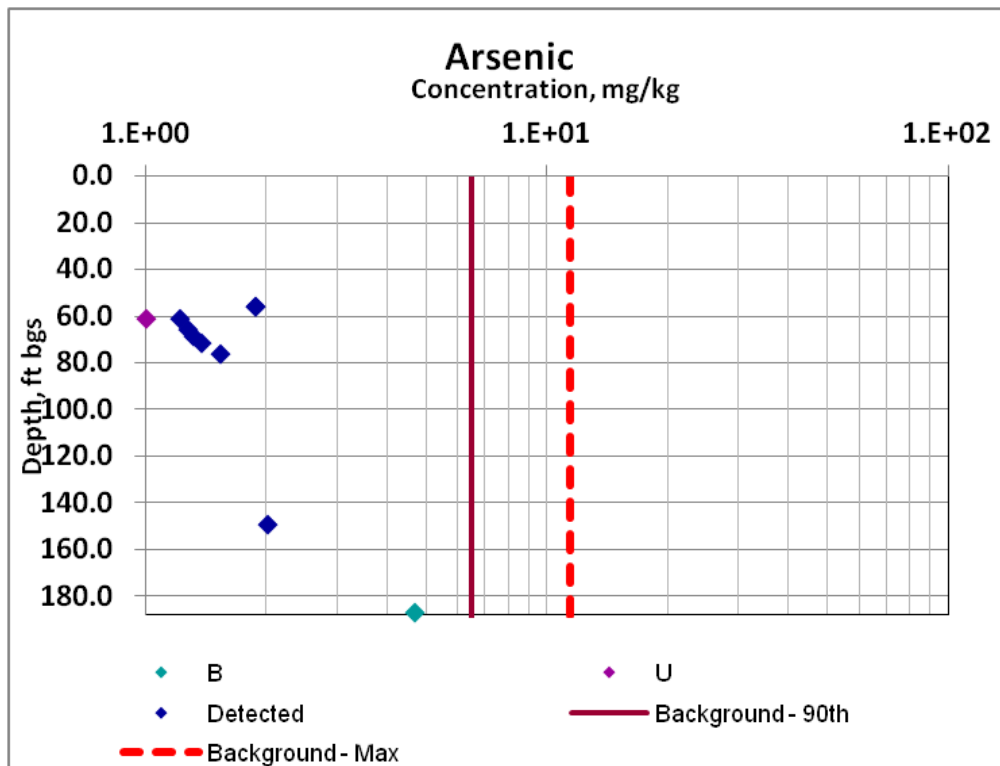


Figure 4-13. Borehole C7683 Arsenic Measurements

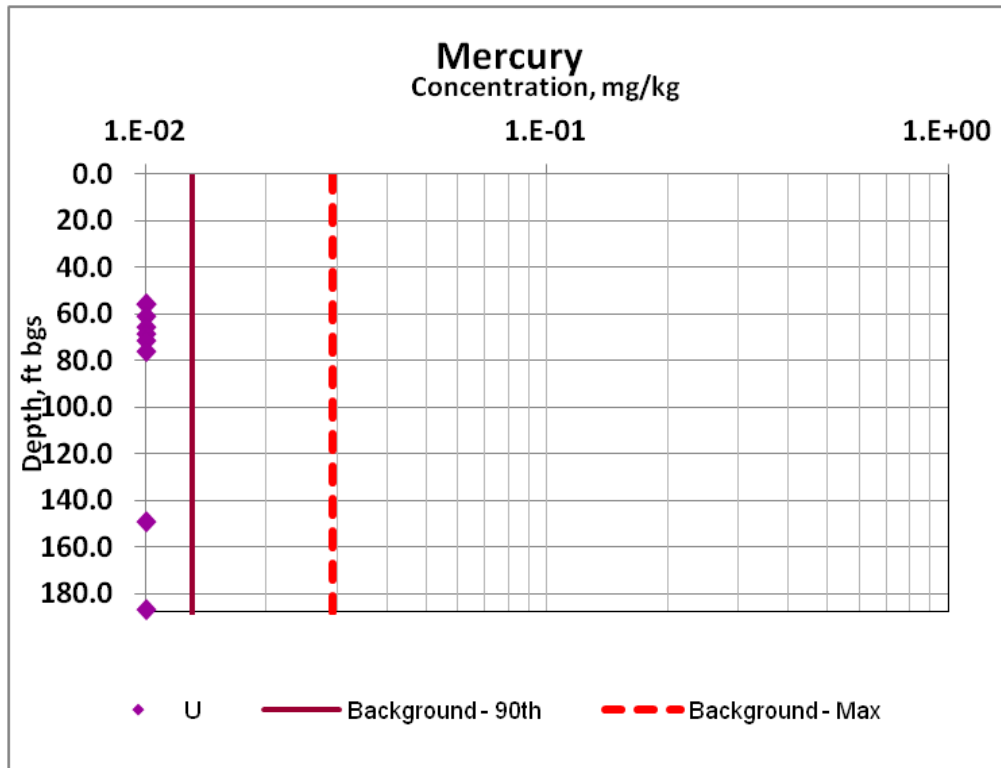


Figure 4-14. Borehole C7683 Mercury Measurements

4.4 Borehole C7689 (100-K Area)

Figure 4-15 shows the borehole C7689 (199-K-189) location. The closest suspect contamination source is the reverse well site 116-KE-3 (Figure 4-15). The site is part of the sub-basin drainage disposal system for the 105-KE Fuel Storage Basin (100-K-42). The site includes the following components: a feed pipe, crib structure, dry well, and test hole. The area of the site is cobble covered and posted with "Underground Radioactive Material" warning signs. A mound of soil, installed in 1977 or 1978, is located nearby and covers some of the ancillary units related to this site.

This site has several types of structures including an injection well and a drain field (crib). The dimensions of the major features are: drain field 20 ft × 20 ft (6.1 m × 6.1 m), injection well 8 in (20.3 cm) in diameter by 78 ft (23.8 m) deep, crib structure 60 ft (18.3 m) × 60 ft (18.3 m) (estimated length) × 41 ft (12.5 m) deep. The fuel storage basin sub-basin drainage disposal system has been modified several times over its operational history to improve the control of contaminated basin water disposal.

Figure 4-16 illustrates the borehole logging data. The lead, arsenic and mercury measurements for C7689 are shown in Figure 4-17, Figure 4-18, and Figure 4-19, respectively. A review of the pertinent data for C7689 suggests the following:

- A zone of higher lead concentration is observed between 40-60 ft (12.2-18.3 m) bgs (Figure 4-17) and corresponds with chromium and strontium-90 contamination.
- C7689 arsenic and mercury data are at or below background (Figure 4-18 and Figure 4-19).
- The water table is located at about 75 ft (22.9 m) bgs.
- The source of lead is most likely anthropogenic and perhaps originates from lead-cadmium rods in the nearby burial ground.
- The nearby reverse well (116-KE-3) that is up to 78 ft (23.8 m) deep could also be a possible source of contamination.
- The zone of contamination corresponds with the contact between the Hanford formation (sandy gravel) and Ringold Formation (muddy sandy gravel) that occurs at about 40 ft (12.2 m) bgs (Figure 4-16). A greater sorption within the fine-grained Ringold Formation probably resulted in retention of contaminants at the contact and below.

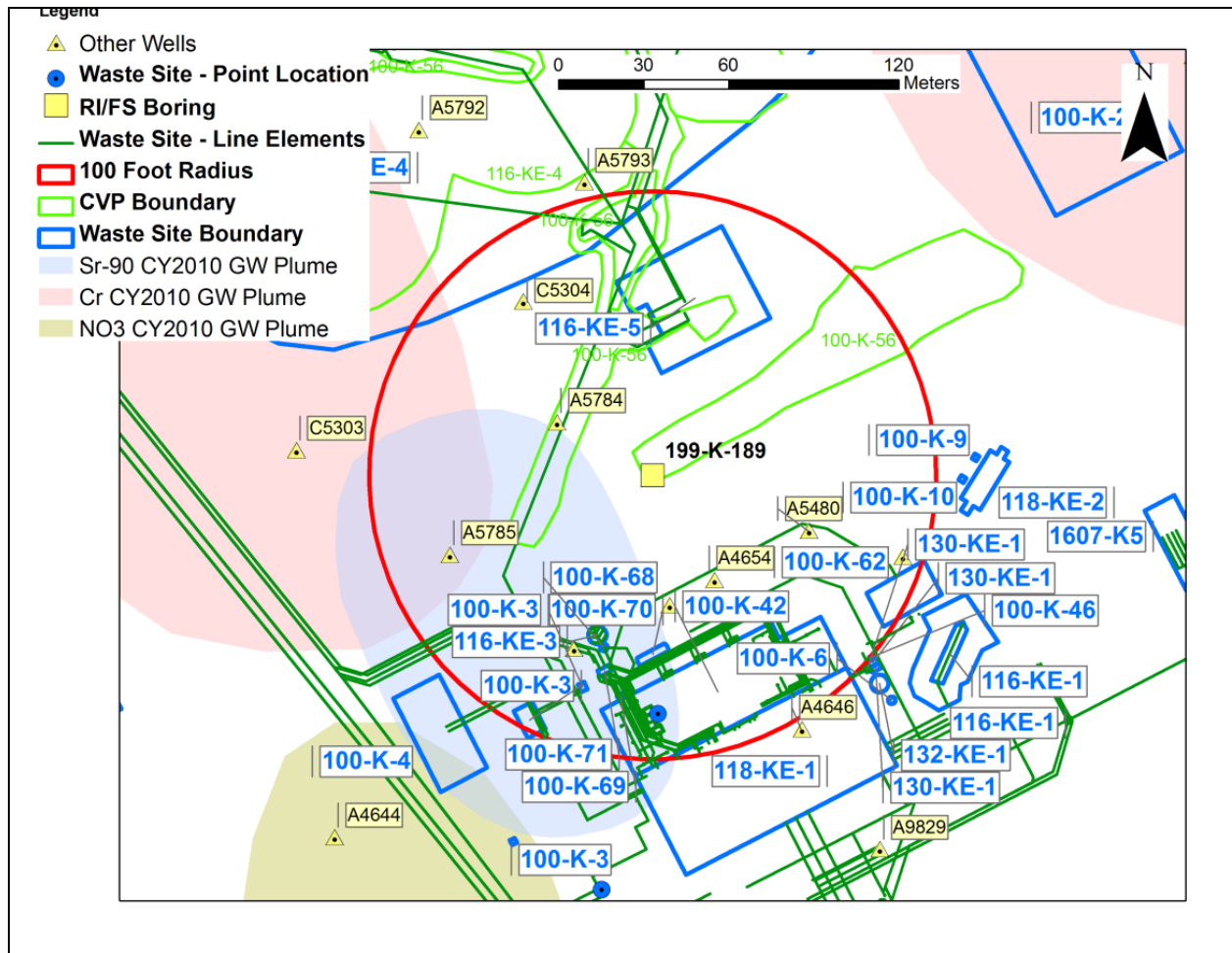


Figure 4-15. Borehole C7689 (199-K-189) Location

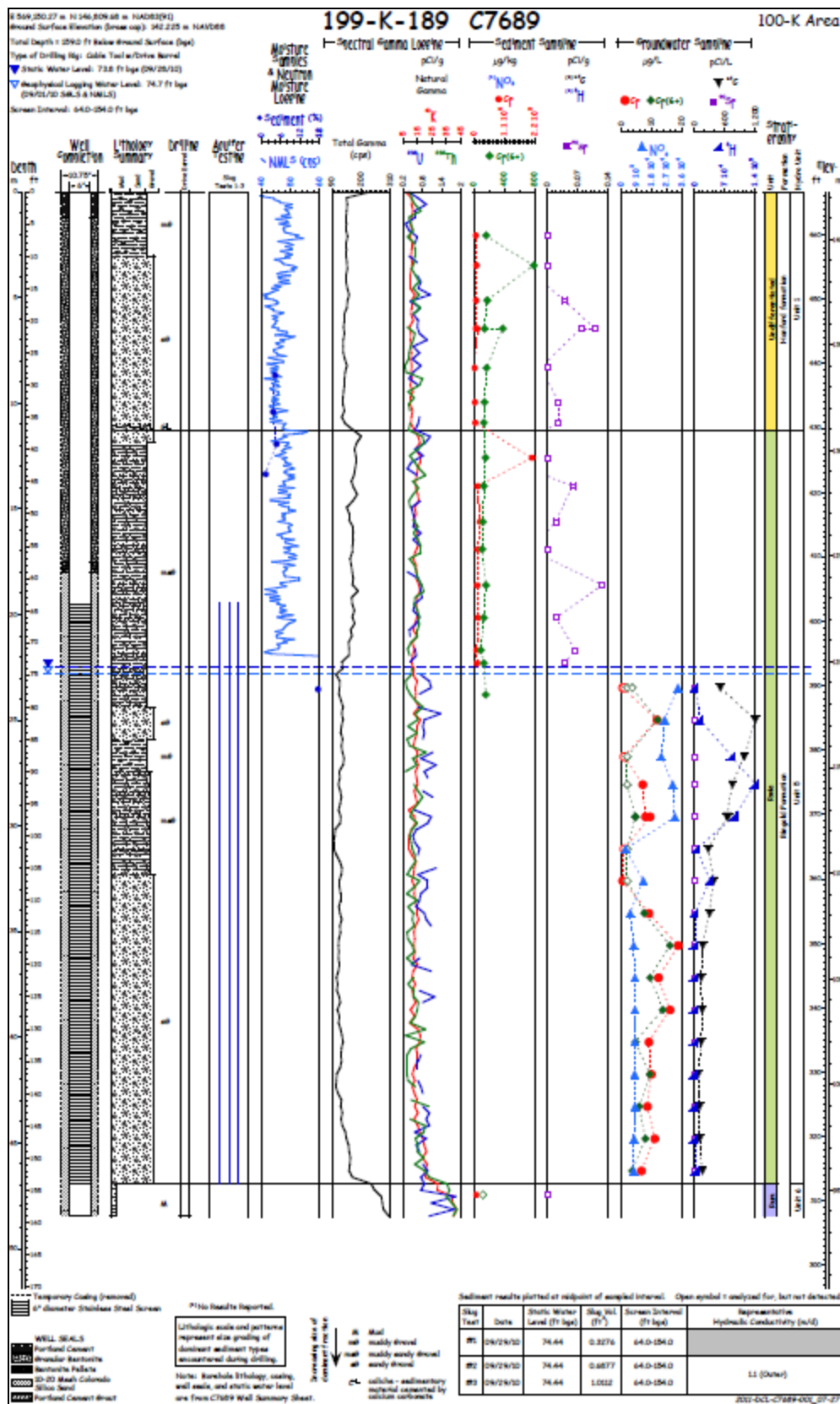


Figure 4-16. Borehole C7689 Logging data

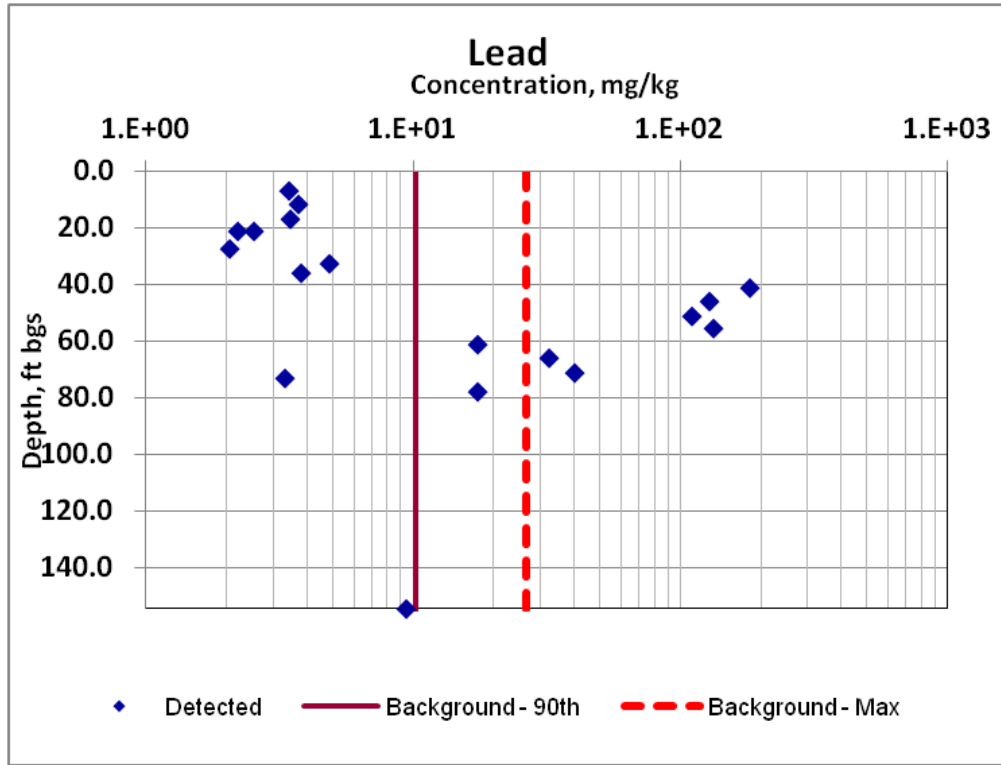


Figure 4-17. Borehole C7689 Lead Measurements

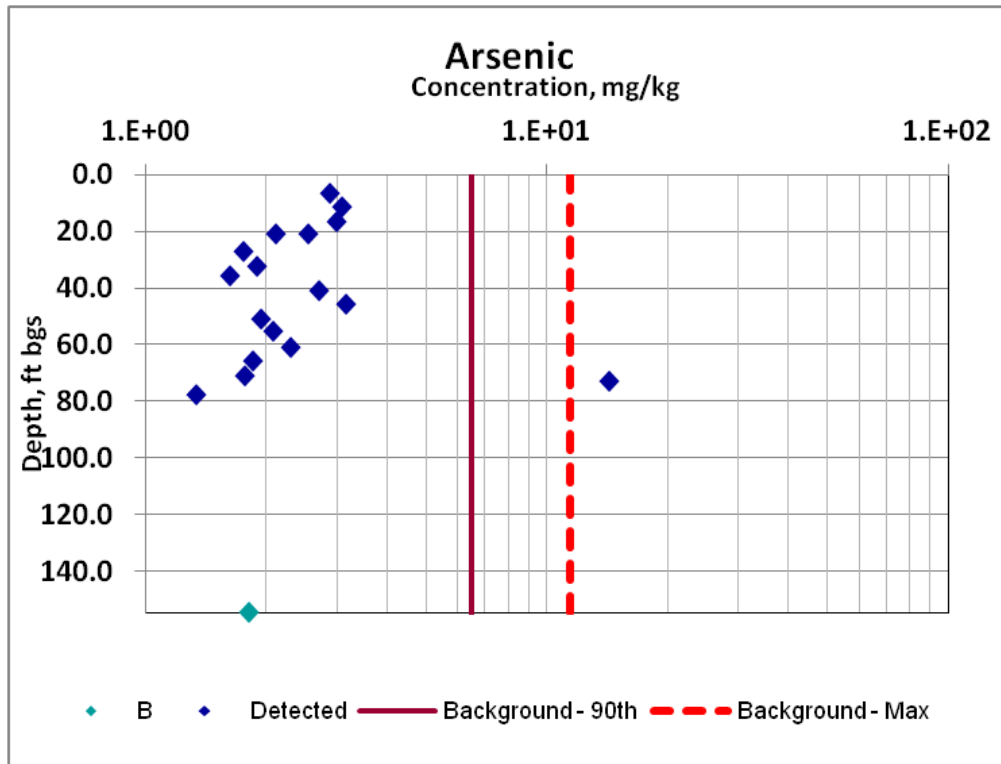


Figure 4-18. Borehole C7689 Arsenic Measurements

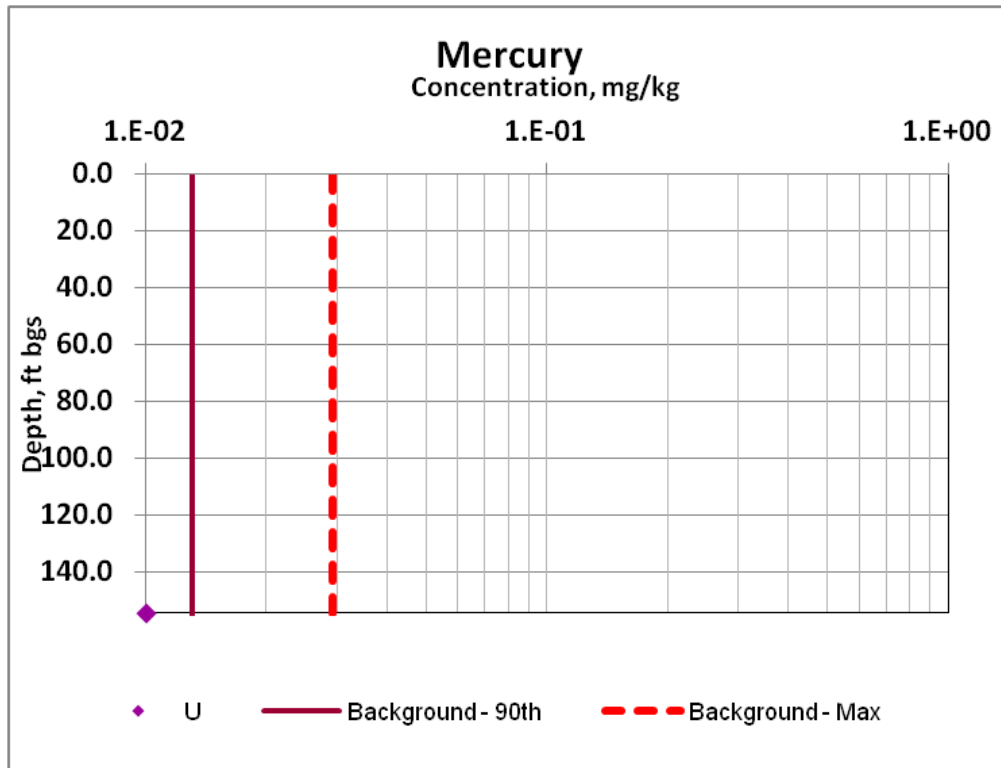


Figure 4-19. Borehole C7689 Mercury Measurements

4.5 Borehole C7506 (100-B/C Area)

Figure 4-20 shows the borehole C7506 (199-B3-50) location. The closest waste site is 100-B-4 (Figure 4-20). The site is a rectangular area: 28 ft (8.5 m) east/west \times 43 ft (13.1 m) north/south, and encircled by large stones neatly stacked 1 ft (0.3 m) high. The surrounding area appears to have been a plowed field that was cleared of large stones. A long line of similar rocks runs parallel to the perimeter road, between the encircled area and the road. The site is distinguishable from the surrounding area only by the arrangement of large stones and soil. The site was possibly associated with farming or some type of military activity. The authors of the 100B Technical Baseline Report believed that the site may be the remains of a building foundation.

Figure 4-21 illustrates the borehole logging data. The lead and arsenic measurements for C7506 are shown in Figure 4-22 and Figure 4-23, respectively. A review of the pertinent data for C7506 suggests the following:

- A zone of higher lead concentration observed between 60-90 ft (18.3-27.4 m) bgs (Figure 4-22).
- Antimony concentration is also higher (above background) at the same depth interval.
- The natural gamma count is high between 60-75 ft (18.3-22.9 m) bgs (Figure 4-21) indicating higher clay content. A change in lithology from muddy gravel to sandy gravel is observed at about 80 ft (24.4 m) bgs.
- The water table is at about 75 ft (22.9 m) bgs.
- There is no evidence of waste site contamination.

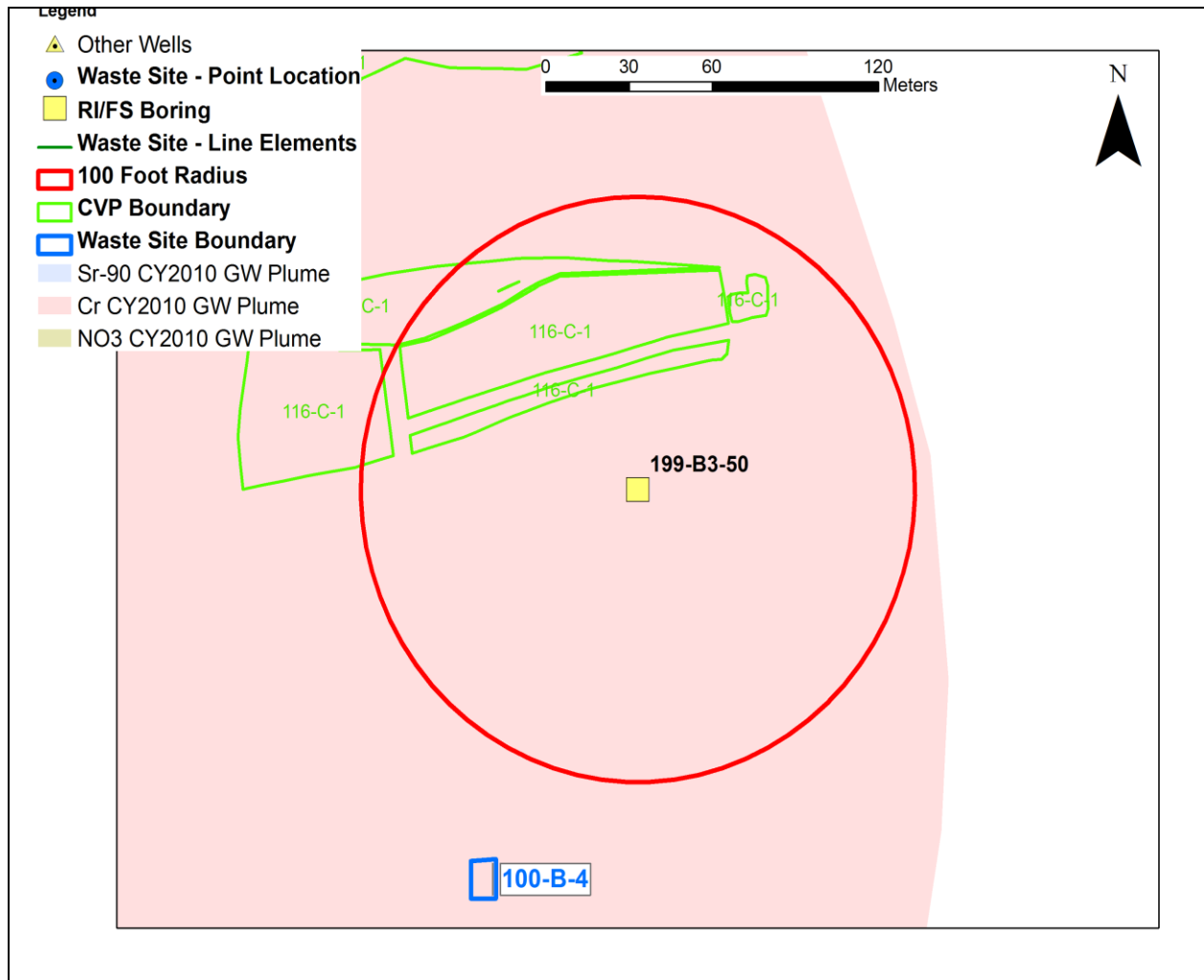


Figure 4-20. Borehole C7506 (199-B3-50) Location

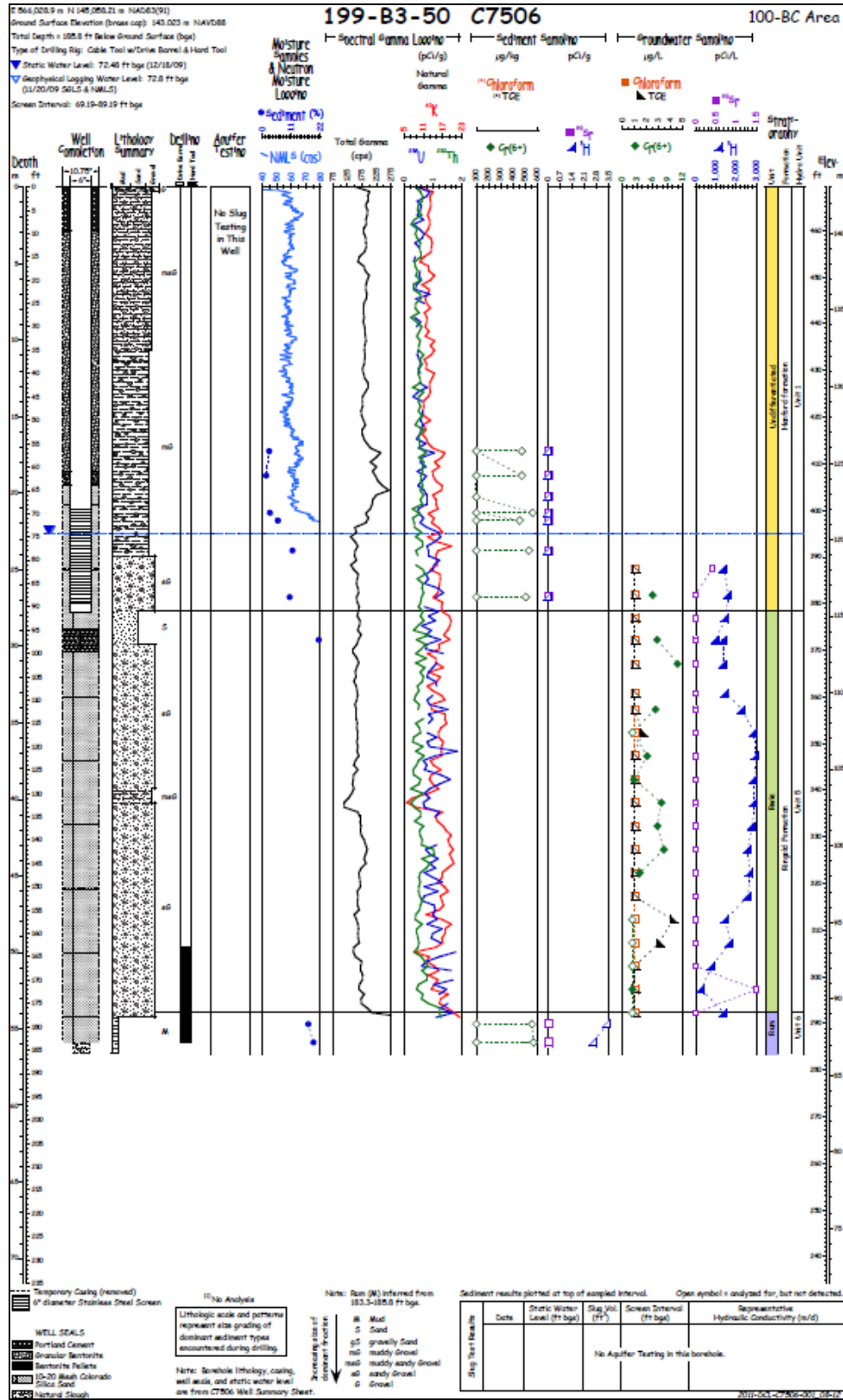


Figure 4-21. Borehole C7506 Logging Data

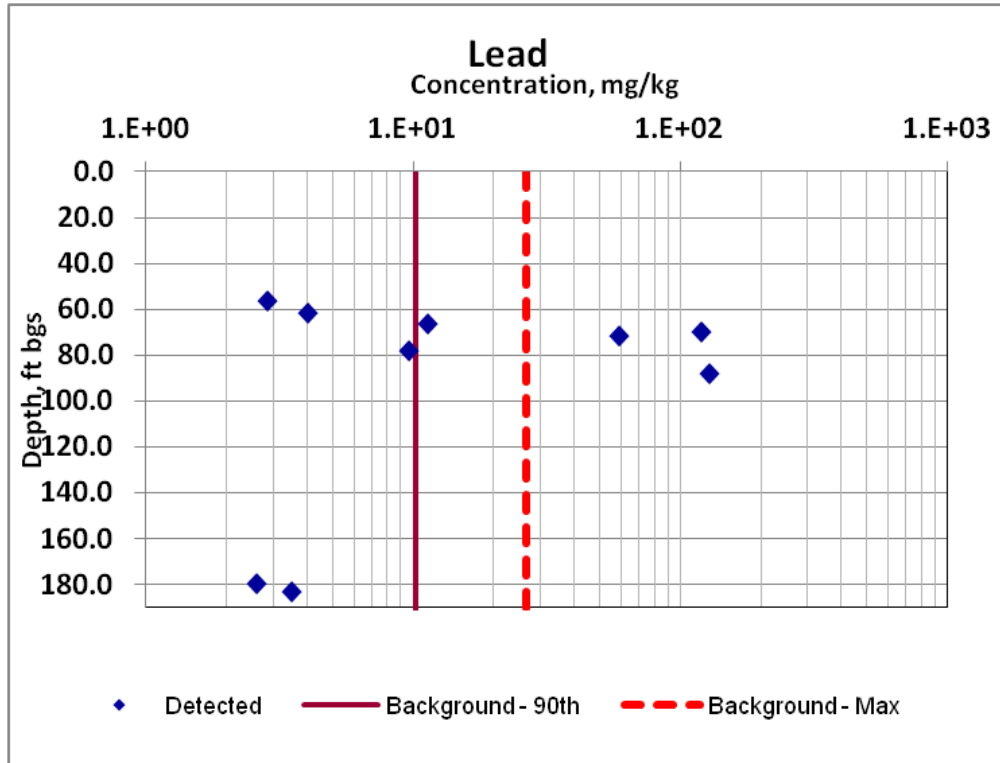


Figure 4-22. Borehole C7506 Lead Measurements

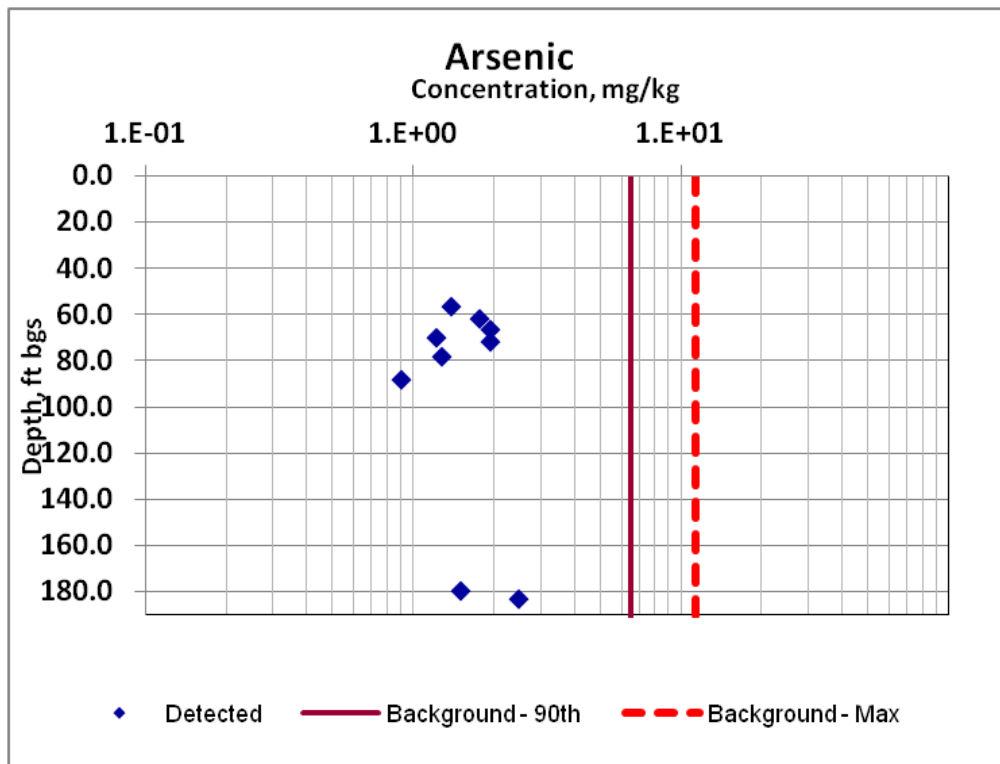


Figure 4-23. Borehole C7506 Arsenic Measurements

4.6 Borehole C7843 (100-B/C Area)

Figure 4-24 shows the borehole C7843 (199-B3-52) location. The closest waste sites are the 116-C-5 and 107-C Retention Basins. The Basins were constructed to hold cooling water effluent from the 105-C Reactor to allow for thermal cooling and radioactive decay prior to release to the Columbia River. After 1954, the effluent from the 105-B Reactor was diverted to the basins because the 116-B-11 Retention Basin had cracked and repair efforts were unsuccessful. Originally, only one tank was filled at a time allowing the option for cooling water contaminated by a ruptured fuel element to be diverted to the second tank. The practice of adding hot water to an empty, cold tank resulted in cracking of the tanks' welded seams. After a series of repair efforts extending into 1958, parallel operation of the tanks became common. The tanks were constructed of welded carbon steel and were set on a reinforced concrete foundation with a crushed rock subfloor.

Figure 4-25 illustrates the borehole logging data. The lead, arsenic and mercury measurements for C7843 are shown in Figure 4-26, Figure 4-27, and Figure 4-28, respectively. A review of the pertinent data for C7843 suggests the following.

- A change in lithology from muddy gravel to muddy sandy gravel occurs at about 29 ft (8.8 m) bgs (Figure 4-25).
- C7843 lead and arsenic concentrations are below background.
- A zone of higher mercury concentration is observed at about 40-50 ft (12.2-15.2 m) bgs (Figure 4-28).
- Chromium and strontium-90 concentration data suggest that the waste site contamination is prevalent throughout the vadose zone. [Note that this is a post-remediation borehole with clean overburden; so no sampling was done above 30 ft (9.1 m)].
- The water table is located at about 48 ft (14.6 m) bgs.
- The anthropogenic source of mercury is likely derived from waste site discharge. Another potential source of mercury could be contaminated sulfuric acid used during the operations.
- There is no mercury contamination currently in the groundwater.

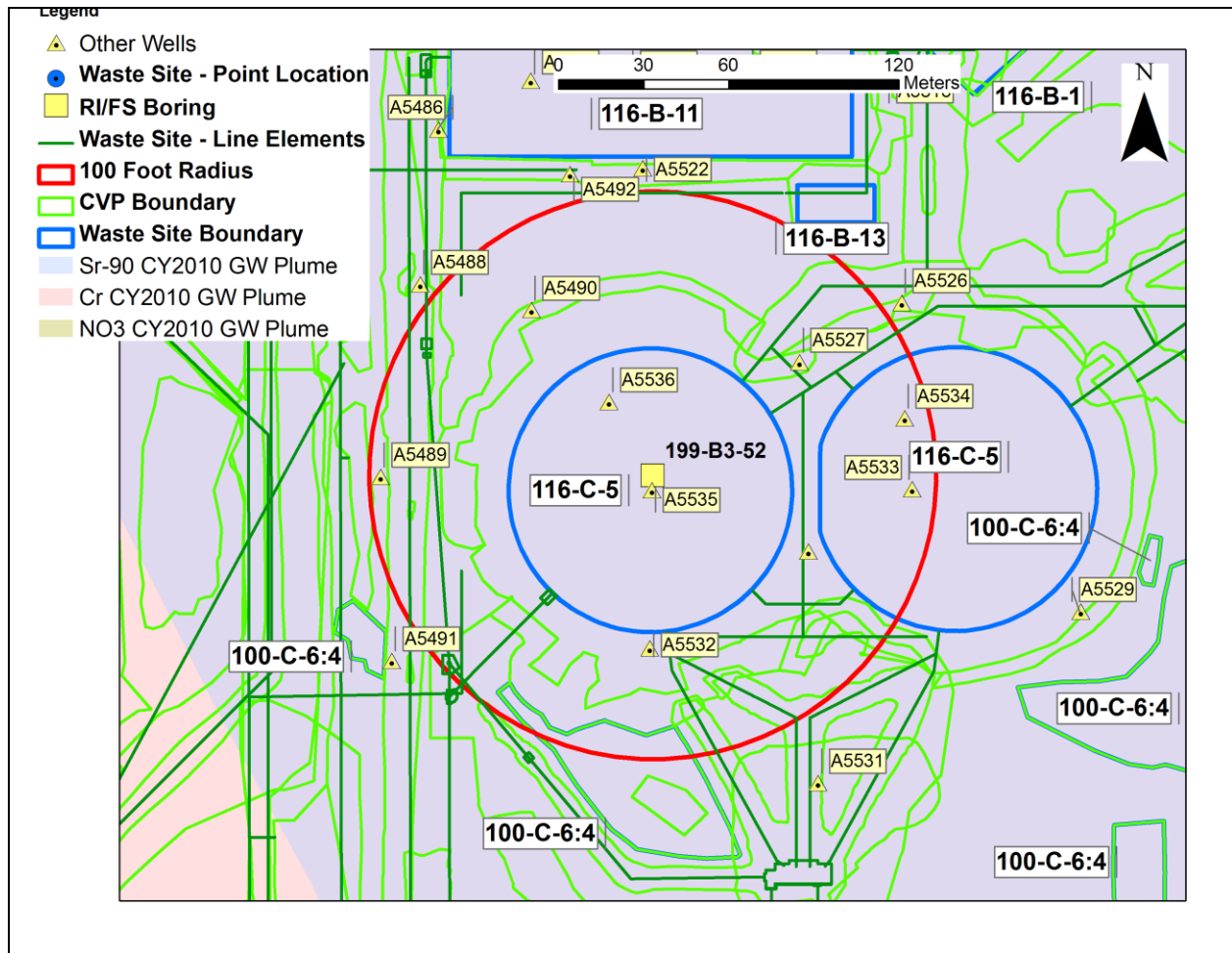


Figure 4-24. Borehole C7843 (199-B3-52) Location

47

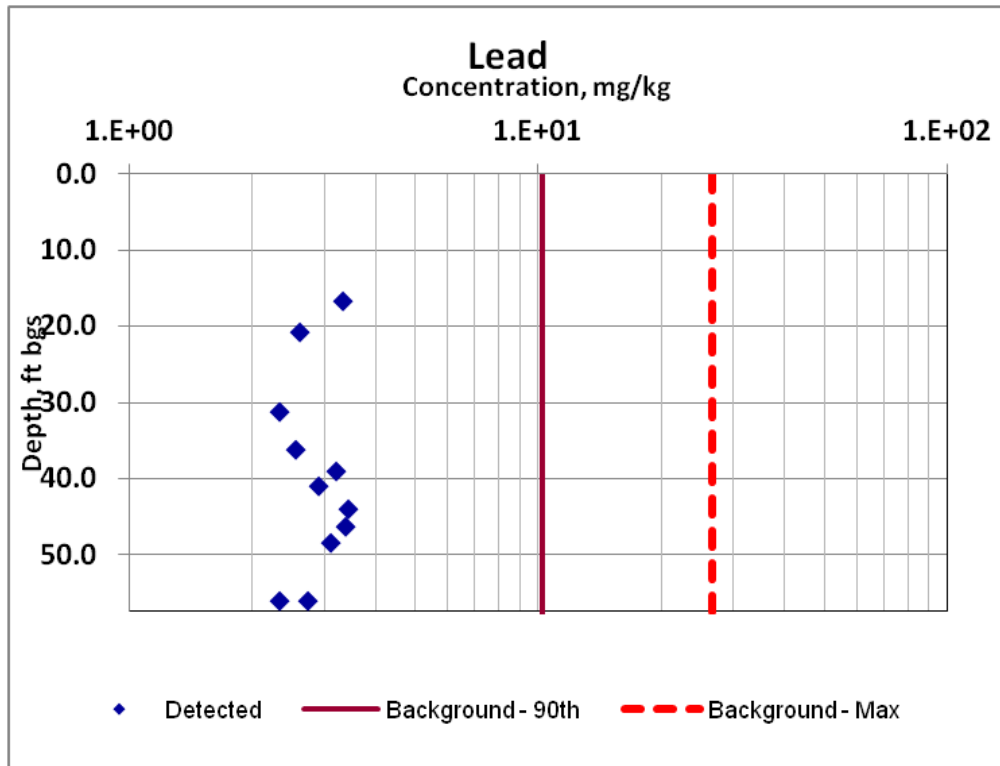


Figure 4-26. Borehole C7843 Lead Measurements

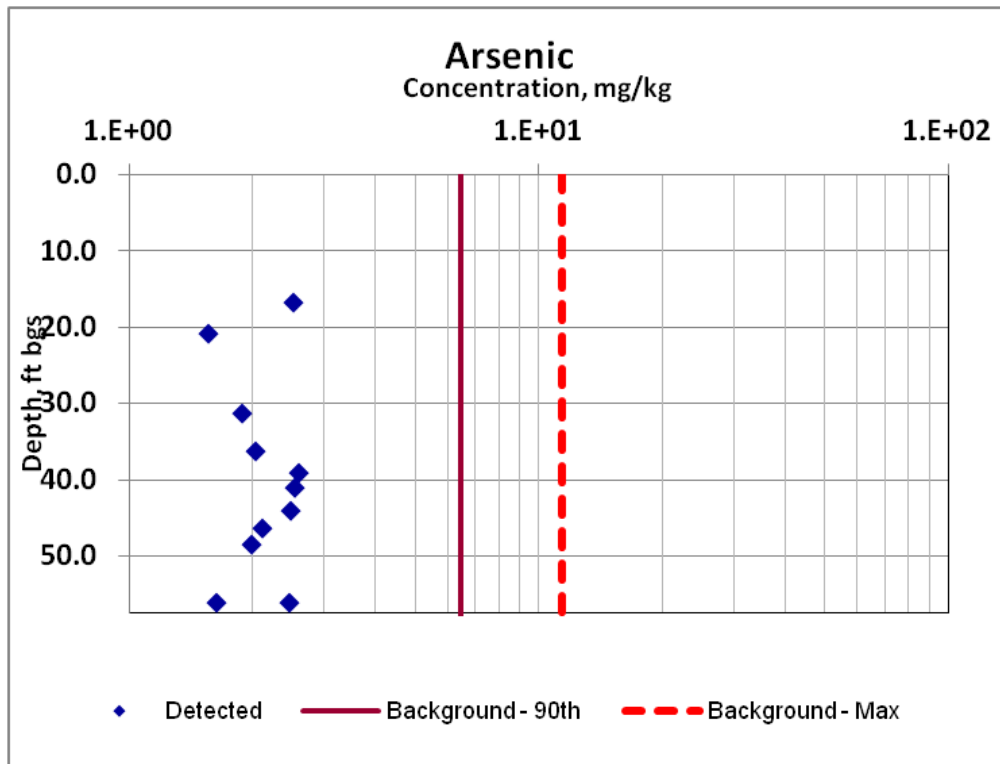


Figure 4-27. Borehole C7843 Arsenic Measurements

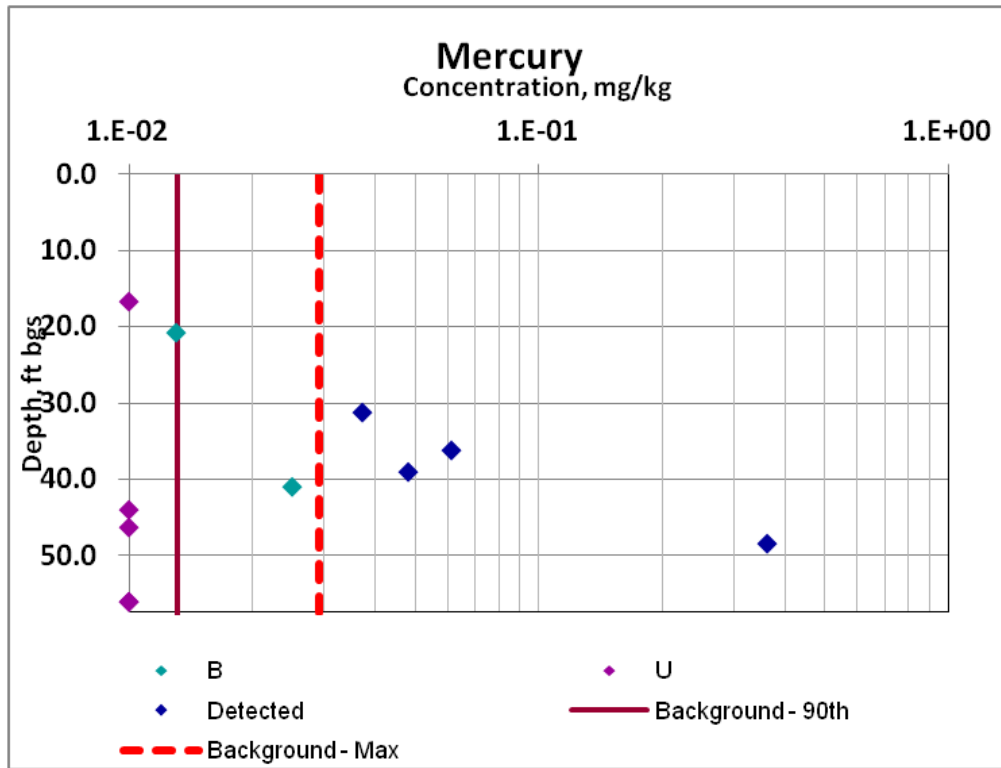


Figure 4-28. Borehole C7843 Mercury Measurements

4.7 Borehole C7844 (100-B/C Area)

Figure 4-29 shows the borehole location; 116-B-5 (Crib) site is the closet waste site. The site received liquid tritium wastes from the 108 Building. Only wastes of less than $1 \mu\text{Ci}/\text{cm}^3$ were discharged to this unit.

In June 1995, the site was excavated as part of the 100-B/C Area Demonstration Project. Remedial action was accomplished by excavating approximately $10,600 \text{ ft}^3$ (300 m^3) of soil from the crib and demolishing the concrete crib structure, leaving an open excavation approximately 112 ft (34 m) long \times 26 ft (8 m) wide \times 16 ft (5 m) depth. The soils within and surrounding the crib were sampled and analyzed. The soils from cells C and D containing levels of tritium above cleanup standards were taken to the Environmental Restoration Disposal Facility (ERDF). All other soils sampled were within cleanup standards.

Figure 4-30 illustrates the borehole logging data. The lead, arsenic and mercury measurements for C7844 are shown in Figure 4-31, Figure 4-32, and Figure 4-33, respectively. A review of the pertinent data for C7844 suggests the following:

- A zone of higher mercury concentration is observed from 15-65 ft (4.6-19.8 m) bgs (Figure 4-33).
- The chromium, strontium-90, tritium, TCE, and chloroform concentrations suggest waste site contamination throughout the vadose zone. [Note that this is a post-remediation borehole with clean overburden to ~15 ft (4.6 m)].
- The water table is at about 67 ft (20.4 m) bgs (Figure 4-30).
- The anthropogenic source of mercury is likely derived from waste site discharge. Another potential source of mercury could be contaminated sulfuric acid used during the operations.
- There is no mercury contamination currently in the groundwater.

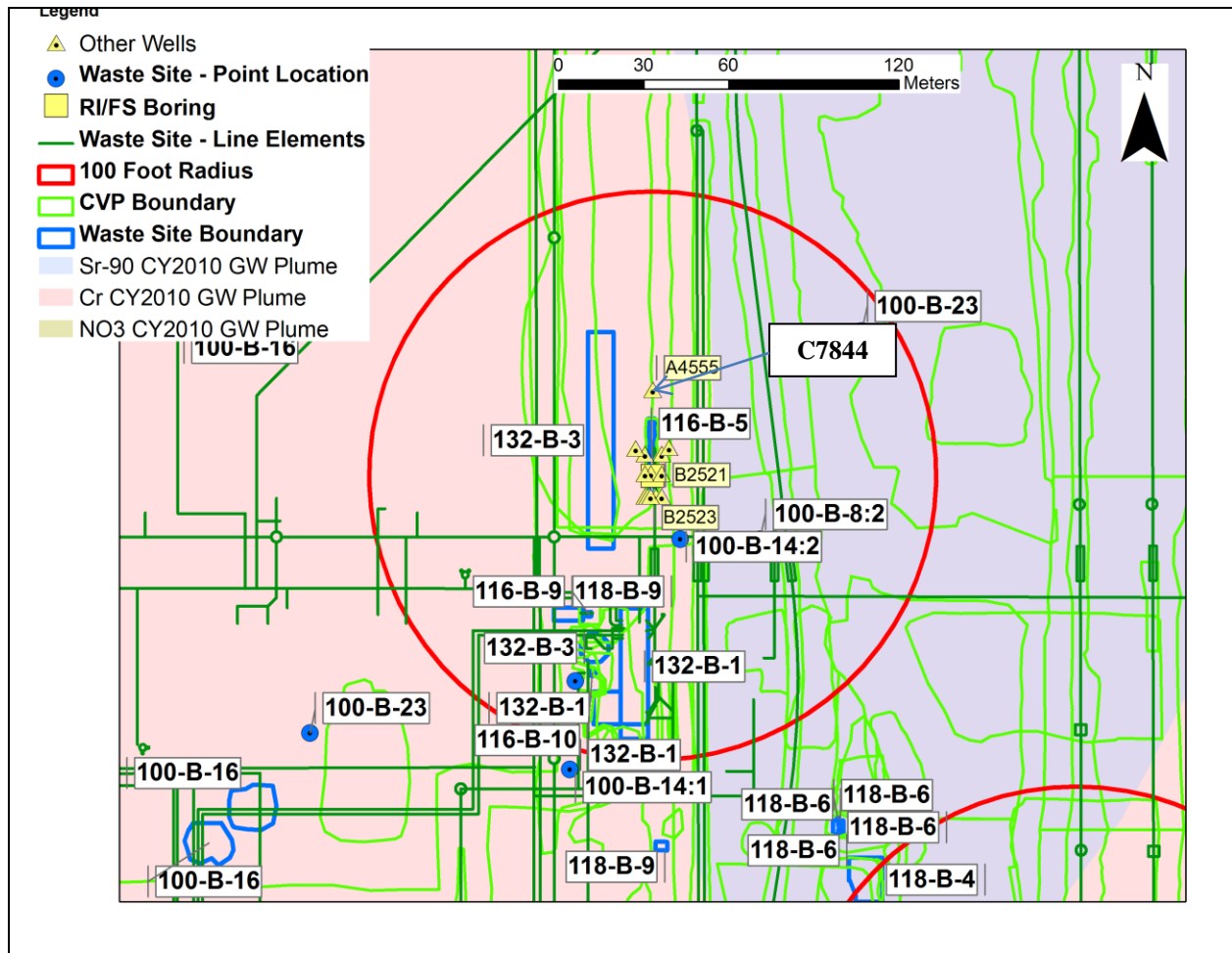


Figure 4-29. Borehole C7844 Location

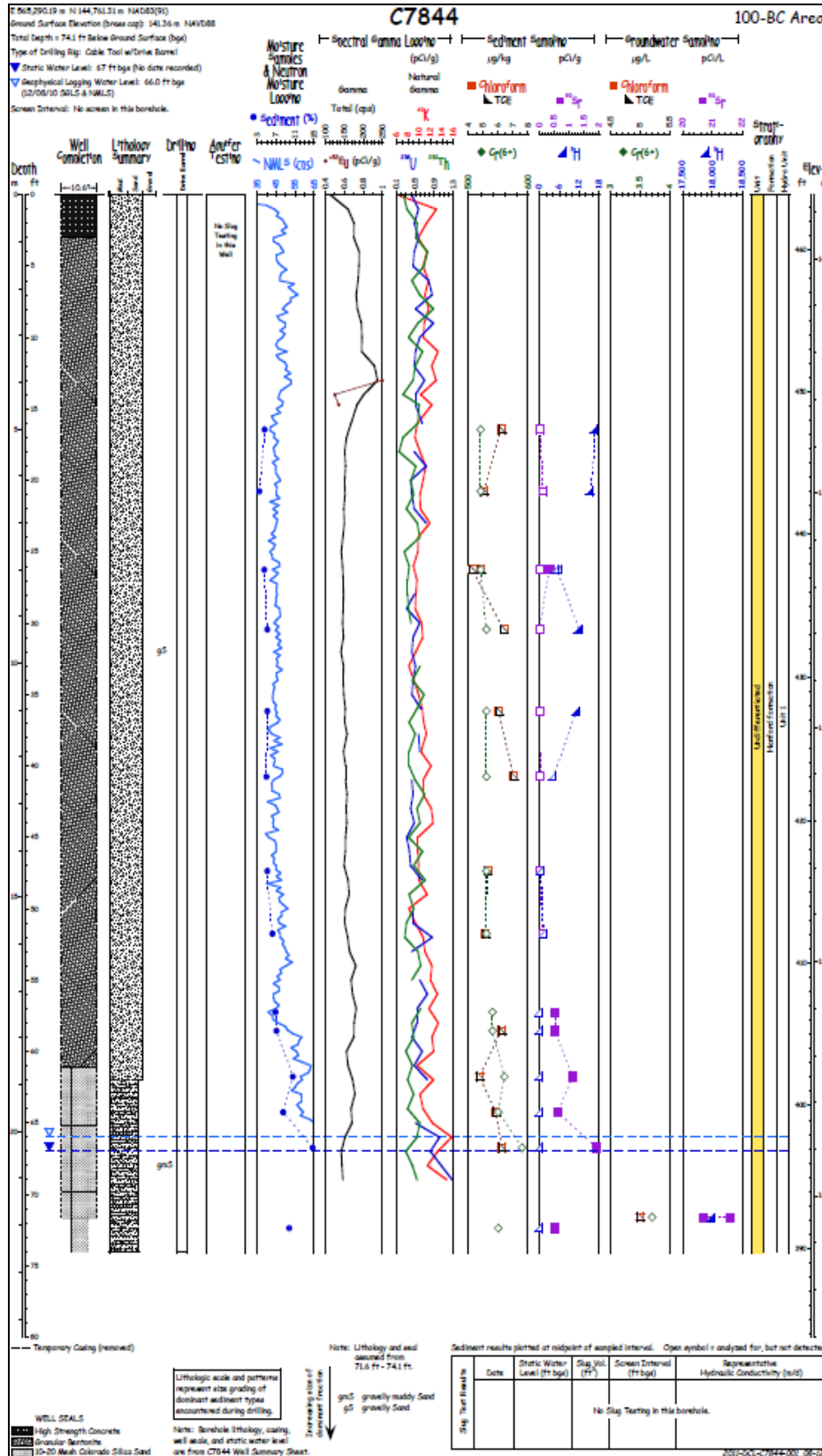


Figure 4-30. Borehole C7844 Logging Data

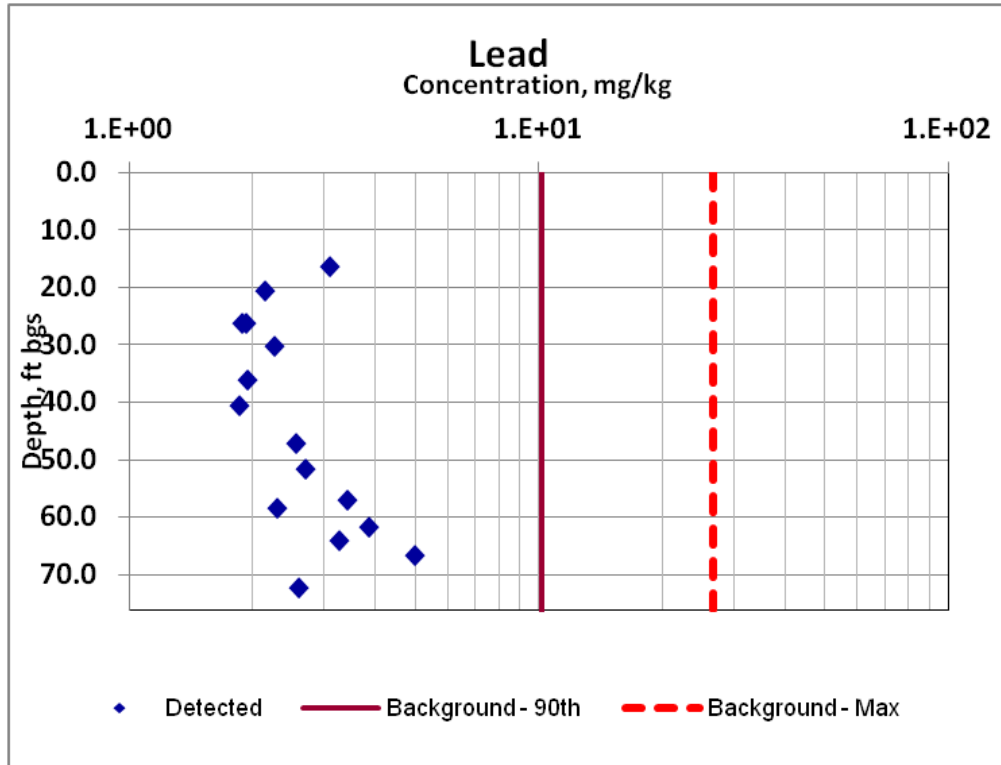


Figure 4-31. Borehole C7844 Lead Measurements

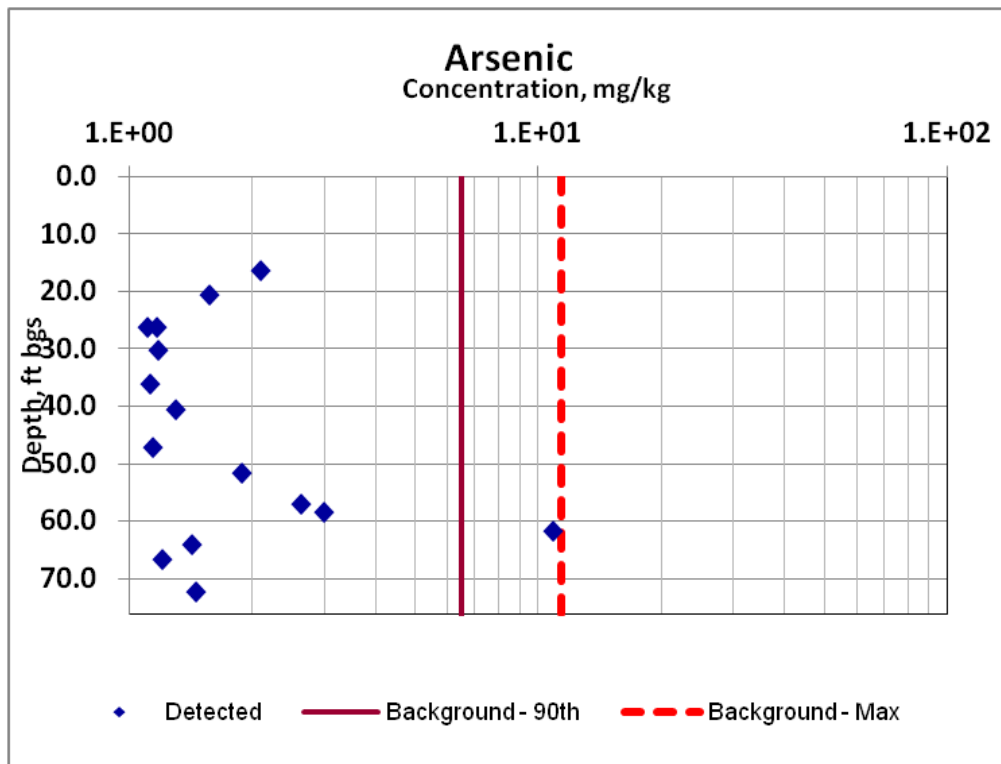


Figure 4-32. Borehole C7844 Arsenic Measurements

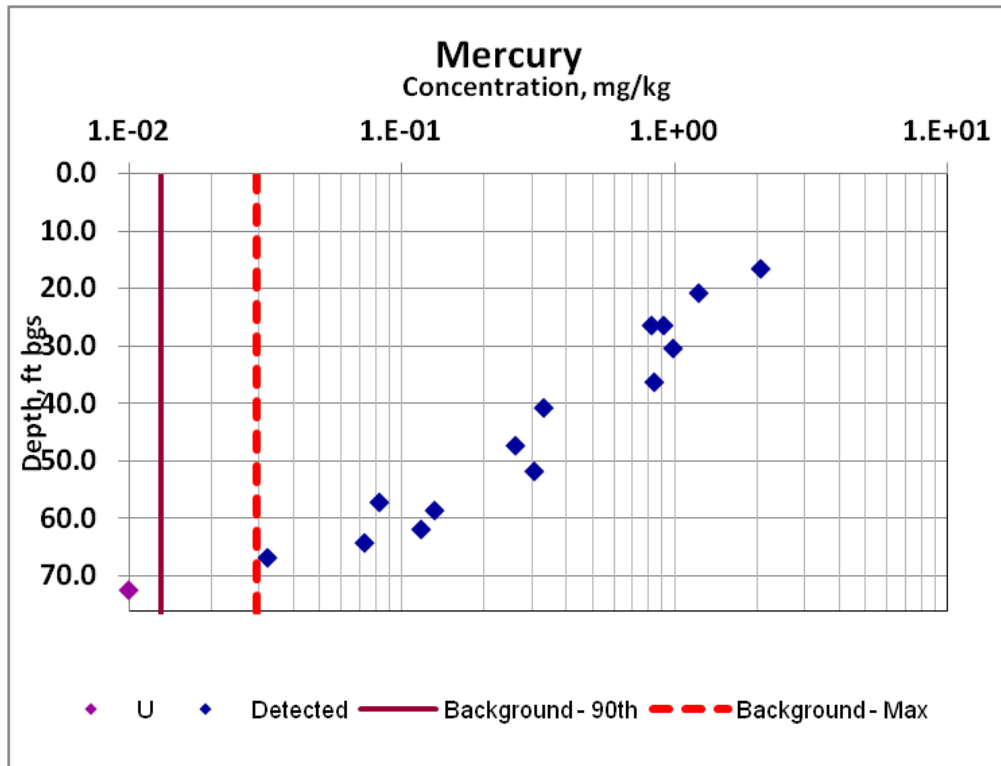


Figure 4-33. Borehole C7844 Mercury Measurements

5. Plausible Conceptual Models

Before discussing plausible conceptual models, a brief discussion is presented on the 100 Areas lead-cadmium sources. The physical and chemical heterogeneities that are important considerations in the context of assigning K_d values for metals are also summarized.

5.1 Lead-Cadmium Burial Grounds.

The location of 100 Areas burial grounds which received the high K_d contaminants is shown in Figure 5-1. The estimated quantity of lead-cadmium used as “reactor poison” and disposed of in the burial grounds in the 100 Areas is 1103 metric tons, of which up to 1059 metric tons are lead and 44 metric tons are cadmium.

The lead-cadmium alloy used as reactor poison was in the form of a solid rod approximately 1.4 in (3.6 cm) in diameter by 6 in (15 cm) long. The rod was sealed in an aluminum can with a wall thickness of 0.035 in (0.09 cm). A total of 38 canned pieces was laid end-to-end to form a process tube column of poison. The word “poison” was used to describe the high neutron-absorbing characteristics of the column (WHC-EP-0087, *Estimates of Solid Waste Buried in the 100 Area Burial Grounds*). Each piece weighed 3.36 lb (1.5 kg). The alloy was composed of the elements shown in Table 5-1.

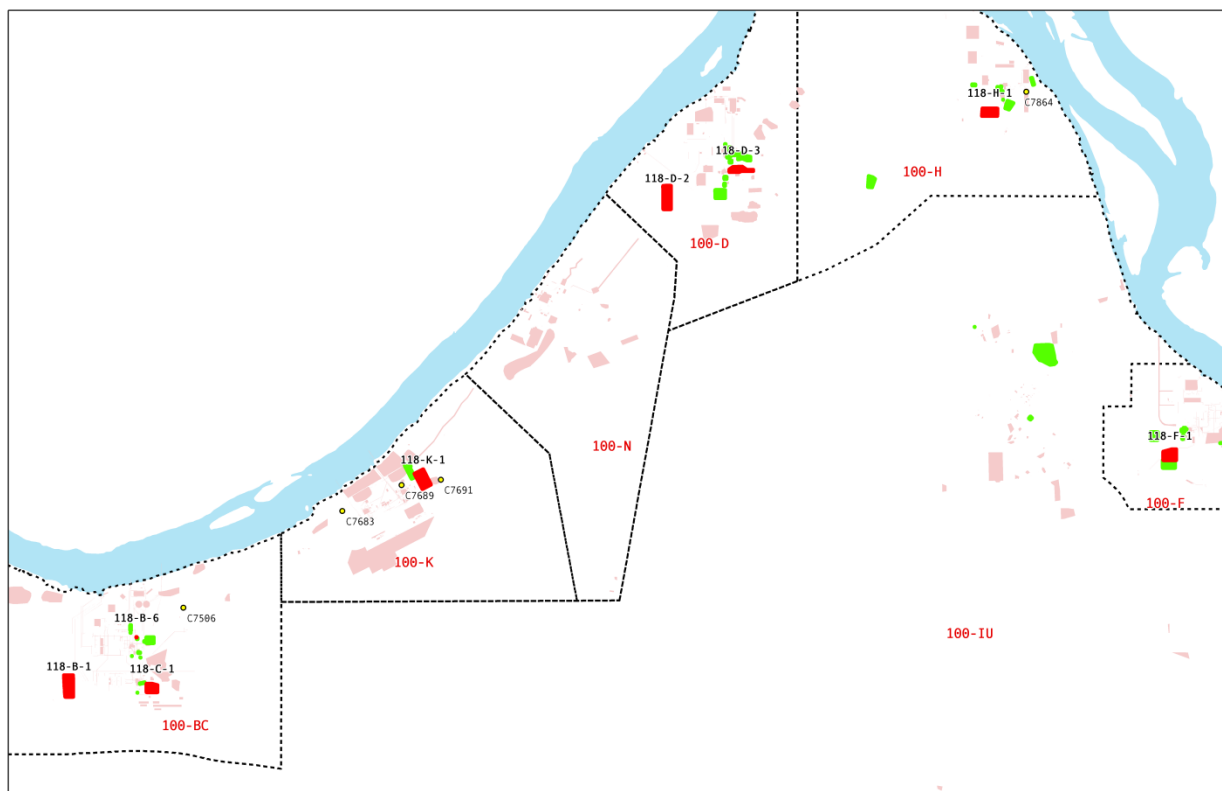


Figure 5-1. Location of 100 Areas Burial Grounds (in red) which received Lead-Cadmium Poison Pieces; Other nearby burial grounds are shown in green

Table 5-1. Composition of Lead-Cadmium Poison Pieces

| Element | Percentage |
|----------------------------|------------|
| Lead | 95.88 |
| Cadmium | 3 to 4 |
| Silver | 0.020 |
| Barium | 0.001 |
| Copper | 0.080 |
| Zinc | 0.001 |
| Iron | 0.002 |
| Bismuth | 0.005 |
| Tin, Antimony, and Arsenic | 0.002 |

5.2 Media and Chemical Heterogeneities

Unlike non-reactive contaminants such as tritium, arsenic, mercury and lead are known to have a higher K_d (DOE/RL-96-17, *Remedial Design Report/Remedial Action Work Plan for the 100 Area*), expected to be relatively immobile, and have a long residence time within the vadose zone. However, as the data in the preceding sections illustrate, a number of sediment samples located close to the water table exceed the background concentrations for lead and arsenic. Three conceptual models are postulated to explain the deeper than expected penetration for the metals.

Adsorption to mineral surfaces is typically the single most important geochemical process affecting transport of contaminants in the vadose zone. It should be noted, however, that a constant value K_d (distribution coefficient) approach is an empirical adsorption model. Also, the K_d value is a lumped parameter and, as a result, neglects many of the chemical complexities of the adsorption process such as saturation of adsorption sites and aqueous complexation. Because there are a finite number of adsorption sites on the solid phases, adsorption will reach a practical upper limit. This can lead to erroneous results when used to predict retardation of metal and radionuclide contaminants in systems with varying chemical conditions (Bethke and Brady 2000; EPA/402/R-99/004A, *Understanding Variation in Partition Coefficient, K_d , Values: Volume I. The K_d Model, Methods of Measurement, and Application of Chemical Reaction Codes*).

In addition to chemical heterogeneities and complexities, significant physical heterogeneities exist for the 100 Areas vadose zone sediments (Figure 2-2). The K_d measurements are generally conducted on Hanford Site sediment material that is <2 mm in size. For 100 Areas sediments that are gravel dominated, K_d values are typically lower than those determined for sandy media (i.e., sediments with <2-mm size material), because the surface area and the corresponding number of adsorption sites per unit mass is much lower [PNNL-13037, *Geochemical Data Package for the Hanford Immobilized Low-Activity Tank Waste Performance Assessment (ILAW PA)*]. As a result, it is necessary to make corrections to K_d values

determined with <2-mm size material. For high K_d contaminants, Equation (1) is recommended (Kaplan et al. 2000):

$$Kd(gc) = (1 - f)Kd(< 2mm) + (f)0.23 Kd(< 2mm) \quad (1)$$

$$\text{or, } Kd(gc) = (1 - 0.77f) Kd(< 2mm)$$

where $Kd(gc)$ = gravel corrected Kd value,

f = weight fraction gravel, and

$Kd(< 2mm)$ = Kd value obtained with <2-mm material.

For the preceding reasons, the constant K_d model is best used to represent adsorption when contaminant concentrations are low relative to the adsorption capacity and the variability in mineralogy and hydrochemistry is minimal along the fluid flow path. The constant K_d model is not adequate for representing adsorption in situations where spatial variability in mineralogy and hydrochemistry is significant along the flow path.

5.3 Conceptual Model #1

As was discussed earlier, the deep borehole measurements targeted in the RI Work Plan were identified with a bias towards locating contaminants throughout the vadose zone and targeted areas at or near the waste sites; i.e., the drilling as well as the sampling was biased towards capturing contamination within the “hot spots.”

For the vadose zone measurements (Sections 3 and 4) for the high K_d contaminants, cable tool drilling was used to drill the RI/FS wells in fiscal year 2011. As part of the review of the measurements, it is investigated first whether it is appropriate, for the high K_d contaminants, to rule out any potential casing contamination and subsequent “drag-down” towards the deeper vadose zone.

Figure 5-2 is one “hot spot” region in 100-H Operable Unit. In the early 1990’s, Limited Field Investigations (LFIs) were conducted to characterize surface and near-surface contamination for the 100 Areas sediments. Figure 5-3 shows the measured data for lead contamination for the waste site 100-H-21, which is located just outside the 100-ft (30.5-m) radius of the RI/FS borehole C7864 (Figure 5-2). The highest measured near-surface sediment concentration for lead is about 750 mg/kg (Figure 5-3).

Figure 5-4 shows the measured vadose zone sediment concentration for lead in the RI/FS borehole C7864. Also shown in the figure are the measured sediment concentrations for antimony and copper. First, as discussed earlier, even though K_d is treated as a constant, in reality, the vadose zone physical heterogeneities (e.g., variability of gravel content and variability of soil moisture contents) as well as chemical heterogeneities (e.g., variable surface adsorption sites, variability of chemical conditions) result in considerable variability of the distribution coefficient for a contaminant.

Figure 5-4, however, suggests otherwise. If porous media continuum flow and transport is what is driving the contaminants, it is unlikely to have such a huge slug appear so close to the water table and line up so perfectly with the co-contaminants at the identical depth of 41.1 ft (12.5 m) bgs for all three analytes. In fact, Figure 5-4 suggests vadose zone transport of three analytes with an identical K_d , whereas, in reality, even the constant K_d values for the three analytes are different, because of physical heterogeneities and chemical complexities. A chromatographic separation is thus expected during their movement through the vadose zone. The K_d values for copper, lead, and antimony for sand-dominated media are 22, 30, and 45

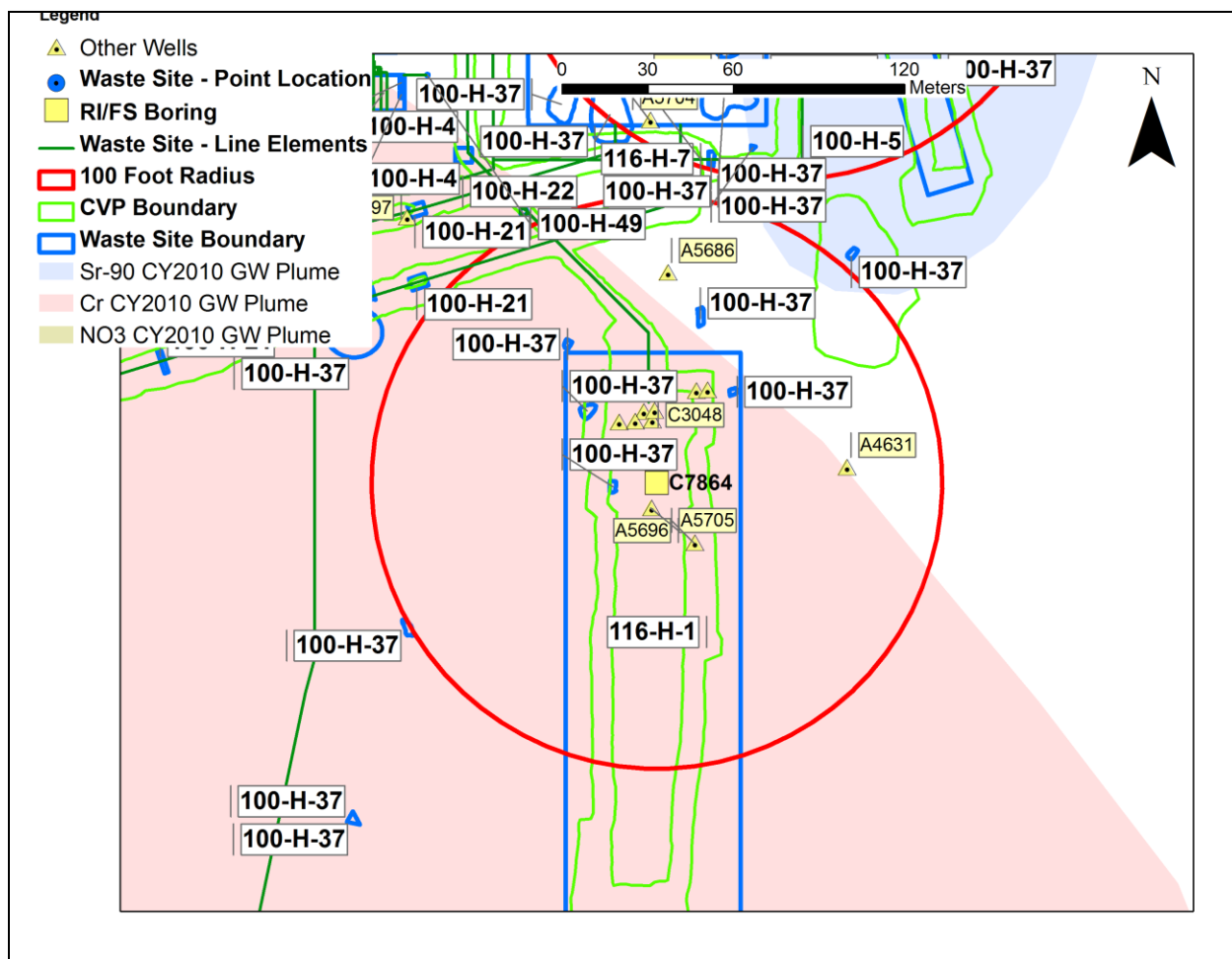


Figure 5-2. Borehole C7864 Location

mL/g, respectively (DOE/RL-96-17). However, for highly gravelly media (Figure 2-2) with an assumed gravel fraction of 80 percent by weight, the respective gravel-corrected K_d values are 8.4, 11.5, and 17.3 for copper, lead, and antimony, for an assumed volumetric moisture content of 5 percent and a sediment bulk density of 1.7 g/cm³. The respective retardation factors (i.e., ratio of porewater velocities for retarded and unretarded species) for copper, lead, and antimony are thus 288, 393, and 589. Therefore, vadose zone residence times or travel times for the three analytes are expected to be different with the copper slug arriving earlier than the antimony slug and the lead slug lying in between. However, such a chromatographic separation is clearly missing for the three analytes, even with the assumption of a constant K_d for the 100 Areas heterogeneous media with a transient chemistry. Rather, all three analytes arrive simultaneously and exhibit considerably high concentrations at the identical depth of 41.1 ft (12.5 m) bgs (Figure 5-4). Therefore, the potential of drag-down from casing contamination during cable-tool drilling for the RI/FS borehole C7864 cannot be discounted.

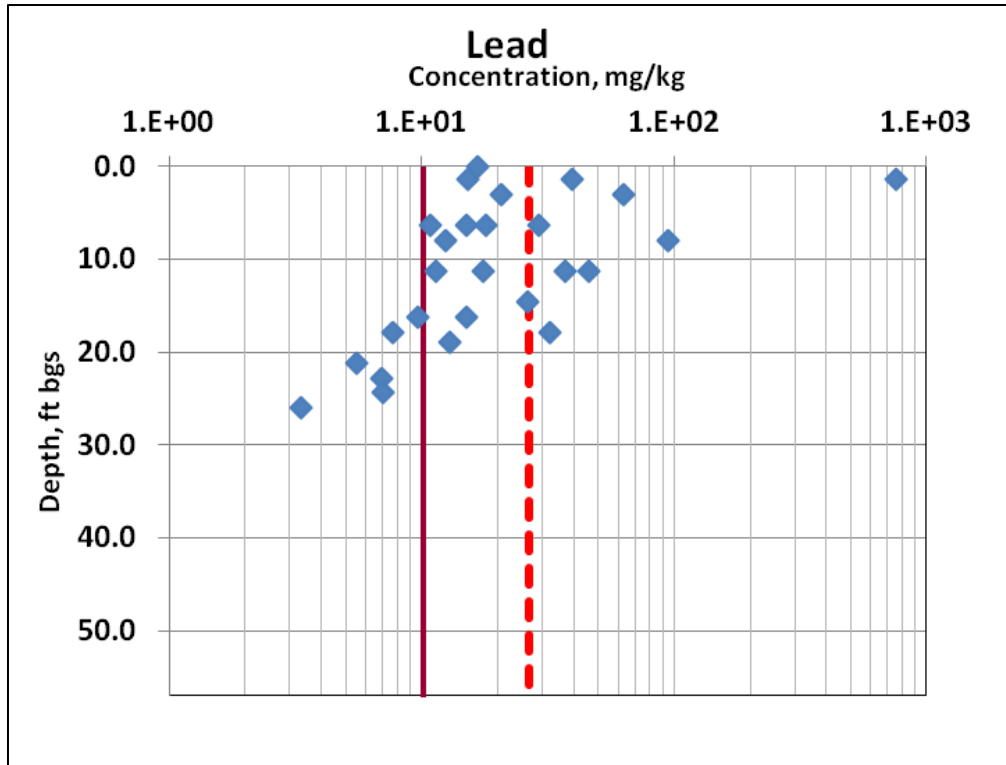


Figure 5-3. Lead Contamination Measurements for Waste Site 100-H-21

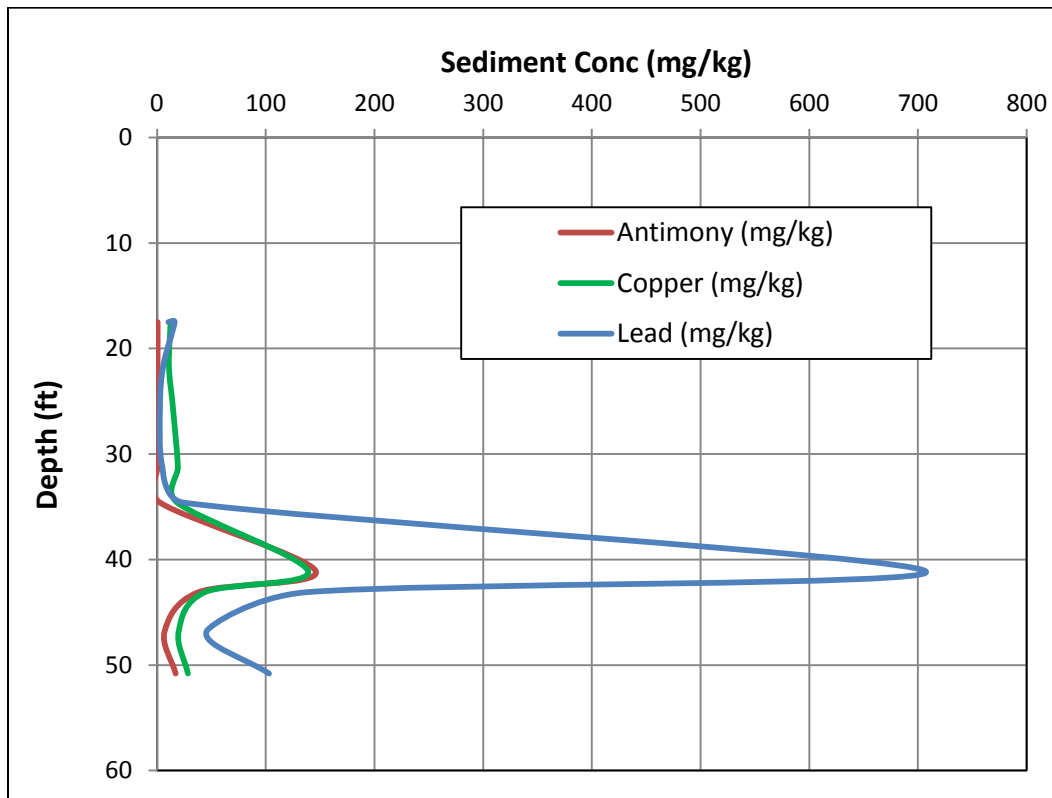


Figure 5-4. Borehole C7864 Lead, Antimony and Copper Concentration Profiles

5.4 Conceptual Model #2

Both Conceptual Models #2 and #3 rely on plausible colloid formation and mobilization. Mobile colloids including mineral fragments are prevalent in the vadose zone porewater. The mineral fragments are derived primarily from the buried waste as well as the soil itself, which includes an abundance of particles in the colloidal size range, especially in fine-textured media. The colloidal size range is about 10 nm to 10 μm . Three key features of the vadose zone can potentially play a significant role in colloid formation or colloid-facilitated transport: (a) the presence of air-water interfaces, (b) transients in flow and chemistry, and (c) sediment structure and heterogeneity.

In general, a plausible conceptual model is based on the scenario that lead could have been derived from nearby lead-cadmium rods disposed in the burial grounds (Figure 5-1); it possibly migrated in colloidal form because of the PRZ smearing with the water table being high and the invasion of a saturated pulse within the vadose zone and then sorbed on to fine-textured media with the dissipation of the pulse.

The salient features of the Conceptual Model #2 for lead contamination, in particular, at borehole C7864, for example, are described below:

- A zone of high lead concentration is observed at about 40-45 ft (12.2-13.7 m) bgs. The high concentration zone also corresponds with increase in copper and antimony concentrations.
- The current water table is at ~43 ft (~13.1 m) bgs. The lead contamination zone is located above but close to the current water table.
- Potential source for lead could be the nearby solid waste burial grounds containing many tons of lead-cadmium “reactor poison” rods – some of which may have undergone corrosion (pitting or general corrosion) along with other metals and therefore provide source of colloidal particles that are carried in suspension.
- The burial grounds being ~20 ft (~6.1 m) deep might have been saturated near their base during the operations period. Some of these burial grounds are located in the vicinity of boreholes where lead is detected above background and it is possible that these burial grounds could be the deep sources when the water table was higher during operations period.
- Lead particles, which include traces of antimony and copper, could have traveled by themselves in colloidal form through the saturated zone and then retained in sediment fines. The iron oxyhydroxide colloids and soil mineral colloids (e.g., smectite) are also potential carriers onto which lead particles may have attached.
- During reactor operations, superheated water was discharged in the subsurface and because of high flow rates, there is potential of colloidal transport due to formation of saturated flow conditions locally. Thermally hot reactor effluent cooling water raised the groundwater temperature from ~16⁰C to 70⁰C (Figure 5-5). Thermal springs were noticed at the edge of the river having temperatures up to 74⁰C. Based on 1962 data, the groundwater mound was at an elevation of about 405 ft (123.4 m) in 100-D/H Area (Figure 5-6); surface elevation is about 426 ft (130 m) in this area and the depth to the water table was about 20 ft (6.5 m), which is about the bottom of the burial grounds. Following operations period when the water table dropped, the colloids carrying lead were likely retained in the sediment fines and now permanently sequestered due to possible anthropogenic overgrowth.

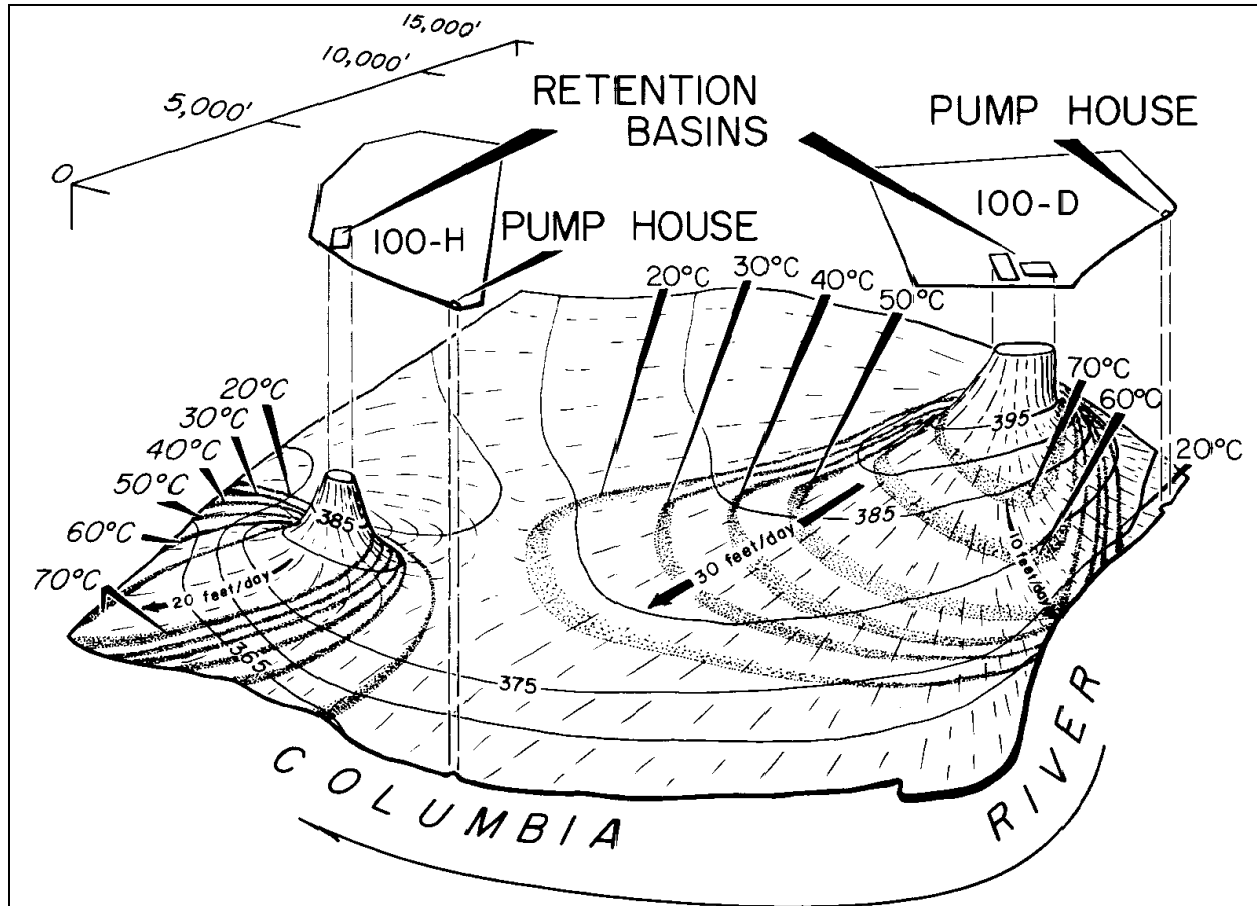


Figure 5-5. Perspective on Thermal Plume Profiles during Reactor Operations in 100-H Area

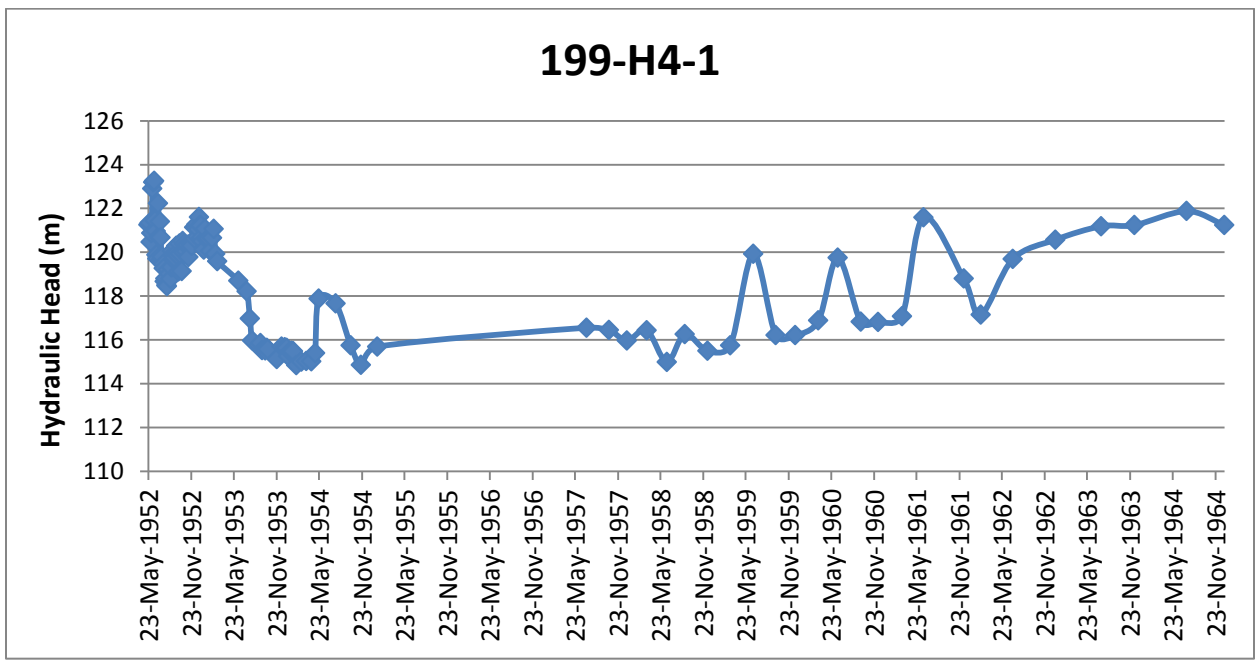


Figure 5-6. Head Data in Well 199-H4-1

- Pipe joints solder is also a potential source of lead, copper, and antimony and could be derived from pipe failures at the waste site. Correlation of lead-antimony-copper near high discharge areas near surface suggests original influent pipe construction as a source. Lead could have also been derived from paint and acid-batteries derived suspension.
- The elevated lead concentrations are located at depths where a change in lithology is observed (e.g., muddy gravel to sandy gravel), which may have influenced the water table locations of the past due to changes in hydraulic properties.
- An alternative explanation for higher lead concentration could be higher clay content in the lithology at similar depths (based on natural gamma measurements observed at some locations) that may have higher sulfide mineral content leading to naturally higher content of lead, copper, and antimony (present in the mineral phase). For such lithologic units the natural (background) concentration can be significantly higher.
- One borehole at 116-H-1 has significant concentration at depth of ~40 ft (~12.2 m). But elevated lead is not consistently detected in multiple boreholes and test pits at this site. Furthermore, the lead is found to be bound strongly to the sediment. Leaching studies indicate that it is not leachable and thus non-labile.
- No lead contamination in the groundwater has been observed (maximum detected concentration in groundwater is 3 parts per billion with a B flag).

Unlike lead and arsenic, mercury concentration profiles often show a different pattern. Low concentrations of residual mercury are observed below the depth of remediation at a number of liquid effluent waste sites. However, even though mercury is present with other low-level residual contamination, it generally decreases to background concentration with depth. The original mercury source for most sites is likely the use of contaminated sulfuric acids in water treatment and direct acid disposal. Some sites are also associated with wastes from P-10 Project where mercury vacuums were used. Sorption of mercury at depth is affected by lithology (variation in fine grained fraction) and perhaps by the degree of saturation.

5.5 Conceptual Model #3

For the base 100 Areas conceptual model (Section 2) under low ambient moisture regime, high K_d for metals keeps contaminants up within the shallow vadose zone. This is especially true for coarse-textured, non-gravelly Hanford sediments. For Hanford sediments that are highly gravel-dominated, K_d values get impacted considerably because of the absence of any significant fine fraction (Equation 1).

While drag-down is a plausible conceptual model for C7864 borehole location, colloid formation and colloid-facilitated transport form the basis for Conceptual Models #2 and #3. Even though both rely on initiation and migration of colloids, the difference in the two models is how the 100 Areas vadose zone is conceptualized (i.e., a porous continuum versus macropore-porous matrix) and how transients in chemistry and preferential flow play a role in colloid mobilization. For both Conceptual Models #2 and #3, the episodic high-volume release from burial grounds as well as the PRZ induced exchange flow can potentially impact initiation of colloid formation and subsequent mobilization.

For Conceptual Model# 3, the 100 Areas gravel-dominated heterogeneous vadose zone is conceptualized as a dual mobile-immobile (macropore-porous matrix) interacting media (Figure 5-7). The flow within macropores is governed by Poiseuille law ("fast flow"), whereas the flow within the porous matrix is

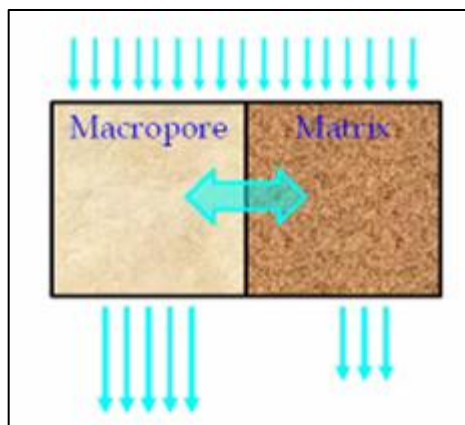


Figure 5-7. An Interacting Dual Media Representation of 100 Area Gravelly Vadose Zone; Macropore (fast flow) and Porous Matrix (slow flow) (after Mohanty et al. 2011)

governed by Darcy-Buckingham law (“slow flow”) (Jury and Horton 2004). In soil physics, macropores are defined as cavities that are larger than 75 μm . Functionally, pores of this size host preferential flow and rapid transport of solutes and colloids. Macropores increase the hydraulic conductivity of soil, allowing water to infiltrate and drain quickly, especially under saturated and near-saturated flow conditions. Literature data suggest the existence of mobile-immobile conditions of the aqueous phase with vadose zone soils, especially those containing large interconnecting system of macropores (DeNovio et al. 2004). Contaminant migration can potentially be enhanced colloidal migration, where the colloidal phase itself is undergoing transport via preferential pathways.

In addition to physical heterogeneity, chemical complexity can exist with the presence of metals in 100 Areas vadose zone. One property of metals (e.g., lead, arsenic and mercury) that distinguishes them from other contaminants is that they potentially can exist in multiple oxidation states that are in thermodynamic equilibrium and can bond with a large number of compounds (i.e., co-contaminants). The resulting complexes that form can vary in toxicity as well as mobility. In addition, many metals participate in oxidation-reduction reactions (i.e., exchange of electrons), and the oxidation state can substantially impact adsorption-desorption reactions at solid-solution interfaces, and the element’s ability to form, for example, a variety of chemical complexes with dissolved contaminants. A quantitative indicator of chemical complexity can be represented by solution ionic strength, which is a function of the concentration of all ions present in that solution.

A possible variation of the base conceptual model (Section 2) is presented as follows. First, detachment of colloidal particles from the soil matrix requires an energy input sufficient to overcome van der Waals and other adsorptive forces binding the particles; the external forces could be due to shear forces of fluid flowing within individual pores during episodic high-volume release. During such episodic events, saturated and/or near-saturated conditions exist for macropore flow, thereby resulting in initiation of colloid generation. Transients in ionic strength can then mobilize colloids and contaminants across the macropore-matrix interface. More colloids are formed and remain stable under low ionic strength conditions, whereas fewer colloids are stable under high ionic strength conditions (Figure 5-8). Also, literature data (Mohanty et al. 2011) suggest that the colloid exchange between macropore and porous matrix can be caused by hysteresis of colloid and metal mobilization due to changes in ionic strength in the porous matrix relative to the macropore (Figure 5-9). In the absence of further high-volume discharges, mobilized colloids reside in fine-textured horizons near the water table.

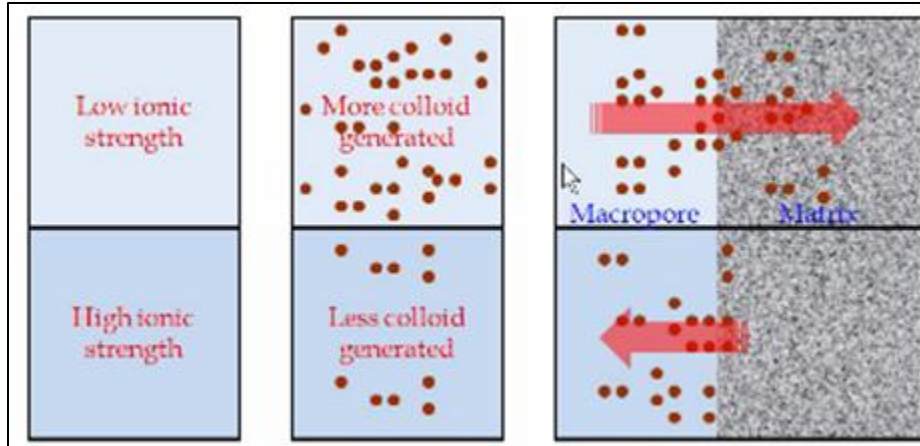


Figure 5-8. An Interacting Physiochemical Hypothesis – Transients in Ionic Strengths May Mobilize Colloids across the Macropore-Matrix Interface (after Mohanty et al. 2011)

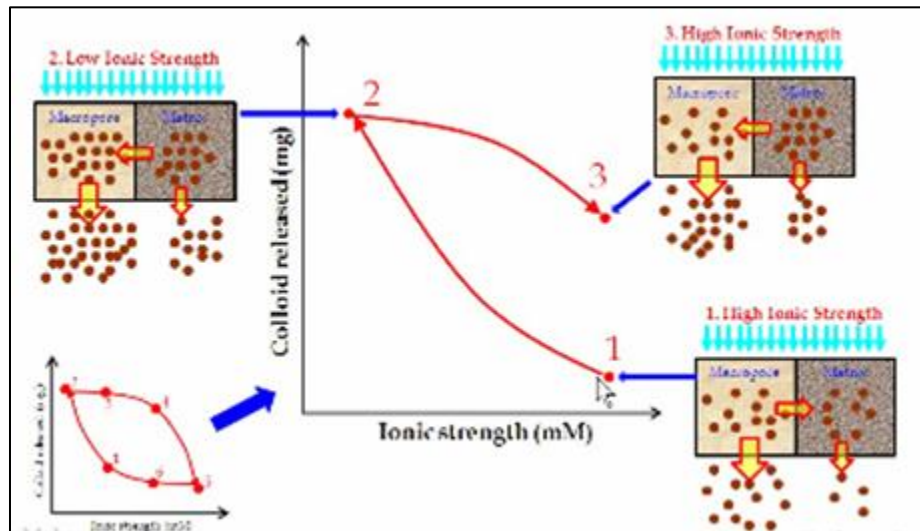


Figure 5-9. Macropore-matrix Exchange Caused by Hysteresis of Colloids and Metal Mobilization (after Mohanty et al. 2011)

It should be noted that bulk of the RI/FS borehole measurements for the metals are located, as expected, within the shallow vadose zone. The deeper penetrations are always located within the fine-textured horizon close to the water table. Experimental data on leaching experiments suggest that the contaminants are essentially immobilized. This is also collaborated by the fact that lead, arsenic and mercury are *not* contaminants of concern in groundwater.

6. Concluding Remarks

Unlike non-reactive contaminants such as tritium, arsenic, mercury and lead are known to have a high K_d , expected to be relatively immobile, and have a long residence time within the 100 Areas vadose zone. However, as the recently collected RI/FS field data illustrate a number of sampling measurements, especially for lead and arsenic, show deeper than expected penetration within the unsaturated media and show migration close to the water table. Three conceptual models are postulated to explain the deep penetration for the metals.

The deep borehole measurements targeted in the RI Work Plan were identified with a bias towards locating contaminants throughout the vadose zone and targeted areas at or near the waste sites; i.e., the drilling as well as the sampling was biased towards capturing contamination within the “hot spots.” For Conceptual Model #1, a comparison of LFI-based characterization data (waste site 100-H-21) with borehole profiles suggests that potential casing contamination and subsequent drag-down during cable-tool drilling cannot be ruled out for the highest measured lead concentration for the 100-H Area Borehole C7864.

While drag-down is a plausible conceptual model for C7864, colloid formation and colloid-facilitated transport form the basis for Conceptual Models #2 and #3 at other 100 Areas sampling locations. Even though both rely on initiation and migration of colloids, the difference in Conceptual Models #2 and #3 is how the 100 Areas vadose zone is conceptualized (i.e., a porous continuum versus macropore-porous matrix) and how transients in chemistry and preferential flow play a role in colloid initiation and mobilization. For both Conceptual Models #2 and #3, the episodic high-volume release from burial grounds as well as the PRZ induced exchange flow can potentially impact initiation of colloid formation and subsequent mobilization.

It should be noted that bulk of the RI/FS borehole measurements for the metals is located, as expected, within the shallow vadose zone. The deeper penetrations are always located within the fine-textured horizon close to the water table. Experimental data on leaching experiments suggest that the contaminants are essentially immobilized. This is also collaborated by the fact that lead, arsenic and mercury are *not* contaminants of concern in groundwater.

The RI/FS borehole data serve an important role in developing soil cleanup decisions along the Columbia River. For high K_d contaminants (generally defined for $K_d \geq 2$) (ECF-Hanford-11-0063, *STOMP 1-D Modeling for Determination of Preliminary Remediation Goals for 100 Area D, H, and K Source Areas*), if the soil column is shown to be not contaminated throughout the vertical profile, the most conservative assumption (i.e., a full contamination in the vadose zone) can be considerably relaxed with respect to soil cleanup decisions at waste sites in the 100 Areas.

7. References

- Bethke, C.M. and P.V. Brady, 2000, "How the Kd Approach Undermines Groundwater Cleanup," *Ground Water*, 38:435-443.
- BNWL-CC-2326, 1969, *Analysis of Travel Time of I-131 from the 1301-N Crib to the Columbia River During July 1969*. Pacific Northwest Laboratory, Richland, Washington. Available at: <http://www2.hanford.gov/arpir/?content=findpage&AKey=D196008312>.
- De Smedt, F. and P.J. Wierenga, 1984, "Solute Transfer through Columns of Glass Beads," *Water Resources Research*, 20:225-232.
- DeNovio, N. M., J. E. Saiers and J. N. Ryan, 2004, "Colloid Movement in Unsaturated Porous Media: Recent Advances and Future Directions," *Vadose Zone Journal* 3(2):338-351, doi: 10.2113/3.2.338
- DOE/RL-96-17, 2009, *Remedial Design Report/Remedial Action Work Plan for the 100 Area*, Rev. 6 Draft A, U.S. Department of Energy, Richland Operations Office, Richland, Washington. Available at: <http://www5.hanford.gov/arpir/?content=findpage&AKey=0810240391>.
- DOE/RL-97-49, 1997, *TWRS Vadose Zone Contamination Issue, Expert Panel Status Report*, Rev. 0, U.S. Department of Energy, Richland Operations Office, Richland, Washington. Available at:
- ECF-Hanford-11-0063, *STOMP 1-D Modeling for Determination of Preliminary Remediation Goals for 100 Area D, H, and K Source Areas*, Rev. 1, CH2M HILL Plateau Remediation Company, Richland, Washington.
- EPA/402/R-99/004A, 1999, *Understanding Variation in Partition Coefficient, Kd, Values: Volume I. The Kd Model, Methods of Measurement, and Application of Chemical Reaction Codes*, prepared for the U.S. Environmental Protection Agency, Washington, D.C. by the Pacific Northwest National Laboratory, Richland, Washington. Available at: <http://epa.gov/radiation/cleanup/402-r-99-004.html#vol1>.
- Mohanty, S., J. Ryan, and J. E. Saiers, 2011, *Mobilization of Colloids and Metals from Intact Cores of a Fractured Soil: Role of Pore Water Exchange Between Macropores and Matrix*, Soil Science Society of America Annual Meetings, October 16-19, San Antonio, Texas.
- Nkedi Kizza, P., J.W. Biggar, M.T. van Genuchten, P.J. Wierenga, H.M. Selim, J.M. Davidson, and D.R. Nielsen, 1983, "Modeling Tritium and Chloride 36 Transport Through an Aggregated Oxisol," *Water Resources Research*, 19:691-700.
- PNL-10899, 1996, *Strontium-90 Adsorption-Desorption Properties and Sediment Characterization at the 100-N Area*, Pacific Northwest Laboratory, Richland, Washington.
- PNNL-13037, 2000, *Geochemical Data Package for the Hanford Immobilized Low-Activity Tank Waste Performance Assessment (ILAW PA)*, Rev. 1, Pacific Northwest National Laboratory, Richland, Washington. Available at: http://www.pnl.gov/main/publications/external/technical_reports/13037rev1.pdf.
- PNNL-14702, 2006, *Vadose Zone Hydrology Data Package for Hanford Assessments*, Rev. 1, Pacific Northwest Laboratory, Richland, Washington. Available at: http://www.pnl.gov/main/publications/external/technical_reports/PNNL-14702rev1.pdf.
- Jury, W. A. and R. Horton, 2004, *Soil Physics*. Wiley, Hoboken, N.J. 370pp.

Kaplan, D.I., I.W. Kutnyakov, A.P. Gamberdinger, R.J. Serne, and K.E. Parker, 2000, "Gravel-Corrected Kd Values." *Ground Water* 38(6):851-857.

SGW-46279, 2011, *Conceptual Framework and Numerical Implementation of 100 Areas Groundwater Flow and Transport Model*, Rev. 1, CH2M Hill Plateau Remediation Company, Richland, Washington.

Wang, J.S. and T.N. Narasimhan, 1985, "Hydrologic Mechanisms Governing Fluid Flow in a Partially Saturated, Fractured, Porous Medium," *Water Resources Research*, 21:1861-74.

WHC-EP-0087, 1987, *Estimates of Solid Waste Buried in the 100 Area Burial Grounds*, Tables 9, 10, 11 and B.7, Westinghouse Hanford Company, Richland, Washington. Available at: <http://www2.hanford.gov/arpir/?content=findpage&AKey=D196008314>.